DEVELOPMENT AND PROCESS EVALUATION OF IMPROVED FISCHER-TROPSCH SLURRY CATALYSTS

QUARTERLY TECHNICAL PROGRESS REPORT

FOR THE PERIOD 1 JULY TO 30 SEPTEMBER 1987

December 21, 1987

by

Howard P. Withers
Air Products and Chemicals, Inc.
Allentown, PA 18105

and

Dragomir B. Bukur and Michael P. Rosynek
Departments of Chemical Engineering and Chemistry
Texas A&M University
College Station, TX 77843

WORK PERFORMED UNDER DOE CONTRACT NO. DE-AC22-85PC80011
FOR THE UNITED STATES DEPARTMENT OF ENERGY
THE PITTSBURGH ENERGY TECHNOLOGY CENTER
PITTSBURGH, PENNSYLVANIA

DEVELOPMENT AND PROCESS EVALUATION OF IMPROVED FISCHER-TROPSCH SLURRY CATALYSTS

QUARTERLY TECHNICAL PROGRESS REPORT

FOR THE PERIOD 1 JULY TO 30 SEPTEMBER 1987

December 21, 1987

by

Howard P. Withers
Air Products and Chemicals, Inc.
Allentown, PA 18105

and

Dragomir B. Bukur and Michael P. Rosynek
Departments of Chemical Engineering and Chemistry
Texas A&M University
College Station, TX 77843

WORK PERFORMED UNDER DOE CONTRACT NO. DE-AC22-85PC80011 -4
FOR THE UNITED STATES DEPARTMENT OF ENERGY
THE PITTSBURGH ENERGY TECHNOLOGY CENTER
PITTSBURGH, PENNSYLVANIA

DISCLAIMER

Project Manager - George Cinquegrane
Liquid Fuels Division
Pittsburgh Energy Technology Center
Pittsburgh, Pennsylvania

Program Manager - John Shen
Office of Coal Preparation & Liquefaction
Department of Energy
Washington, DC

TABLE OF CONTENTS

I. ABSTRACT

Nine runs in fixed bed reactors were performed during this period using the precipitated iron catalysts prepared in our laboratory. These tests were made to investigate the effect of copper and potassium promoters on catalyst activity and selectivity at various process conditions. Catalysts with 0 and 0.05 parts potassium were less stable and less active than catalysts with higher potassium loadings. Potassium and copper also influence product selectivity. One additional run was also made with United Catalyst, Inc. fused iron catalyst as a repeat of a previous run.

The investigation of catalyst activation/reduction procedures was begun in this period. The reductant type, temperature and pressure of the reduction will be studied as parameters, using a 100 Fe/3.0 Cu/0.2 K catalyst. One run was made following the CO reduction procedure used in previous catalyst tests, but a power failure interrupted the run, causing the catalyst to deactivate prematurely.

The elemental analysis of all precipitated, unsupported catalysts has been completed. The values for copper and potassium are in good agreement with the expected values for most catalysts. Surface area and pore size distribution measurements have been continued for the doubly promoted catalysts. Temperature programmed reduction (TPR) has also been applied to the doubly promoted catalysts. The effects of copper and potassium on catalyst reduction are similar to those observed for singly promoted catalysts. Work on isothermal reduction tests has also been performed. The promotional effect of copper on iron reduction is also seen at isothermal conditions, in agreement with the TPR results. Also, it was found that isothermal CO reduction occurs more rapidly than with H_2. Fourier Transform Infrared Spectrophotometry, using NO as a probe molecule, has been continued to investigate the chemical nature of surface iron species on the precipitated iron catalysts.

The trapping scheme of both fixed bed reactors and the existing slurry reactor have been modified to allow for the high pressure collection of products. Improvements in the temperature

control of the fixed bed reactors have been made by increasing the reactor volume to allow for higher catalyst dilution ratios, and by installing separate heaters and controllers on the top and bottom portions of the reactor bed. A new slurry reactor, including a computer data acquisition/control system, has been built. The preliminary tests of this system have been completed.

II. OBJECTIVE AND SCOPE OF WORK

The objective of this contract is to develop a consistent technical data base on the use of iron-based catalysts in Fischer–Tropsch (F–T) synthesis reactions. This data base will be developed to allow the unambiguous comparison of the performance of these catalysts with each other and with state-of-the-art iron catalyst compositions. Particular attention will be devoted to generating reproducible kinetic and selectivity data and to developing reproducible improved catalyst compositions. To accomplish these objectives, the following specific tasks will be undertaken.

TASK 1 – Project Work Plan

The objective of this task is to establish a detailed project work plan covering the entire period of performance of the contract. This includes estimated costs and manhours expended by month for each task.

TASK 2 – Slurry Catalyst Improvement

The primary purpose of this task is to develop improved iron-based catalysts, both precipitated and supported, that show enhanced activity and selectivity in slurry phase testing. This will be accomplished by gaining systematic understanding of the role of promoters, binders, supports and activation procedures in determining the activity and selectivity of iron-based catalysts. The catalyst development program will incorporate extensive physical and chemical characterization of these materials with the objective to establish correlations between the physical/chemical properties of these catalysts and the corresponding catalytic behavior for synthesis gas conversion.

TASK 3 – Process Evaluation Research

The purpose of this task is to subject the most improved catalysts (based on activity and selectivity) to a thorough process evaluation. This involves long term stability studies, investigation of a wide range of process variables, and determination of kinetic parameters. These kinetic parameters will be utilized to simulate catalyst performance under actual bubble column conditions.

Task 4 - Economic Evaluation

The aim of this task is to develop the relative economic impact for each improved catalyst composition and compare these economics with the economics of using the base case catalyst. Data obtained from tasks 2 and 3 will be used to generate a product yield structure, Fischer-Tropsch reactor residence time, and key process flow rates. These economic studies will include relative capital costs, operating costs, and required revenues for each catalyst, as well as a sensitivity study of the assigned relative values of the principal products (i.e. diesel and gasoline).

III. SUMMARY OF PROGRESS

Eight calcined, precipitated, unsupported catalysts have been tested in the past quarter, using the fixed bed reactors to study the effect of copper and potassium promotion on catalyst activity, selectivity, and stability. At a nominal 0.3 parts copper, catalysts with two levels of potassium promotion were tested, 100 Fe/0.3 Cu/0.2 K (run FB–05–2287) and 100 Fe/0.3 Cu/0.5 K (run FB-07–2657). Three sets of conditions were tested during run FB–05–2287: 220 °C, 1.48 MPa, 2 Nl/g-cat·h, and 235 °C, 1.48 MPa, at both 2 and 4 Nl/g-cat·h. During run FB–07–2657, one balance was completed, at 220 °C, 1.48 MPa, and 2 Nl/g-cat·h. Before a second balance at 235 °C could be completed, a power failure occurred and interrupted the operation of the reactor. After power was resumed and the reactor brought to the desired conditions, the catalyst activity was lower than before the interruption. Increasing the temperature further, to 250 °C , gave (H_2+CO) conversion lower than expected, and the run was terminated.

Four catalysts with nominal 1 part copper were tested: 100 Fe/1.0 Cu/0.0 K (run FA–33–2287), 100 Fe/1.0 Cu/0.05 K (run FA–13–2217), 100 Fe/1.0 Cu/0.2 K (run FA–15–2097), and 100 Fe/1.0 Cu/0.5 K (run FA–17–2367). The nominal composition of the 100 Fe/1.0 Cu/0.5 K catalyst was significantly different from the measured composition. The measured composition, from atomic absorption spectroscopy, was 100 Fe/1.05 Cu/0.83 K. The catalysts with low potassium concentrations (0 and 0.05 K) deactivated after only two balances. Their poor water–gas shift activity may have contributed to deactivation by decreasing the (H_2/CO) ratio in the gas phase, enhancing carbon deposition. The catalysts with higher potassium concentrations were more stable. The catalysts tested in runs FA–15–2097 and FA–17–2367 were deactivated only at high (2.86 MPa) pressure, which was the last condition tested in both of these runs.

Two catalysts with a nominal 3 parts copper were tested, 100 Fe/3.0 Cu/0.2 K (run FB–25–2447) and 100 Fe/3.0 Cu/0.5 K (runs FA–27–2457 and FA–27–2557). In the first test of the 100 Fe/3.0/0.5 K catalyst, a plug developed in the reactor after about 51 h on stream. and although the plug was later cleared, the pressure and flowrates remained unstable and the run was terminated. The retest of the catalyst was successful (run FA–27–2557) as was run FB–25–2447. Both of these runs consisted of five balances, and the catalyst deactivated only at the last set of conditions with high pressure (2.86 MPa).

Uncalcined 100 Fe/1 Cu/0.2 K catalyst was tested in run FA–15–1947 as a repeat of the run FA–02–1687 made in the previous quarter. At the first set of conditions, a hot spot 25 °C above the average reactor temperature (220 °C) was present in the top of the reactor and persisted throughout the balance. The hot spot was eventually eliminated by cooling the reactor and installing a two-zone heater, but after the process conditions were reestablished, the catalyst was found to be deactivated. Two additional balances, at 222 and 236 °C, 1.48 MPa, and 1.9 Nl/g-cat·h were performed, after the modification to the reactor, but the conversions were lower than expected.

A run using United Catalyst, Inc. C–73 fused iron was also made (run FA–01–1807) as a retest of a run made during the last quarter (run FA–01–1547). At 234 °C, 0.79 MPa, 1.52 Nl/g-cat·h, the conversion was 22.8 %, which is lower than the 29.9 % conversion obtained in run FA–01–1547–1. A second balance was made at 235 °C, 1.48 MPa, and 2 Nl/g-cat·h, but the conversion decreased to 19.1 %, and the run was terminated, due to obvious catalyst deactivation.

The investigation of activation/reduction procedures has begun, using a nominal 100 Fe/3.0 Cu/0.2 K catalyst, which has been shown in previous tests to have good activity and stability. One run (FB–25–2667) has been performed as part of this investigation. After 5 h at the process conditions (250 °C, 200 $psig$, 2 Nl/g-cat·h, (H_2/CO) = 1.07), the (H_2+CO) conversion was 84 %, but at 20 h on stream, a power failure occurred and temporarily shut down the reactor. After power was resumed and the system was returned to the desired process conditions, the (H_2+CO) conversion dropped to 68.7 % and continued to decline with time on stream. The run was stopped after 60 h due to the deactivation. Work on the activation/reduction procedure research will continue during the next quarter.

Several modifications have been made to the fixed bed reactor systems during this reporting period. In order to improve the temperature control of the fixed bed reactors, their volumes have been increased to 30 *cc* which allows higher dilution ratios to be used. Also, two-zone heaters have been installed, which allows the top one-third and bottom two-thirds of the reactor to be controlled separately. Two high pressure product traps have been installed on each system to collect condensed products before reaching the back pressure regulator. Pressure and flowrate fluctuations have been caused in the past by liquid or solid products accumulating in the lines or back pressure regulator. Finally, a new feed section for the systems has been built in order to simplify the switching of feed gases to the reactors during operation.

The existing slurry reactor system has been modified to allow for the high pressure collection of products before the back pressure regulator. Two low pressure product traps have also been installed on this system. A separate reactor head heater is now used to control the head temperature independently of the reactor furnace. A second slurry reactor has been built and pressure tested. The new system incorporates the improvements of the existing slurry system into its design. A computer data acquisition/control system, including software, has been built and tested for the new slurry reactor. The computer will perform data logging on the reactor and provide for simple temperature control.

Work has been performed on a procedure to analyze wax. Four columns were tested for the analysis, and a fused silica capillary column (RSL-150, Alltech) was found to give the best overall results. Response factors were determined with this column, and a sample paraffin wax, FT-300 (Dura Commodities, New York) was used to test the procedure. Only 43 % of the wax was analyzed, which may be due to the high $C_{50}+$ fraction in FT-300.

All of the precipitated, unsupported catalysts have been analyzed for iron, copper, and potassium by atomic absorption spectroscopy. The compositions of the catalysts have been found to be acceptably close to the predicted (nominal) compositions in most cases. Both copper and potassium concentrations tend to be slightly lower than the predicted values.

The measurement of surface areas and pore size distributions of uncalcined, calcined, and reduced samples has been continued. The surface area measured by N_2 physisorption of unpromoted, unreduced iron is 180 m^2/g, and the area increases to 200–210 m^2/g after impregnation with $KHCO_3$. Copper promotion, even at very low levels, increases the surface areas substantially, to 280–380 m^2/g. Calcination in air has been found to decrease the surface area, to 60 m^2/g for most samples, and H_2 reduction decreased the surface areas of all catalysts to 5–10 m^2/g. Mercury porosimetry has been used to characterize the pore size distributions of the calcined and reduced catalysts. Calcination of the unpromoted catalyst increased the average pore diameter to 90 Å, from 40–45 Å for the uncalcined catalyst (determined by N_2 desorption). The reduced catalyst has a bimodal pore size distribution, with a principal maximum at 250 Å and a secondary maximum at 90 Å. Copper (0.1 and 0.3 parts) promoted catalyst also exhibited a bimodal distribution, with the principal maximum increased to 400 Å.

The temperature–programmed reduction (TPR) technique used previously for unpromoted or singly promoted catalyst has been applied to the doubly promoted catalysts. Copper has the same promotional effect on potassium–containing catalysts as it does on potassium–free catalysts, that is, the reduction of Fe_2O_3 to Fe_3O_4 is shifted to lower temperature. Potassium broadens and intensifies the peak associated with the reduction of Fe_3O_4 to metallic iron, which is the same effect observed for copper–free catalysts. Isothermal reduction experiments have also been performed, and the promotional effect of copper on iron reduction evident in the TPR experiments are also observed in the isothermal experiments. For example, the H_2 reduction at 300 °C of copper–free catalyst is incomplete after 16 h, while complete reduction is attained after 10 h when 0.3 parts copper is present, and 7 h when 3 parts copper is present. Potassium has little effect on the reduction, although high (> 0.5 part K) levels of potassium inhibits the reduction.

The work with Fourier Transform Infrared Spectrophotometry (FT–IR) has been continued to investigate the chemical nature of surface iron species on the precipitated iron catalysts. Nitric oxide (NO) has been used as a probe molecule in these studies. Three preparations have been used: undiluted precipitate deposited as a thin film on a BaF_2 crystal, silica supported sample (25 weight % Fe) prepared by incipient wetness impregnation, and a physical mixture of silica and calcined, unpromoted catalyst.

IIII. DETAILED DESCRIPTION OF TECHNICAL PROGRESS

TASK 1 – Project Work Plan

The project work plan was completed during the first quarter of this project and the detailed work plan was submitted to APCI.

TASK 2 – Slurry Catalyst Improvement

2.1. Design and Construction of Reactor Systems.

Several modifications have been made to both fixed bed reactor systems and the existing slurry system in order to improve the trapping of liquid products and facilitate reactor operation. Also. a second slurry reactor system (reactor "SB") has been constructed with the new trapping procedure implemented.

2.1.1. Fixed Bed Reactor Systems.

A process schematic of the modified fixed bed reactor systems is shown in Figure 1. Both systems ("FA" and "FB") share essentially the same design, and share a new feed section for helium and feed gas delivery. The new feed section was built to deliver two types of gas (H_2, CO, or synthesis gas) to each fixed bed reactor system. This modification allows for switching from reducing gas (CO or H_2, for example) to synthesis gas immediately, without changing cylinders. Also, the feed section can deliver helium to the fixed beds to dilute the feed, as well as for purging. A new product trapping scheme has also been implemented. Two high pressure traps are now used to collect products upstream of the back pressure regulator. These traps were installed to remove products that condense or solidify at lower temperatures from the reactor effluent before they reach the back pressure regulator. In the past, operational problems have been caused by condensation and/or solidification of products in the back pressure regulator, leading to pressure fluctuations and an unstable system outlet flowrate. The two low pressure ice traps downstream of the back pressure regulator have been retained.

During system startup, or during an unsteady period, the reactor effluent flows through the high pressure waste trap, which operates at system pressure and ambient temperature. The gas then flows through the back pressure regulator to the unsteady ice trap, where any condensible products remaining in the exit gas are removed. Immediately before a mass balance period, gas flow is directed from the waste trap to the high pressure (wax) trap, and from the unsteady state ice trap to the steady state ice trap. The wax trap, operating at system pressure and 190–210 °C, is used to remove high molecular weight products which are solids at room temperature (*i.e.*, "wax"). The steady state ice trap removes any remaining condensible organic products and the aqueous phase products.

Two–zone heaters have also been installed on the fixed bed reactor systems to control reactor temperature. The zoned heaters allow for independent temperature control of the heating blocks on the top one–third and bottom two–thirds of the reactor. This modification was made to obtain better temperature control and thus decrease the likelihood of a hot spot developing in the top of the reactor during catalyst tests. Also, larger volume reactors have been built and installed so that higher dilution ratios can be used, which will also help to reduce the possibility of hot spots. The new reactors have effective volumes of 30 *cc*, with 5 thermocouple wells installed radially in the reactor, spaced every 6.4 *cm* along the length of the bed in order to monitor the axial temperature profile during a run.

2.1.2. Slurry Reactor Systems.

The existing slurry reactor system has also been modified to allow for the high pressure collection of products. The process schematic of the modified slurry reactor system is shown in Figure 2. Four traps are now used in place of the single C_5/C_6 splitter. It was difficult to maintain a low temperature in the C_5/C_6 splitter, and incomplete product condensation was a problem during the shakedown run.

During system startup, or during an unsteady period, the reactor effluent passes through the refluxer to the unsteady state trap, which operates at ambient temperature and system pressure.

The gas flows through the back pressure regulator to an unsteady state ice trap, and then to the system outlet where the gas flowrate is measured. During a mass balance period, the flow is diverted through the high and low pressure steady state traps. The high pressure steady state trap is operated at ambient, or mildly elevated temperature and system pressure, and the low pressure trap is operated at 0 °C and ambient pressure. Before draining, the pressure in the high pressure trap is relieved through the ice trap to minimize product loss due to flashing.

Several other minor modifications have been made to the slurry reactor system. A separate heater/controller for the reactor head has been installed to ensure true isothermal temperatures of both the gas and slurry phases in the reactor. Previously, the reactor head was insulated and heated only by conduction from the reactor furnace. Also, a wax receiver vessel has been added to collect wax from the reactor when it is withdrawn at high pressure at the end of a mass balance period.

A second slurry reactor system has been built, incorporating all modifications to the existing slurry reactor system. The flow path of the new system is identical to that of the existing system (Figure 2).

The second slurry reactor system utilizes IBM–PC based data acquisition/control to monitor process variables, implement alarms, and provide simple temperature control. The reactor head and reactor furnace are controlled from separate, independent controllers; other heaters for the preheater, reflux condenser, and outlet lines are controlled by the computer. All computer interface hardware was purchased from Interactive Microware, Inc. (State College, PA). An ADALAB–PC board provides for the interface between the computer and reactor system. Additional 16–channel and a 32–channel multiplexer boards provide up to 48 channels of analog input, 8 bits of digital input, and 8 bits of digital output. An additional 8 bits of digital output are available directly from the ADALAB–PC board. A 16–channel relay board, using the 16 bits of digital output, is used to drive relays for alarms and temperature control.

All system temperatures are monitored by Type J thermocouples. System pressure is monitored with a pressure transducer on the reactor inlet line, and the feed flowrate is obtained as a 0–5 V signal from the mass flow controller. In the event of an excessively high reactor temperature, or abnormally high or low system pressure, the computer initiates a controlled shutdown by cutting all power to heaters, turns off the reactor stirrer, diverts air to the reactor cooling coils, and switches the feed from synthesis gas to helium. All process conditions continue to be monitored during the shutdown. The computer also controls the temperature of the reactor preheater, reflux condenser, and outlet lines, and provides high/low temperature alarms for these devices, as well as high/low temperature alarms for the reactor head and reactor furnace.

2.2. Product Analysis System.

2.2.1. Wax Analysis Procedure.

During the past quarter, we have initiated the development of a wax analysis procedure. To date, our study has included:

- Establishment of a wax dissolution and injection procedure.
- Evaluation of different chromatograph columns.
- Establishment of optimum chromatographic conditions.
- Determination of response factors.
- Analysis of a Fischer–Tropsch wax.

Equipment employed in this study include a Sigma 1 chromatograph, which has been modified for capillary application. A "cold" on–column injector is employed with a capillary column providing the component separation. Quantitative analysis is obtained from a flame ionization detector (FID) maintained at 375 °C.

The wax analysis procedure employed a carrier flow rate of 15 ml/min (STP) of helium. The oven was temperature programmed from 90 to 325 °C at a rate of 10 °C $/min$ with the final temperature being maintained for 20 minutes, for a total analysis time of 45 minutes. Lower carrier flow rates and/or decreased heating rates were found to result in excessive peak broadening and a loss of resolution at higher hydrocarbon numbers.

In order to obtain an accurate quantitative analysis of reactor wax, it is necessary to dissolve the wax as completely as possible in an appropriate solvent. It is also necessary that the wax remain dissolved in the solvent during the sample injection. The dissolution procedure employed in this study involved adding 0.25 to 0.30 *g* of reactor wax to approximately 5.0 *g* of toluene. A small quantity, typically 0.05 *g*, of *n*–hexadecane (or similar hydrocarbon) was added to the solvent to serve as an internal standard. The mixture was then heated to near boiling in order to completely dissolve the wax. Once dissolved, about 0.25 *g* of the hot solution was removed and further diluted with toluene to achieve a final dilution between 200 and 400:1 (weight basis). The final solution was maintained at 50 to 60 °C to avoid condensation of the heavier components. 1.5 to 2.0 *μl* of solution was drawn into a heated 10 *μl* syringe for injection onto the GC column. Heating of the syringe was accomplished by using a small aluminum block, heated at about 60 °C . No condensation of heavy components was observed with this procedure.

Four different chromatograph columns were evaluated for the wax analysis. The columns were evaluated based on their ability to resolve high carbon number components while maintaining good separation of *n*–paraffin species. The four columns investigated were: a 10–*m* × 0.53–*mm* ID, 0.2 *μ* RSL–150 fused silica capillary column (Alltech), a 15–*m* × 0.32–*mm* ID, 1.0 *μ* DB–5 fused silica capillary column (J&W Scientific), a 8–*m* × 0.32–*mm* ID, 1.0 *μ* DB–5 fused silica capillary column (J&W Scientific), and a 6–*ft* × 1/8–*in*, 60/80 mesh SP–2100 packed column (Supelco). All columns provided a good separation of *n*–paraffins; however, the 8–*m* DB–5 and the SP–2100 column exhibited excessive peak broadening at about C_{35}. The RSL–150 column was the only column capable of eluting *n*–paraffins greater than C_{42}. Using the RSL–150 column, analysis up to *n*–C_{55} could be achieved, as illustrated in Figure 3.

Response factors were determined at selected carbon numbers for C_{16} to C_{40} *n*–paraffins using the RSL–150 fused silica column. These values are reported in Table 1. Response factors were determined on a weight basis using the equation:

$$RF_i = (A_i/A_{ref})(w_{ref}/w_i) \tag{1}$$

Where RF is the response factor, A is the area of integration and w is the weight fraction of the component. The subscripts i and ref refer to the component of interest and the reference component, respectively. Note from Table 1 that all response factors are close to 1. This indicates that none of the species are lost during the analysis. Based on these results, a response factor of 1.0 will be used for all hydrocarbons present in the wax sample.

A hard n–paraffin wax FT–300 (purchased from Dura Commodities, New York) was used as a standard material for evaluation of the above procedure, and n–hexadecane was used as an internal standard. Paraffins with carbon numbers between 24 and 50 were quantified, but only 43 % of the total product has been analyzed. Possible reasons for the low wax recovery are: (1) part of the wax (mostly $C_{50}+$) does not elute from the column, (2) the sample which is injected onto the column is not representative of the "true" sample, (3) errors in integration due to the baseline shift. All of these factors may be responsible for the low wax recovery in one form or another. Further work will be required to adequately evaluate our techniques and make improvements where necessary.

Recently, in Mobil's work (Kuo, 1985) it was reported that the reactor waxes from runs CT–256–4 and –5 (the high reactor–wax yield operation) contained 64.8 and 74.8 % of the $C_{55}+$ hydrocarbons, respectively. Thus, our finding that about 57 weight % of FT–300 wax may be in the $C_{50}+$ range is consistent with these results.

Problems with the equipment hardware were encountered during this quarter. The polarizer of one of the FID's on the Sigma 1 GC became defective. We plan to replace this part, and obtain a new gas chromatograph, both of which will improve the speed and quality of the product analysis by capillary gas chromatography.

2.3. Promoter Effect Research.

2.3.1. Catalyst Tests in Fixed Bed Reactors.

Eight of the precipitated, unsupported catalysts have been tested during the period 1 July – 30 September, 1987. Also, a single run was made with United Catalyst. Inc. C–73 fused iron (run FA–01–1807). A nominal 100 Fe/1 Cu/ 0.2 K (1 part by weight of copper and 0.2 part by weight of potassium per 100 parts of iron) precipitated, unsupported catalyst was tested in both calcined (run FA–15–2097) and uncalcined (run FA–15–1947) form. The remaining precipitated catalysts were all tested after calcination. Calcination of the catalysts was performed in flowing air at 3.0 Nl/g-cat·h, 300 °C, and ambient pressure for 5 h. Details of the catalyst calcination procedure are given in Appendix I. All precipitated catalysts were reduced prior to testing using pure CO following the procedure described in Appendix I.

Run numbers have the following format: the first two characters designate the reactor unit used for the test, ("FA" = fixed bed reactor A; "FB" = fixed bed reactor B), followed by a two digit catalyst code. The last four digits of the run number indicate the day and year of the start of the run. The catalyst codes for the precipitated, unsupported series of catalysts are given in Table 2. Unpromoted, unsupported, precipitated iron catalyst was given the code "00" and United Catalyst, Inc. C–73 fused iron was given the code "01". Precipitated iron catalysts singly promoted with copper have the codes "3x", where "x" is an integer indicating the concentration of copper promoter (x = 1 → 9). Precipitated iron catalysts singly promoted with potassium have a similar type of code, "4x", where x now indicates the level of potassium promotion. Doubly promoted precipitated catalysts are assigned the codes "0x" (0.3 parts copper), "1x" (1.0 parts copper), and "2x" (3.0 parts copper), where x again indicates the level of potassium promotion.

Run FA – 01 – 1807 (United Catalyst, Inc. C – 73 fused iron catalyst)

This run was made using United Catalyst, Inc. C–73 fused iron catalyst ground to 170/230 mesh, diluted 4:1 by volume with glass beads of the same mesh size range. The catalyst was activated using pure H_2 flowing at 20 000 h^{-1} (volume of gas at STP/volume of catalyst·h) and atmospheric pressure, following the procedure described in the Technical Progress Report for the period 1 April – 30 June 1987. Two mass balances were performed during this run, which are summarized in Table 3 with the results of a previous run at the same conditions (run FA–01-1547).

The first balance was made at 234 °C, 0.79 MPa, using an $(H_2/CO) = 1$ feed gas at 1.5 Nl/g-cat·h. The $(H_2{+}CO)$ and CO conversions, 22.8 and 24.1 % at these conditions was significantly lower than in the previous run, 29.9 and 35.9 %. The CO conversion was also much less than the 49 % conversion obtained by workers at Exxon (Satterfield, *et al.*, 1985) using the same catalyst and particle size at comparable process conditions (run 746: 233 °C, 0.79 MPa, $(H_2/CO) = 1$, 1.51 Nl/g-cat·h). A second balance was made at 235 °C, 1.48 MPa, 2 Nl/g-cat·h, again using an $(H_2/CO) = 1$ synthesis gas. The $(H_2{+}CO)$ conversion dropped to 19.1 % at these conditions, which indicates that the catalyst had deactivated. At slightly higher space velocity, but double the pressure, the space time yield increased only 11 %, from 0.015 to 0.017 *mols* $(H_2{+}CO)$ converted/g-cat·h. The weight % of hydrocarbons for methane and C_2–C_4 products increased at higher pressure and space velocity, from 3.51 (methane) and 19.5 % (C_2–C_4) during the first balance to 5.71 (methane) and 36.6 % (C_2–C_4) during the second balance, while the weight % of hydrocarbons decreased for the C_5–C_{11} and $C_{12}+$ products, 48.9 (C_5–C_{11}) and 28.5 % ($C_{12}+$) to 41.2 (C_5–C_{11}) and 16.5 % ($C_{12}+$). The run was terminated as it was apparent that the catalyst had deactivated.

Run FA – 15 – 1947 (Uncalcined 100 Fe/0.96Cu/0.18K)

This run was made to evaluate precipitated, unsupported catalyst in an uncalcined form, and was a repeat of run FA–02–1687, reported in the Technical Progress Report for the period 1 April – 30 June, 1987. The same catalyst was used in both of the runs (a change in catalyst codes is responsible for the different run numbering format). The first set of conditions used were 225 °C, 1.48 MPa, using an $(H_2/CO) = 1$ feed at a space velocity of 1.86 Nl/g-cat·h. The $(H_2{+}CO)$ conversion measured at these conditions was 78.0 %, however, a hot spot persisted in the top of the catalyst bed throughout the mass balance period. The temperature at the top of the bed was about 242 °C while the remainder of the bed operated at about 220 °C. On increasing the temperature to 235 °C, the temperature increase in the top of the bed grew worse, and after several unsuccessful attempts were made to raise the reactor temperature without propagating the hot spot, the reactor was allowed to cool to room temperature after 51 *h* on stream. A two–zone heater was installed on the system in order to control the top and bottom bed temperatures separately, and the reactor temperature was brought up to 222 °C at about 57 *h* on stream. A second mass balance was made at 222 °C, 1.48 *MPa*, with a space velocity of 1.9 *Nl*/*g*-cat·*h*. The (H_2+CO) conversion at these conditions was 25.3 %, significantly lower than in the previous balance. The decrease in conversion was due to both catalyst deactivation and the elimination of the temperature gradient in the reactor. A third balance was made after increasing the reactor temperature to 236 °C, and the (H_2+CO) conversion increased to 34.8 %. In run FA–02–1687–2, the same operating conditions were used and an (H_2+CO) conversion of 37.2 % was obtained, however, run FA–02–1687–2 had a 18 °C hot spot in the first balance which probably caused catalyst deactivation also. The weight % of hydrocarbons for methane, C_2–C_4 , and C_5–C_{11} products increased from 2.8 (methane), 22.7 (C_2–C_4), and 19.6 % (C_5–C_{11}) at 222 °C to 3.8 (methane), 23.1 (C_2–C_4), and 24.5 % (C_5–C_{11}) at 236 °C. The weight % of hydrocarbons for the C_{12}+ products decreased accordingly, from 54.9 (222 °C) to 48.6 % (236 °C). The results from this run are summarized in Table 4.

2.3.2. Fixed Bed Reactor Runs with Calcined Catalysts.

The conditions for the fixed bed catalyst tests of precipitated, unsupported, calcined catalysts made during this period are shown in Table 5. For all of these runs, the catalyst was diluted approximately 1:7 by volume with glass beads before loading the reactor, and both catalyst and glass were ground and sized to 30/60 mesh. All tests were made using a synthesis gas with an (H_2/CO) molar feed ratio of approximately 1. The effect of temperature was studied with the first, second, and fifth sets of conditions shown, at 220, 235, and 250 °C. The effect of pressure was studied in the second and sixth sets of conditions at 1.48 and 2.86 MPa. Finally, the effect of space velocity was studied in the second, third, and fourth sets of conditions, at 2 and 4 Nl/g-cat·h as well as an unspecified space velocity at the fourth set of conditions. The unspecified space velocity was selected to complement the conversion data of the tests at 2 and 4 Nl/g-cat·h, *i.e.*, if both previous space velocities gave low (H_2+CO) conversions, the space velocity would be decreased to give high conversion level data. Likewise, if the previous space velocities gave high conversions, a higher space velocity would be used to give data at lower (H_2+CO) conversions. This set of conditions was optional, and not performed for all runs. Also, if catalyst deactivation became apparent before all sets of process conditions were tested, the remaining conditions were not run on the deactivated catalyst.

Run FB – 05 – 2287 (100 Fe/0.28 Cu/0.19K)

Three sets of conditions were used during this run, and the results are summarized in Table 6. Following reduction, the reactor was brought to 220 °C, 1.48 MPa, with a space velocity of 2 Nl/g-cat·h. At the first set of conditions, the (H_2+CO) conversion was 43.5 %. Increasing the temperature to 235 °C, while holding all remaining conditions constant, increased the (H_2+CO) conversion to 64.8 %. The weight % of methane, C_2–C_4 , and C_5–C_{11} products remained about the same at the two temperatures, 7.96 (methane), 30.4 (C_2–C_4) and 20.2 % (C_5–C_{11}) at 235 °C, as compared to 7.38 (methane), 32.3 (C_2–C_4), and 24.9 % (C_5–C_{11}) at 220 °C. The C_{12}+ fraction increased by 17 % at the higher temperature, from 35.4 to 41.5 %, while the yield of oxygenates dropped from 10.1 to 3.9 g/Nm^3 (H_2+CO) converted . Increasing the space velocity to 4 Nl/g-cat·h at 235 °C led to a decrease in (H_2+CO) conversion to 27.6 %. The hydrocarbon fractions of methane, C_2–C_4 , and C_5–C_{11} products increased at the higher space velocity, to 8.72, 37.5, and 31.2 %, respectively. A significant decrease in the C_{12}+ products to 22.6 % was observed. A fourth set of conditions at lower space velocity, 1.4 Nl/g-cat·h, was attempted following the balance at 4 Nl/g-cat·h. The measured (H_2+CO) conversion was 52.4 %, which is less than the conversion obtained in balance 2 at the same temperature and pressure, but higher space velocity (2 *Nl*/*g*-cat·*h*). The conversion decrease was due to catalyst deactivation, and the run was terminated. Hot spots were present in the reactor at all three sets of process conditions tested in this run: 10, 20, and 13 °C during balances 1, 2, and 3, respectively. The persistent hot spots were a probable cause of catalyst deactivation during this run.

Run FB – 07 – 2657 (100 Fe/0.28 Cu/0.48 K)

Only two balances were performed during this run, at 220 and 235 °C, 1.48 *MPa*, at a space velocity of 2 *Nl*/*g*-cat·*h*. The results of these two balances are summarized in Table 7. The (H_2+CO) conversion at 220 °C was 39.9 %. Following the balance at 220 °C, the temperature was increased to 235 °C, however, approximately 15 *h* after the change of conditions, and before a mass balance could be completed, an electrical power failure shut down the system for roughly 45 minutes, during which time the reactor cooled to 90 °C. During the power failure, helium at atmospheric pressure was fed to the reactor. When electrical power was resumed, the system was gradually returned to the conditions of the second mass balance, but an (H_2+CO) conversion of only 43.3 % was obtained. Since this is only slightly higher than that obtained at 220 °C, catalyst deactivation was apparently caused by the process interruption. Although conversions were not measured at 235 °C before the power failure, the gas contraction was measured at 43 %, as compared to a contraction of 31.2 % after power was resumed. Following the mass balance at 235 °C the reactor temperature was raised to 250 °C, and after 17 *h* on stream at these conditions, an (H_2+CO) conversion of only 54.7 % was obtained. Since this conversion was significantly less than expected (~ 70 %), the run was terminated.

Run FA – 33 – 2287 (100 Fe/1.03Cu/0.0K)

During run FA-33-2287, only two mass balances were performed, at 220 and 235 °C, 1.48 *MPa*, using a space velocity of 2 *Nl*/*g*-cat·*h*. The results of this run are summarized in Table 8. The (H_2+CO) conversions at the two temperatures were 37.1 % (220 °C) and 45.4 % (235 °C).

The relatively small change in (H_2+CO) conversion with temperature indicates that deactivation occurred. The olefin/paraffin ratios at the two temperatures were similar, as was the hydrocarbon weight % of methane. The weight % of hydrocarbon for the C_2–C_4 , and C_5–C_{11} products decreased with temperature, from 43.1 (C_2–C_4) and 31.4 % (C_5–C_{11}) at 220 °C to 35.5 (C_2–C_4) and 26.8 % (C_5–C_{11}) at 235 °C. The C_{12}+ products increased from 14.5 % at 220 °C to 28.2 % at 235 °C. At the end of the second balance, the space velocity was decreased to 1 Nl/g-cat·h in an attempt to increase conversion; however, the (H_2+CO) conversion at the lower space velocity was only 43.1 %, less than the conversion obtained during balance at the same temperature and pressure but higher space velocity. The run was terminated due to catalyst deactivation.

Run FA – 13 – 2217 (100 Fe/0.94Cu/0.05K)

Two balances were performed during this run, and the results are summarized in Table 9. Following reduction, the reactor was first brought to 220 °C, 1.48 MPa, with a space velocity of 2 Nl/g-cat·h. At these conditions, the (H_2+CO) conversion was 45.1 %. Increasing the reactor temperature to 235 °C, with all remaining conditions held constant, increased the (H_2+CO) conversion to only 47.5 %. This indicates that the catalyst had deactivated, although no hot spots or other operational difficulties were encountered. The olefin/paraffin ratios and the weight % of hydrocarbons for methane and C_2–C_4 products were about the same at both temperatures. As the temperature was increased to 235 °C, the weight % of hydrocarbons for C_5–C_{11} products decreased from 39.1 to 33.8 %, while the weight % of hydrocarbons for the C_{12}+ products increased from 23.4 to 29.2 %. Since deactivation was apparent from the second balance, no additional conditions were tested.

Run FA – 15 – 2097 (100 Fe/0.96Cu/0.18K)

A total of six sets of operating conditions were used during this run, the results of which are summarized in Table 10. Following reduction, the reactor was brought to 220 °C, 1.48 MPa, with a space velocity of 2 Nl/g-cat·h. At these conditions, the (H_2+CO) conversion was 39.4 %

and the (H_2/CO) usage was 0.84. Increasing the reactor temperature to 235 °C, with all other conditions the same, led to an increase in (H_2+CO) conversion to 72.8 %. The higher temperature increased the weight % of hydrocarbons for methane and C_2–C_4 products, 7.22 (methane) and 26.6 % (C_2–C_4) at 220 °C to 9.85 and 33.3 % at 235 °C. The weight % of hydrocarbons for the C_5–C_{11} products decreased to 25.6 % at 235 °C from 37.1 % at 220 °C. The C_{12}+ weight % remained approximately constant. A further increase in temperature for the fifth balance to 250 °C yielded a higher (H_2+CO) conversion, 78.9 %, but the reaction was probably reactant limited by CO as the CO conversion was 91.6 %. For an (H_2/CO) = 1 feed, CO will be the limiting reactant whenever the (H_2/CO) usage ratio is less than 1; the usage ratio at 250 °C was 0.75.

Balances 3 and 4 show the effect of space velocity at 4 and 5.5 *Nl/g*-cat·*h*. The reactor was held at 235 °C and 1.48 *MPa*, which are the same as for balance 2 at 2 *Nl/g*-cat·*h*. The (H_2+CO) conversion decreased as expected as the space velocity increased, 72.8, 49.6, and 26.9 % (H_2+CO) conversion at 2, 4, and 5.5 *Nl/g*-cat·*h*, respectively. The olefin/paraffin ratios are also higher at 5.5 *Nl/g*-cat·*h*, indicative of secondary olefin hydrogenation at the lower flowrates. The effect of pressure was studied in balance 6, with the reactor at 235 °C, 2.86 *MPa*, and a space velocity of 4 *Nl/g*-cat·*h*. The catalyst deactivated rapidly at the high pressure, and the (H_2+CO) conversion was measured at only 23.6 %, as compared to the 72.8 % (H_2+CO) conversion obtained during balance 2. The (H_2+CO) conversions of these two balances should be comparable, as the gas phase residence times are approximately the same under both sets of conditions. The high pressure produced low weight % of hydrocarbons for methane and C_2–C_4 products, decreasing to 4.63 (methane) and 23.7 % (C_2–C_4) at 2.86 *MPa* from the 9.85 (methane) and 33.3 % (C_2 - C_4) obtained during balance 2 at lower pressure. The C_5–C_{11} products remained approximately the same, and the C_{12}+ products increased with pressure to 44.1 % from 31.2 % at 1.48 *MPa*.

The Anderson–Schulz–Flory (ASF) plots for balances 1, 2, and 5 are shown in Figures 4–6. The data plotted in these figures consist only of the liquid products collected in the ice trap, and gaseous products. Products collected in the high pressure trap were not analyzed, and do not appear in these figures. The data from all three balances generally fall on a straight line, however, negative deviations appear in Figures 4–6 in the C_7–C_{10} carbon number range. These negative deviations are due to sample loss by evaporation during sample collection and handling. Positive deviations occur beginning about C_{17} for balances 2 and 5. This type of behavior has been observed by others (*e.g.*, Huff and Satterfield, 1984). The negative deviations above C_{22}–C_{23} in Figure 6 are probably due to the collection of high molecular weight products in the high pressure trap during the mass balance.

Run FA – 17 – 2367 (100 Fe/1.05 Cu/0.83 K)

Five sets of conditions were used during this run, and the results are summarized in Table 11. The first set of conditions tested were 220 °C, 1.48 *MPa*, and a space velocity of 2 *Nl/g*-cat·*h*. At these conditions, the (H_2+CO) conversion was 40.4 %, and increased to 56.1 % when the temperature was increased to 235 °C for the second balance, with all remaining conditions constant. The increase in temperature had little effect on the weight % of hydrocarbons for methane and C_2–C_4 products, but decreased the percentage of C_5–C_{11} products by 35 %, from 32.6 % (220 °C) to 21.3 % (235 °C). The $C_{12}+$ products increased with temperature, from 28.5 % (220 °C) to 40.9 % (235 °C). A second increase in temperature to 250 °C (balance 5) increased the (H_2+CO) conversion to 64.6 %. The weight % hydrocarbon distribution remained fairly stable from 235 to 250 °C, with a slight increase (6.6 %) for the $C_{12}+$ products and a decrease (9.9 %) for the C_5–C_{11} products.

The effect of space velocity was also studied, at 235 °C, 1.48 *MPa*, and 1.36 (balance 4), 2.1 (balance 2) and 4.2 *Nl/g*-cat·*h* (balance 4). As would be expected, the conversion decreased with increasing space velocity: 60.2, 56.1, and 33 % (H_2+CO) conversion at 1.36, 2.1 and 4.2 *Nl/g*-cat·*h*, respectively. *Nl/g*-cat·*h*, respectively. After balance 5, the process conditions were adjusted to 235 °C, 2.86 *MPa*, and 4.2 *Nl/g*-cat·*h*, which resulted in rapid catalyst deactivation. After 1 and

19 *h* at these conditions the (H_2+CO) conversion was 46.4 and 13 %, respectively. The run was terminated after a total of 156 *h* on stream.

Run FB – 25 – 2447 (100 Fe/2.93 Cu/0.18 K)

The results at the five sets of conditions used during this run are summarized in Table 12. The first set of conditions following reduction were 220 °C, 1.48 *MPa*, with a space velocity of 2 *Nl/g*-cat·*h*. The (H_2+CO) conversion during this test was 42.9 %. Increasing the temperature to 235 °C , while holding all other conditions constant, increased the (H_2+CO) conversion to 54.5 % (balance 2). The weight % of hydrocarbons for methane, C_2–C_4 , and C_5–C_{11} products all increased at the higher temperature, from 4.31, 19.9, and 20.2 % (220 °C) to 7.80, 37.3, and 29.6 % (235 °C) for methane, C_2–C_4 , and C_5–C_{11} products, respectively. The weight % of hydrocarbons for C_{12}+ products decreased by 54 % at 235 °C, from 55.6 % to 25.3 %. A second increase in temperature to 250 °C (balance 4) increased the (H_2+CO) conversion to 72.2 %. The weight percent of hydrocarbons followed the same trend found at lower temperatures. The methane, C_2–C_4 , and C_5–C_{11} weight % increased with temperature, to 10.3, 75.2, and 32.8 %, while the weight percent of hydrocarbons for the C_{12}+ products decreased to 20 %. The ASF plots for balances 1, 2, and 4 are given in Figures 7–9. Only gaseous products and liquid products collected in the ice trap will appear in these figures, products collected in the high pressure trap were not analyzed. The negative deviations in the C_7–C_{10} range are caused by product loss through evaporation. A negative deviation in the C_2 products appears in Figures 8 and 9, and is probably due to secondary reactions of these products. At 221 °C, positive deviations begin about carbon number 15, and negative deviations at high carbon numbers, caused by collection of products in the high pressure trap, appear at about C_{21}.

The effect of space velocity was studied in balance 3, at 235 °C, 1.48 *MPa*, with a space velocity of 4 *Nl/g*-cat·*h*. The (H_2+CO) conversion decreased relative to balance 2, as expected, to 26 % at the higher flowrate. The weight % of hydrocarbons for methane, C_2–C_4 , and C_5–C_{11}

products decreased at the higher space velocity, with the largest change appearing in the C_5–C_{11} products, 37.3 % at 2 Nl/g-cat·h , compared to 26.9 % at 4 Nl/g-cat·h. The weight % of $C_{12}+$ products increased to 38.3 % (4 Nl/g-cat·h) from 25.3 % (2 Nl/g-cat·h).

Increasing the system pressure to 2.86 MPa (balance 5), with a temperature of 235 °C and a space velocity of 4 Nl/g-cat·h deactivated the catalyst. The (H_2+CO) conversion at these conditions was only 19.5 %. The (H_2+CO) conversion was expected to be comparable to that obtained in balance 2 (54.4 %). The higher pressure decreased the weight % of methane and C_2–C_4 products from 7.80 and 37.3 % at 1.48 MPa to 4.06 and 26.5 % at 2.86 MPa. The weight % of hydrocarbons for the C_5–C_{11} and $C_{12}+$ products increased, from 29.6 and 25.3 % at 1.48 MPa to 36.6 and 32.9 % at 2.86 MPa.

Run FA – 27 – 2457 (100 Fe/2.95 Cu/0.45 K)

Only a single mass balance was performed with this catalyst, at 247 °C, 1.48 MPa, using a space velocity of 2 Nl/g-cat·h. The (H_2+CO) conversion obtained at these conditions was 38.5 %. Decreasing the reactor temperature to 220 °C, a plug developed in the reactor after about 51 h on stream. The pressure differential across the reactor ranged from 100 to 200 *psi*. The plug was removed by increasing the reactor temperature to 235 °C, however the exit flowrates continued to be unstable and the run was terminated after 97 h on stream.

Run FA – 27 – 2557 (100 Fe/2.95 Cu/0.45 K)

Five sets of conditions were used during this run, which was a retest of run FA–27–2457. The results of this run are summarized in Table 13. Following reduction, the reactor was brought to 220 °C, 1.48 MPa, at a space velocity of 2 Nl/g-cat·h. The (H_2+CO) conversion at these conditions was 42.7 %. Increasing the temperature to 235 °C (balance 2) increased the (H_2+CO) conversion to 62.9 %, but the weight % of hydrocarbons was about the same at both sets of conditions. Increasing the temperature further to 250 °C, while still at 1.48 MPa and 2 Nl/g-cat·h, increased the (H_2+CO) conversion to 70.4 %. The weight % of methane and C_2–C_4 products decreased at the higher temperature, 5.80 (methane) and 25.2 % (C_2–C_4) at 235 °C as compared to 4.07 (methane) and 17.8 % (C_2–C_4) at 250 °C. The weight % of the higher products increased from 22.4 (C_5–C_{11}) and 46.6 % (C_{12}+) at 235 °C to 25.9 (C_5–C_{11}) and 52.3 % (C_{12}+) at 250 °C. The ASF plots for balances 2 and 4 appear in Figures 10 and 11. Both balances show the positive deviations beginning at C_16, as seen in previous runs. The balance at 249 °C also has negative deviations: C_2 is low due to reaction of these products, and C_7–C_9 is low due to product loss from evaporation.

An increase in space velocity to 4 *Nl*/*g*-cat·*h* at 235 °C (balance 3) decreased the (H_2+CO) conversion to 35.7 %, as should be expected. The weight fraction of methane and C_2–C_4 products decreased slightly at higher space velocity, dropping 16 % to 4.86 % for methane, and 17 % to 20.9 % for the C_2–C_4 range. The higher products increased correspondingly to 24.7 % (C_5–C_{11}) and 38.3 % (C_{12}+), an increase of 10 and 6 %, respectively, above the hydrocarbon weight percentages obtained at 2 *Nl*/*g*-cat·*h*. In the fifth balance, the pressure was increased to 2.86 *MPa* at 235 °C and 4 *Nl*/*g*-cat·*h*, and the (H_2+CO) conversion was measured at 28.6 %. This is again substantially lower than what would be expected, and shows that the catalyst deactivated at the higher pressure. The higher pressure decreased the weight % of methane by 25 % to 4.36 % and the C_2–C_4 products by 19 % to 20.5 % from the results obtained in balance 3 at lower pressure. The weight % of the C_5–C_{11} products remained virtually the same, while the C_{12}+ products increased by 9.7 % to 51.1 %.

2.3.3. Summary

The most promising catalyst tested has been the 100 Fe/0.95 Cu/0.18 K catalyst (FA–15–2097). The activity (as indicated by space time yield) for this catalyst was superior or comparable to all other catalysts tested at all conditions. The 100 Fe/2.84 Cu/0.18 K (run FB–25–2447), 100 Fe/2.85 Cu/0.44 K (run FA–27–2557), and 100 Fe/1.03 Cu/0.82 K (run FA–17–2367) catalysts also showed promise. These catalysts also proved to be the most stable. The fixed bed testing of catalysts for promoter effect research will be continued during the next quarter. A more detailed comparison of the catalysts tested, with a discussion of the effect of copper and potassium promoter on catalyst activity and selectivity, will be made in future reports.

2.4. Activation/Reduction Procedure Research.

It is generally recognized that the activation/reduction procedure has a significant effect on subsequent catalyst activity, stability, and selectivity. Various reduction procedures have been employed in previous studies of F–T synthesis with precipitated iron catalysts, but very few studies have been undertaken with the objective to investigate the effect of reduction parameters in a systematic manner. A brief review of some of the previous work in this area is given below.

The first systematic study on the effect of reduction conditions on the stability of precipitated iron catalysts was done at the Kaiser–Wilhelm Institute in Germany by Pichler and co-workers (Anderson, 1956, pp. 176–181). They varied the temperature (225–425 °C) and pressure (0.1–15 atm) of activation using carbon monoxide or synthesis gas with $(H_2/CO) = 0.67$. The duration of activation was usually 25 h, and the gas flowrate was 0.4 l/g–Fe·h. The optimum pretreatment conditions were 325 °C and 0.1 atmosphere (absolute), with CO being somewhat better than synthesis gas as a pretreating agent. However, the activation at 1 atm was not greatly inferior.

In the early studies at the U.S. Bureau of Mines, synthesis gas ($(H_2/CO) = 1$, $T = 230$ °C, $GHSV = 100\ h^{-1}$ for 23 h) and H_2 ($T = 300$ °C, $GHSV = 1000\text{–}1500\ h^{-1}$ for 9–18 h) were used for activation at atmospheric pressure. The average activities in these experiments were about the same, but selectivities were markedly different. The catalyst sample activated in synthesis gas yielded more higher molecular weight products than the ones reduced in hydrogen.

Recently, studies were conducted at the U.S. DOE Pittsburgh Energy Technology Center (PETC) on the effect of activation parameters on activity, stability, and selectivity of precipitated iron catalysts in slurry bed reactors. In the studies by Pennline *et al.* (1987) using iron–manganese F–T catalysts, CO, CO followed by H_2 (Kölbel type of activation), and H_2 were employed as reducing agents at 275 or 300 °C, $P = 0$ or 200 *psig*, and $WHSV = 2.25\ h^{-1}$. The activating gas composition had the most dramatic effect, with the catalyst exhibiting no activity after a hydrogen activation. The effect of other activation parameters was rather small.

Zarochak and Anderson (1986) reported results of experiments with CO and $(H_2/CO) = 1.0$ as reducing agents using a precipitated iron catalyst (65 % Fe, 0.6 % Cu, 0.29 % K, by weight, and the balance oxygen). The pretreatment was conducted at 200 *psig*, a weight hourly space velocity of about 1.7, and temperatures of 260 and 280 °C for the synthesis gas and CO pretreatments, respectively. It was found that CO–pretreated catalyst was more active and stable, whereas no major differences were found in selectivities after about 200 *h* on stream. Additional studies on the effect of pretreatment conditions are under way at PETC.

In the present study, CO reduction at atmospheric pressure, 280 °C for 8 *h* and a gas hourly space velocity of 4 Nl/g-Fe·h was chosen as a base case on the basis of findings reported in the literature. Since the number of parameters which effect the catalyst activation is large (*e.g.* reductant type, reductant flowrate, pressure and temperature at reduction conditions, and duration of reduction) a systematic study of all variables is not feasible. Thus, we have decided to keep some parameters constant (reduction at atmospheric pressure and a space velocity of 4.5 Nl/g-Fe·h) and investigate the effect of reductant type (H_2 and CO), reduction temperature (250 and 280 °C), and duration (8 and 24 *h*). After the reduction, the catalyst activity, stability, and selectivity will be determined at a fixed set of process conditions ($T = 250$ °C, $P = 200$ *psig* (1.48 *MPa*), $(H_2/CO) = 1$, and a space velocity of 3.0 Nl/g-Fe·h) up to 120 *h* on stream. In order to minimize transient effects and hot spots, the reactor is brought to reaction conditions gradually following the reduction. First, the fixed bed is cooled to 190 °C in helium at 4.5 Nl/g-Fe·h and the system pressure is increased to 200 *psig*. At this point the synthesis gas feed is introduced and the bed temperature is raised from 190 to 250 °C over a period of about 30 *h*, according to the following schedule:

Table 14 . Time–Temperature Schedule Following Reduction (H_2/CO = 1.0, 3.0 Nl/g-Fe·h , 1.48 MPa).

Temperature (°C)	Duration (h)	Heating Rate
190	1	0
190–200	1	2 °C every 10 min
200	1	0
200–210	1	2 °C every 10 min
210	3	0
210–220	1	2 °C every 10 min
220	3	0
220–230	1	2 °C every 10 min
230	11	0
230–240	1	2 °C every 10 min
240	4	0
240–250	1–3	Slowly to avoid temperature overshoot

We have selected a doubly promoted precipitated iron catalyst with a nominal composition 100 Fe/3.0 Cu/0.2 K (on a weight basis) for these studies. This catalyst has shown good activity and stability (run FB–25–2447) and a sufficient amount is available for both activation/reduction studies and subsequent slurry bed testing.

Run FA – 25 – 2667 (100 Fe/2.93 Cu/0.18 K)

The standard reduction procedure described in Appendix I was used for this run. After 5 h at the desired process conditions (250 °C, 200 *psig*, 2 Nl/g-cat·h, (H_2/CO) = 1.07) the tail gas contraction was 59.8 % and the (H_2+CO) and CO conversions were 84 and 95.3 %, respectively. After about 20 h at these conditions, an electrical power failure occurred and helium purge at atmospheric pressure was introduced to prevent potential damage to the catalyst and solidification of heavy molecular weight products in the reactor and/or exit lines. After the power was resumed and the process conditions reestablished, the (H_2+CO) conversion and tail gas contraction were lower than before the upset and continued to decline with time on stream. For example, one hour after the process conditions were established the (H_2+CO) conversion and tail gas contraction were

68.7 and 49.6 %, respectively, whereas after 42 *h* these values were 54.5 and 38.7 %, respectively. A mass balance was made 20 *h* after the process conditions were reestablished, and the (H_2+CO) conversion was 62.3 %. The weight % hydrocarbon distribution was: methane: 6.8; C_2–C_4 : 26.9; C_5–C_{11} 30.1; and C_{12}+ : 36.2 %. This run was discontinued after 60 *h* at the process conditions (including the period before the power failure) due to relatively rapid catalyst deactivation, which may be attributed to the temporary disruption caused by the power failure. We plan to make one more run using the same reduction procedure early next month. Other activation/reduction procedures will be studied during the next quarter.

2.5. Catalyst Preparation and Characterization.

During the current reporting period, we have completed the elemental analyses of all of the precipitated, unsupported iron catalysts that will be investigated during this project. We have also continued our catalyst characterization experiments, including surface area and pore size distribution measurements, temperature–programmed and isothermal reduction studies, and spectroscopic examination of adsorbed probe molecules aimed at elucidating the chemical nature of surface iron species on these catalysts. The following sections contain detailed presentations of research progress in each of these areas.

2.5.1. Catalyst Synthesis and Drying Procedure.

For reference purposes, a complete description of the procedure employed for the synthesis and drying of the precipitated iron catalysts, as contained in a previous report, is provided in Appendix II.

2.5.2. Catalyst Elemental Analyses.

Each of the 24 catalysts, whose syntheses have been described in previous reports, was separately analyzed for iron, copper, and potassium contents by atomic absorption spectroscopy. All samples were prepared for analysis by calcination in air for 15 *h* at 300 °C, followed by dissolution in hot HCl; the results are summarized in Table 15. Values for copper and potassium levels in each catalyst are reported in parts by weight of the metal relative to 100 parts by weight of iron. It is apparent that, with only a few exceptions, the analyzed copper and potassium contents of all catalysts are acceptably close to the nominal values that have heretofore been assumed. Most copper analyses are only slightly lower than predicted, indicating that the deleterious effect of increasing pH on copper precipitation described in a previous report was correctly assessed. The precipitation pH of 6.0 ± 0.2 employed in all catalyst syntheses effects virtually quantitative precipitation of $Cu(OH)_2$, with minimal formation of the complex ion $Cu(NH_3)_4^{2+}$ that leads to incomplete precipitation. Most potassium analyses are, in general, also somewhat lower than predicted, probably due to slight retention of the $KHCO_3$ solution on the walls of the impregnation vessel.

2.5.3. Physical Characterization of Catalysts.

Surface Areas

Surface areas have been measured by physical adsorption of N_2 at -196 °C for each of the seven precipitated materials containing differing copper contents, as well as for selected additional catalysts following impregnation with $KHCO_3$. Results are shown in Table 16. The unreduced materials were treated in a vacuum oven for 16 h at 120 °C prior to adsorption measurements, while the reduced samples were exposed to flowing H_2 for 4 h at 300 °C and $GHSV = 3500$ hr^{-1}. As reported previously, the surface area of the unreduced, unpromoted iron precipitate is 180 m^2/g; impregnation with varying levels of $KHCO_3$ causes a slight increase in surface area to 200–210 m^2/g. The presence of copper promoter in the unreduced precipitate, however, results in a substantially higher surface area (280–380 m^2/g) than that of the copper–free material. The effect is manifested, moreover, at copper levels as low as 0.1 part; only the catalyst containing 1.0 part Cu had a surface area (230 m^2/g) that appeared anomalously low. Calcination in air for 16 h at 300 °C decreased the surface area of most samples to 60 m^2/g. However, following reduction treatment in H_2 at 300 °C, the surface areas of all catalysts decreased markedly to 5–10 m^2/g, regardless of copper content. As discussed in a previous report, the absence of a support or binder leads to collapse of the precipitates' pore structures upon thermal treatment.

Pore Size Distributions

As discussed in a previous report, the pore size distribution of the unpromoted, unreduced iron precipitate is very narrow, and exhibits an average pore diameter of 40–45 Å, as determined by application of the Kelvin equation to the desorption branch of a N_2 adsorption isotherm obtained at – 196 °C. Thermal treatment, *i.e.*, calcination and/or reduction, leads to collapse of the micropore structure, as described above, and results in a much broader pore size distribution with larger average pore openings. Since the adsorption method is not accurately applicable for large (*i.e.*, > 100 Å) pores, the technique of mercury porosimetry has been employed to obtain further information about the pore size distributions of calcined/reduced catalysts. The instrument used for these measurements has an upper pressure limit of 30,000 *psig*, corresponding to a minimum observable pore diameter of 60 Å. Prior to porosimetry measurements, all catalysts were calcined for 4 *h* at 300 °C, and then reduced in H_2 for 4 *h* at the same temperature.

The differential pore volume curve shown in Figure 12 for the calcined. but unreduced, precipitate confirms that calcination causes the average pore diameter to increase from the value of 40–45 Å reported previously for the uncalcined material to 90 Å. Subsequent reduction leads to further change in the curve (Figure 13) and generates a bimodal pore size distribution, with the principal maximum at 250 Å pore diameter and a secondary maximum at 90 Å. Similar bimodal distributions were observed for the reduced precipitates containing 0.1 and 0.3 parts copper, as shown in Figures 14 and 15, respectively; the presence of even these low copper levels, however, results in a principal maxima (400 Å) in both cases that is higher than that of the unpromoted precipitate. Porosimetry measurements of the pore size distributions for the remaining copper–promoted catalysts will be completed during the next quarter.

2.5.4. Chemical Characterization of Catalysts.

Reduction Studies

As discussed in previous reports, temperature–programmed reduction (TPR) studies of pure and singly– (copper– or potassium–) promoted iron catalysts indicate that reduction of precipitated $FeOOH/Fe_2O_3$ in H_2 or CO occurs in two stages, the first leading to Fe_3O_4 formation and the second to metallic Fe. Increasing amounts of copper promoter, up to 3 %, facilitate both reduction steps. Potassium promoter, on the other hand, has little effect on the first reduction step, and broadens the TPR peak corresponding to the second step. During the past quarter, we have extended application of the TPR technique to certain of the doubly–promoted iron catalysts that have been synthesized for catalytic testing. As in previous studies, all TPR experiments were performed using 10 *mg* catalyst samples, a 12 cm^3/min flow rate of H_2/N_2 reductant, and a temperature program rate of 20 °C/*min*.

Figures 16 and 17 illustrate the effect of increasing levels of copper promoter on the TPR profiles of uncalcined samples, having two different potassium contents (0.05 and 0.2 parts, respectively). It is clear that, at both levels of potassium, copper displays the essentially the same promotional effect on iron reduction as has been reported previously for potassium–free catalysts. In both figures, the lowest temperature peak that occurs at 300 °C is due to reduction of both residual $Fe(NO_3)_3$ and $Cu(OH)_2/CuO$ promoter, while the peak that shifts from 370 to 300 °C with increasing copper level corresponds to reduction of Fe_2O_3 to Fe_3O_4. The origin of the third peak that occurs at 325 °C in both figures only for the catalysts containing 0.3 part copper is unclear. The presence of such a peak may indicate that a copper level of only 0.3 part is insufficient to facilitate intimate contact with all of the iron, leading to both copper–promoted and unpromoted iron reduction. The effect of increased potassium promoter is similar to that reported previously for copper–free catalysts, *viz.*, to broaden and intensify the peak due to the second reduction step, in which Fe_3O_4 is transformed into metallic iron. Increasing the potassium content further to 0.5 part, at a constant copper level of 3 parts, had little additional effect over that of the catalyst containing 0.2 part K, as shown in Figure 18.

In the case of samples that had been pre–calcined in air for 16 *h* at 300 °C prior to TPR measurements, the low–temperature peak due to $Fe(NO_3)_3$ reduction is absent (Figures 19 and 20), as had been observed previously for unpromoted and for singly–promoted catalysts. As was the case for the uncalcined materials, two low–temperature peaks were evident at both potassium contents (0.05 and 0.2 part) for the catalysts containing only 0.3 part copper promoter. This result suggests again that reduction of Fe_2O_3 to Fe_3O_4 may occur both with and without copper promotion at sufficiently low copper levels.

In a previous report in this series, it has been stressed that the temperatures at which reduction peak maxima occur in TPR profiles are of comparative, rather than absolute importance due to the thermally dynamic nature of the technique. The location of peaks is a sensitive function of several experimental parameters, particularly the rate of temperature programming; increases in the latter lead inevitably to corresponding increases in the temperatures of reduction peak maxima. In order to gain further insight into the nature of the reduction process for precipitated iron materials, and to more closely approximate conditions used during actual catalyst pretreatment, we have begun to employ the TPR experimental apparatus to study reduction under isothermal conditions. In all cases, catalyst samples were programmed at 20 $°C/min$ from ambient temperature to 300 °C and then maintained at the latter temperature, while continuously monitoring the rate of uptake of H_2 or CO reductant by thermal conductivity measurement.

The data in Figure 21 demonstrate that the promotional effect of increasing levels of copper on the rate of both steps of iron reduction, which were observed in TPR experiments, is also evident under isothermal conditions. In the absence of copper, reduction of $FeOOH/Fe_2O_3$ in H_2 is incomplete, even after 16 *h* at 300 °C. However, the presence of only 0.3 part Cu results in virtually complete reduction after less than 10 *h* at 300 °C, while 3 parts Cu effects complete reduction in less than 7 *h* under these conditions. By contrast, although the presence of 0.2 part potassium has little effect on reduction behavior, the effect of 1 and 2 parts K, in the absence of Cu, actually inhibits the rate of reduction of Fe_3O_4, as shown in Figure 22. Isothermal H_2 reduction behaviors of two doubly-promoted catalysts are presented in Figure 23. As in the cases of copper-free catalysts, the presence of 0.2 part K has little effect on the reduction behavior. The profiles shown are quite similar to the corresponding curves in Figure 21 for potassium-free samples.

We have also begun to investigate isothermal reduction behaviors using CO reductant at 300 °C; results for selected catalyst compositions are provided in Figure 24. It is apparent that, in all cases, both steps of iron reduction occur more rapidly in CO than in H_2. (Note the difference in abscissa scale between Figure 24 and Figures 21-23). The promotional effect of copper and the inhibiting effect of excessive ($>$ 0.5 part) potassium is again evident, as was observed with H_2 reductant. It is noteworthy that reduction in CO of the 100 Fe/1 Cu/0.2 K catalyst shown in Figure 24 is essentially complete after only 1 *h* of treatment.

Spectroscopic Studies

We have continued to apply Fourier Transform Infrared Spectrophotometry (FT-IR) in an attempt to obtain further information about the chemical nature of surface iron species on the precipitated catalysts. Because of the relatively weak binding and low coverage of CO adsorption on iron under ambient conditions, we have focused on the use of nitric oxide (NO) as a probe molecule for these investigations. NO adsorbs on both oxidized and reduced forms of Fe, producing several types of surface species that are spectroscopically distinguishable. In order to obtain adequate transmittance to observe spectral evidence for NO adsorption, the strongly adsorbing precipitated catalysts were studied by evaporative deposition of a thin film of finely powdered sample onto a BaF_2 crystal from an acetone slurry. For comparison purposes, silica-supported samples containing 25 wt % of Fe were prepared by incipient wetness impregnation from aqueous solutions of $Fe(NO_3)_3$.

In a previous report, FT-IR spectra for NO adsorption on a calcined, unpromoted iron catalyst diluted (not supported) with silica gave rise to two principal adsorption bands due to the N–O stretching vibration of mononitrosyls, at 1805 and 1710 cm^{-1}, suggesting the presence of at least two types of oxidized Fe adsorption sites. By contrast, the calcined (in O_2 for 1 h at 230 °C), undiluted precipitate when deposited on the BaF_2 crystal produced bands at 1775 and 1720 cm^{-1}, as shown in Figure 25. This difference in frequencies between the two samples may be caused by differing extents of surface iron coordination to oxide species in the calcined precipitate. Other investigators have reported previously that NO adsorbed on sites of high oxygen coordination produces N–O stretching bands having higher frequencies than does NO adsorbed on low coordination sites (Rethwisch and Dumesic, 1986; Yeun *et al.*, 1982). Following subsequent reduction in H_2 at 500 °C, the silica–diluted sample produced bands at 1810 and 1740 cm^{-1} upon exposure to NO. The latter band is due to NO adsorption on a reduced, metallic Fe site, but the continued presence of a band at 1810 cm^{-1} is evidence for oxidized Fe sites and indicates that reduction is incomplete under the conditions employed.

Much greater transmittance and, hence, more intense and reliable spectra were obtained for the silica–supported samples than for the precipitated materials. Exposure to gaseous NO of a 25 wt % Fe/SiO_2 that had been calcined in O_2 for 1 h at 500 °C produced an intense band at 1815 cm^{-1} and a weaker band at 1765 cm^{-1}, both due to mononitrosyl species adsorbed on oxidized Fe sites (Figure 26). The latter band becomes better resolved after cryogenic removal of residual gaseous NO. In addition, a weak band occurs at 1905 cm^{-1} that is probably one of a pair of bands (the other is masked by the intense band at 1815 cm^{-1}) due to a dinitrosyl species. (Additional broad spectral features are observed at > 2000 cm^{-1} and at < 1600 cm^{-1}, whose origins have not yet been elucidated. These features disappear after removal of gas–phase NO.) By way of comparison, exposure to gaseous NO of a calcined 25 wt % Fe/SiO_2 sample containing 1 wt % K_2O produced only a single band at 1785 cm^{-1}, due to mononitrosyl formation, that was, moreover, an order of magnitude less intense than the bands observed with the unpromoted supported catalyst

(Figure 27). Bands due to a dinitrosyl species were never observed with the potassium-containing samples. It is clear that the presence of potassium promoter inhibits adsorption of NO on the calcined catalyst.

Figures 28 and 29 show corresponding spectra for NO adsorption on unpromoted and potassium promoted supported catalysts that had been reduced by exposure to excess H_2 for 1 *h* at 500 °C. In both cases, an intense band at 1735 cm^{-1} is observed that may be ascribed to the N–O stretching vibration of a mononitrosyl adsorbed on a reduced, metallic Fe site. However, the continued presence of a strong band at 1815 cm^{-1} indicates that iron reduction is incomplete, even after treatment in H_2 at 500 °C.

TASK 3 – Process Evaluation Research

No work on this task was scheduled during this quarter.

TASK 4 - Economic Evaluation

No work on this task was scheduled during this quarter.

V. LITERATURE REFERENCES

Anderson, R. B., "Catalysts for the Fischer-Tropsch Synthesis," in *Catalysis*, P. H. Emmet, Ed., Reinhold, New York, 4, 29 (1956).

Anderson, R. B., *The Fischer-Tropsch Synthesis*, Academic Press, Orlando, Florida (1984).

Huff, G. A., Jr., and C. N. Satterfield, *J. Catal.*, **80**, 370 (1984).

Kuo, J. C. W., "Two Stage Process for Conversion of Synthesis Gas to High Quality Transportation Fuels," Final Report, Contract No. DE-AC22-83PC60019 (1985).

Pennline, H. W., Zarochak, M. F., Stencel, J. M., and Diehl, J. R., *Ind. Eng. Chem. Res.*, **26**, 595 (1987).

Rethwisch, D. G., and Dumesic, J. A., *J. Phys. Chem.*, **90**, 1625 (1986).

Satterfield, C. N., Huff, G. A., Jr., Stenger, H. G., Carter, J. L., and Madon, R. J., *Ind. Eng. Chem. Fundam.*, **24**, 450 (1985).

Yeun, S., Chen, Y., Kubsh, J. E. and Dumesic, J. A., *J. Phys. Chem.*, **86**, 3022 (1982).

Zarochak, M. F., and McDonald, M. A., "Slurry-Phase Fischer-Tropsch Synthesis," Proc. of the DOE Contractors Conference on Indirect Liquefaction, December 2-4, Pittsburgh, Pennsylvania, 58 (1986).

Table 1. Response factors of *n*–paraffins in wax analysis.

Component	Response Factor
n–$C_{16}H_{34}$	0.92±0.05
n–$C_{20}H_{42}$	0.99±0.04
n–$C_{24}H_{50}$	0.99±0.03
n–$C_{28}H_{58}$	1.00±0.03
n–$C_{36}H_{74}$	1.03±0.05
n–$C_{40}H_{82}$	1.07±0.09

Chromatograph: Sigma 1
Column: RSL–150 fused silica
Detector: FID
Sample dilution: 200 to 400:1
Sample size: 1.5 – 2.0 μl

Table 2. Catalyst codes for run numbers.

Wt % Composition			
Fe	Cu	K	Code
	UCI C–73 Fused		01
100	0.0	0.00	00
100	0.0	0.01	41
100	0.0	0.02	42
100	0.0	0.05	43
100	0.0	0.10	44
100	0.0	0.20	45
100	0.0	0.50	46
100	0.0	1.00	47
100	0.0	2.00	48
100	0.1	0.00	31
100	0.3	0.00	32
100	0.3	0.05	03
100	0.3	0.20	05
100	0.3	0.50	07
100	1.0	0.00	33
100	1.0	0.05	13
100	1.0	0.20	15
100	1.0	0.50	17
100	3.0	0.00	34
100	3.0	0.05	23
100	3.0	0.20	25
100	3.0	0.50	27
100	10.	0.00	35
100	20.	0.00	36

Table 3. Summary of results for fixed bed run FA-01-1807.

Catalyst: 5.70[a] *g*, United Catalyst, Inc. C-73 fused iron (170/230 mesh)
Catalyst Volume: 2.50 *cc*

Diluent: 14.0 *g*, Glass Beads (170/230 mesh)
Diluent Volume: 10.0 *cc*

Period	1	2	FB-01-1547-1
Date	7/1/87	7/3/87	6/4/87
Time on Stream (h)	6.0	72.5	18.0
Balance Duration (h)	6.0	7.0	6.0
Average Temperature (°C)	234	235	234
Maximum Δ Temperature (°C)[b]	1.7	1.4	4.0
Pressure (MPa)	0.79	1.48	0.83
H_2/CO Feed Ratio	1.05	1.05	0.97
Space Velocity (Nl/g-cat·h)[a]	1.52	2.01	1.51
Space Velocity (Nl/g-Fe·h)[a]	2.27	3.00	2.25
GHSV (h^{-1})[c]	3471	4584	3924
Weight Closure (%)	99.7	97.7	93.2
CO Conversion (%)	24.1	20.1	35.9
H_2+CO Conversion (%)	22.8	19.1	29.9
H_2/CO Usage	0.93	0.95	0.64
STY (*mols* H_2+CO/g-cat·h)[a]	0.015	0.017	0.020
$P_{CO_2} \cdot P_{H_2} / P_{CO} \cdot P_{H_2O}$	2.72	1.40	5.70
Weight % of Outlet			
H_2	5.53	5.88	5.35
H_2O	2.07	3.14	1.78
CO	70.8	76.0	64.3
CO_2	12.7	9.98	21.5
Hydrocarbons	8.02	4.06	5.94
Oxygenates	0.76	0.76	0.63
Wax[d]	0.18	0.14	0.44
Yield (g/Nm^3 H_2+CO Converted)			
CH_4	7.42	8.05	12.8
C_2-C_4 Hydrocarbons	45.9	51.6	51.6
C_5-C_{11} Hydrocarbons	115	58.0	53.7
C_{12}+ Hydrocarbons	67.0	33.6	7.31
Oxygenates	21.7	25.5	16.7
Wax[d]	5.07	4.77	9.33
Total	257	166	148

[a] Based on unreduced catalyst

[c] Based on catalyst volume

[b] Maximum axial temperature difference

[d] Unanalyzed products collected from hot trap

Table 3 (cont'd). Summary of results for fixed bed run FA-01-1807.

Period	1	2	FB-01-1547-1
Weight % of Hydrocarbons			
CH_4	3.51	5.71	9.51
Ethane	2.09	5.09	2.44
Ethylene	4.85	7.99	9.57
Propane	1.15	2.50	2.14
Propylene	5.66	10.1	11.8
n-Butane	1.02	2.18	2.15
1+2 Butenes	4.64	8.54	9.16
C_4 Isomers	0.09	0.21	1.03
n-Pentane	1.23	2.52	1.82
1+2 Pentenes	3.37	6.29	8.07
C_5 Isomers	0.41	0.95	0.78
n-Hexane	0.70	1.69	0.02
1+2 Hexenes	10.7	5.11	7.55
C_6 Isomers	2.16	1.13	1.38
n–Heptane	0.17	1.29	0.04
1+2 Heptenes	9.38	2.85	4.65
C_7 Isomers	0.99	0.70	0.77
n–Octane	0.20	0.81	0.30
1+2 Octenes	6.80	1.78	2.81
C_8 Isomers	1.65	0.61	0.35
n–Nonane	0.62	0.99	0.67
1+2 Nonenes	1.44	2.10	2.20
C_9 Isomers	0.08	0.10	0.05
n–Decane	1.01	1.54	0.79
1+2 Decenes	2.55	3.66	2.70
C_{10} Isomers	0.50	0.44	0.19
n–Undecane	1.03	1.40	0.68
1+2 Undecenes	3.01	4.16	2.50
C_{11} Isomers	0.88	1.04	0.50
C_2^e+	94.7	90.9	83.6
C_2–C_4	19.5	36.6	38.3
C_5–C_{11}	48.9	41.2	39.8
$C_{12}+$	28.5	16.5	12.4
Wax[d]	2.15	3.38	6.92

[d] Unanalyzed products collected in hot trap

[e] Does not include wax

Table 4. Summary of results for fixed bed run FA-15-1947.

Catalyst: 5.10^a g, 100 Fe/0.95 Cu/0.18 K (Uncalcined 60/100 mesh)
Catalyst Volume: 4.1 cc

Diluent: 25.6 g, Glass Beads(60/100 mesh)
Diluent Volume: 16.4 cc

Period	1	2	3
Date	7/13/87	7/15/87	7/16/87
Time on Stream (h)	25.0	72.0	97.0
Balance Duration (h)	6.0	6.0	6.0
Average Temperature (°C)	225	222	236
Maximum Δ Temperature (°C)^b	24.5	5.0	1.6
Pressure (MPa)	1.48	1.48	1.48
H_2/CO Feed Ratio	1.00	1.00	1.00
Space Velocity (Nl/g-cat$\cdot h$)^a	1.86	1.87	1.87
Space Velocity (Nl/g-Fe$\cdot h$)^a	2.99	3.00	3.00
GHSV (h^{-1})^c	2312	2320	2320
Weight Closure (%)	90.0	93.9	99.7
CO Conversion (%)	91.6	27.1	35.9
H_2+CO Conversion (%)	78.0	25.3	34.8
H_2/CO Usage	0.71	0.87	0.95
STY ($mols$ H_2+CO/g-cat$\cdot h$)^a	0.065	0.021	0.029
$P_{CO_2} \cdot P_{H_2} / P_{CO} \cdot P_{H_2O}$	13.9	1.3	1.7
Weight % of Outlet			
H_2	2.66	5.49	4.48
H_2O	7.35	4.03	5.18
CO	8.67	72.5	60.0
CO_2	58.8	12.1	21.2
Hydrocarbons	19.9	2.86	4.97
Oxygenates	0.91	0.28	0.29
Wax^d	1.74	2.74	3.86
Yield (g/Nm^3 H_2+CO Converted)			
CH_4	25.3	3.88	6.43
C_2–C_4 Hydrocarbons	64.6	31.6	39.1
C_5–C_{11} Hydrocarbons	55.0	27.3	41.3
C_{12}+ Hydrocarbons	22.1	76.2	82.0
Oxygenates	7.01	7.03	5.55
Wax^d	13.5	68.0	73.9
Total	174	146	175

[a] Based on unreduced catalyst
[c] Based on catalyst volume

[b] Maximum axial temperature difference
[d] Unanalyzed products collected from hot trap

Table 4 (cont'd). Summary of results for fixed bed run FA-15-1947.

Period	1	2	3
Weight % of Hydrocarbons			
CH_4	15.1	2.80	3.80
Ethane	7.70	3.14	2.75
Ethylene	2.53	5.44	4.38
Propane	4.13	1.42	1.39
Propylene	11.2	5.88	6.89
n-Butane	2.75	1.30	1.30
1+2 Butenes	9.29	2.91	3.34
C_4 Isomers	1.09	2.62	3.05
n Pentane	2.82	1.57	1.60
1+2 Pentenes	6.00	5.44	4.83
C_5 Isomers	2.03	1.23	0.65
n-Hexane	1.70	0.04	1.35
1+2 Hexenes	4.74	0.16	2.72
C_6 Isomers	0.79	0.01	3.31
n-Heptane	1.37	0.12	0.45
1+2 Heptenes	2.77	0.44	2.04
C_7 Isomers	0.55	0.03	0.36
n-Octane	1.11	0.52	0.93
1+2 Octenes	2.27	1.33	2.40
C_8 Isomers	0.43	0.12	0.13
n-Nonane	0.86	0.98	0.39
1+2 Nonenes	1.39	1.93	0.80
C_9 Isomers	0.29	0.22	0.20
n Decane	0.72	0.99	0.38
1+2 Decenes	1.10	1.80	0.68
C_{10} Isomers	0.31	0.25	0.20
n-Undecane	0.61	0.83	0.34
1+2 Undecenes	0.80	1.39	0.54
C_{11} Isomers	0.30	0.23	0.16
C_2^e+	76.8	48.2	52.5
C_2-C_4	38.7	22.7	23.1
C_5-C_{11}	33.0	19.6	24.5
$C_{12}+$	13.2	54.9	48.7
Wax[d]	8.05	49.0	43.7

[d] Unanalyzed products collected in hot trap

[e] Does not include wax

Table 5. Summary of fixed bed tests and testing conditions for precipitated iron catalysts.

Run[1]	220 °C 1.48 MPa 2 Nl/g–cat·h	235 °C 1.48 MPa 2 Nl/g–cat·h	235 °C 1.48 MPa 4 Nl/g–cat·h	235 °C 1.48 MPa	250 °C 1.48 MPa 2 Nl/g–cat·h	235 °C 2.86 MPa 4 Nl/g–cat·h
FB-05-2287 100 Fe/0.28 Cu/0.19 K	*	*	*			
FB-07-2657 100 Fe/0.28 Cu/0.48 K	*	*				
FA-33-2287 100 Fe/1.04 Cu/0.0 K	*	*				
FA-13-2217 100 Fe/0.94 Cu/0.05 K	*	*				
FA-15-2097 100 Fe/0.96 Cu/0.18 K	*	*	*	5.5 Nl/g–cat·h	*	*
FA-17-2367 100 Fe/1.05 Cu/0.83 K	*	*	*	1.4 Nl/g–cat·h	*	
FB-25-2447 100 Fe/2.93 Cu/0.18 K	*	*	*		*	*
FA-27-2457 100 Fe/2.95 Cu/0.45 K					*	
FB-27-2557 100 Fe/2.95 Cu/0.45 K	*	*	*		*	*

[1] Nominal values of process conditions listed

* indicates balance performed at conditions shown

Table 6. Summary of results for fixed bed run FB-05-2287.

Catalyst: 4.03[a] *g*, 100 Fe/0.28 Cu/0.19 K (30/60 mesh)
Catalyst volume: 3.00 *cc*

Diluent: 38.3 *g*, Glass Beads (30/60 mesh)
Diluent volume: 26.0 *cc*

Period	1	2	3
Date	8/17/87	8/19/87	8/20/87
Time on Stream (h)	48.0	96.0	120.5
Balance Duration (h)	6.0	6.0	6.0
Average Temperature ($^\circ$C)	220	235	234
Maximum Δ Temperature ($^\circ$C)[b]	10.0	20.0	13.0
Pressure (MPa)	1.48	1.48	1.48
H_2/CO Feed Ratio	1.07	1.07	1.07
Space Velocity (Nl/g-cat$\cdot h$)[a]	2.08	2.08	4.17
Space Velocity (Nl/g-Fe$\cdot h$)[a]	2.99	2.99	5.99
GHSV (h^{-1})[c]	2800	2800	5600
Weight Closure (%)	98.9	94.1	97.5
CO Conversion (%)	46.7	74.0	30.8
H_2+CO Conversion (%)	43.4	64.7	27.6
H_2/CO Usage	0.93	0.81	0.85
STY (*mols* H_2+CO/g-cat$\cdot h$)[a]	0.040	0.060	0.051
$P_{CO_2} \cdot P_{H_2} / P_{CO} \cdot P_{H_2O}$	1.9	1.1	2.5
Weight % of Outlet			
H_2	4.32	3.34	5.55
H_2O	6.78	6.65	3.53
CO	50.1	25.6	65.9
CO_2	26.9	47.6	18.5
Hydrocarbons	7.44	16.3	5.06
Oxygenates	0.69	0.41	0.23
Wax[d]	3.85	0.03	1.22
Yield (g/Nm^3 H_2+CO Converted)			
CH_4	12.3	13.0	12.6
C_2–C_4 Hydrocarbons	53.9	50.2	54.0
C_5–C_{11} Hydrocarbons	41.6	31.6	45.1
C_{12}+ Hydrocarbons	59.1	64.4	32.5
Oxygenates	10.1	3.88	5.21
Wax[d]	57.0	0.31	27.9
Total	177	159	149

[a] Based on unreduced catalyst
[c] Based on catalyst volume

[b] Maximum axial temperature difference
[d] Unanalyzed products collected from hot trap

Table 6 (cont'd). Summary of results for fixed bed run FB-05-2287.

Period	1	2	3
Weight % of Hydrocarbons			
CH_4	7.38	7.95	8.72
Ethane	5.28	3.85	6.96
Ethylene	5.51	4.08	7.03
Propane	1.73	1.82	1.95
Propylene	9.55	9.93	10.3
n Butane	1.60	1.63	1.77
1+2 Butenes	7.82	8.23	8.60
C_4 Isomers	0.80	0.84	0.88
n-Pentane	2.04	2.03	2.26
1+2 Pentenes	6.50	6.72	7.27
C_5 Isomers	0.55	0.69	0.65
n-Hexane	1.57	1.17	1.70
1+2 Hexenes	3.90	3.74	6.33
C_6 Isomers	1.37	0.84	1.40
n-Heptane	0.87	0.67	1.06
1+2 Heptenes	2.15	1.94	4.01
C_7 Isomers	0.66	0.53	0.94
n-Octane	0.49	0.26	0.57
1+2 Octenes	1.17	0.0	2.12
C_8 Isomers	0.35	0.0	0.52
n-Nonane	0.25	0.0	0.14
1+2 Nonenes	0.83	0.0	0.41
C_9 Isomers	0.06	0.0	0.07
n-Decane	0.29	0.26	0.19
1+2 Decenes	0.87	0.0	0.57
C_{10} Isomers	0.10	0.0	0.12
n-Undecane	0.22	0.01	0.21
1+2 Undecenes	0.61	0.14	0.59
C_{11} Isomers	0.07	0.0	0.14
C_2+[e]	58.5	92.2	71.9
C_2–C_4	32.3	30.4	37.5
C_5–C_{11}	24.9	20.2	31.3
$C_{12}+$	35.4	52.5	22.6
Wax[d]	34.1	0.20	19.4

[d] Unanalyzed products collected in hot trap

[e] Does not include wax

Table 7. Summary of results for fixed bed run FB-07-2657.

Catalyst: 4.01[a]g, 100 Fe/0.28 Cu/0.48 K (30/60 mesh)
Catalyst volume: 3.40 cc

Diluent: 38.5 g, Glass Beads (30/60 mesh)
Diluent volume: 25.0 cc

Period	1	2
Date	9/24/87	9/26/87
Time on Stream (h)	46.0	93.5
Balance Duration (h)	6.0	6.0
Average Temperature ($^\circ$C)	220	235
Maximum Δ Temperature ($^\circ$C)[b]	4.0	4.0
Pressure (MPa)	1.38	1.38
H_2/CO Feed Ratio	1.07	1.07
Space Velocity (Nl/g-cat$\cdot h$)[a]	2.09	2.09
Space Velocity (Nl/g-Fe$\cdot h$)[a]	3.01	3.01
GHSV (h^{-1})[c]	2471	2471
Weight Closure (%)	94.3	100.4
CO Conversion (%)	40.1	50.6
H_2+CO Conversion (%)	39.9	43.3
H_2/CO Usage	1.07	0.78
STY ($mols$ H_2+CO/g-cat$\cdot h$)[a]	0.037	0.040
$P_{CO_2} \cdot P_{H_2} / P_{CO} \cdot P_{H_2O}$	2.32	2.49
Weight % of Outlet		
H_2	4.57	4.55
H_2O	4.21	7.12
CO	59.0	45.7
CO_2	22.2	31.2
Hydrocarbons	6.02	6.43
Oxygenates	0.45	0.65
Wax[d]	3.56	4.36
Yield (g/Nm^3 H_2+CO Converted)		
CH_4	6.25	7.60
C_2–C_4 Hydrocarbons	34.9	37.6
C_5–C_{11} Hydrocarbons	44.4	37.5
C_{12}+ Hydrocarbons	61.3	79.3
Oxygenates	6.87	9.70
Wax[d]	54.5	65.4
Total	154	172

[a] Based on unreduced catalyst

[b] Maximum axial temperature difference

[c] Based on catalyst volume

[d] Unanalyzed products collected from hot trap

Table 7 (cont'd). Summary of results for fixed bed run FB-07-2657.

Period	1	2
Weight % of Hydrocarbons		
CH_4	4.26	4.69
Ethane	3.03	2.26
Ethylene	5.58	5.25
Propane	1.28	1.23
Propylene	6.53	7.13
n–Butane	1.27	1.12
1+2 Butenes	5.42	5.58
C_4 Isomers	0.64	0.65
n–Pentane	1.69	1.56
1+2 Pentenes	6.32	4.98
C_5 Isomers	0.73	0.40
n–Hexane	1.47	1.24
1+2 Hexenes	2.83	2.94
C_6 Isomers	1.31	0.78
n–Heptane	0.94	0.76
1+2 Heptenes	1.94	2.32
C_7 Isomers	1.58	0.33
n–Octane	0.54	0.36
1+2 Octenes	1.40	1.11
C_8 Isomers	0.26	0.19
n–Nonane	0.45	0.24
1+2 Nonenes	1.60	1.22
C_9 Isomers	0.37	0.09
n–Decane	0.70	0.40
1+2 Decenes	1.59	1.65
C_{10} Isomers	1.26	0.21
n–Undecane	0.68	0.44
1+2 Undecenes	2.01	1.66
C_{11} Isomers	0.59	0.25
C_2+^e	58.1	54.9
C_2–C_4	23.7	23.2
C_5–C_{11}	30.3	23.1
$C_{12}+$	41.7	49.0
Wax[d]	37.1	40.4

[d] Unanalyzed products collected in hot trap

[e] Does not include wax

Table 8. Summary of results for fixed bed run FA-33-2287.

Catalyst: 4.03[a] *g*, 100 Fe/1.04 Cu/0.0 K (30/60 mesh)
Catalyst volume: 3.80 *cc*

Diluent: 40.4 *g*, Glass Beads (30/60 mesh)
Diluent volume: 27.0 *cc*

Period	1	2
Date	8/17/87	8/18/87
Time on Stream (h)	48.5	73.0
Balance Duration (h)	6.0	6.0
Average Temperature (°C)	221	235
Maximum Δ Temperature (°C)[b]	4.7	4.8
Pressure (MPa)	1.48	1.48
H_2/CO Feed Ratio	1.07	1.07
Space Velocity (Nl/g-cat$\cdot h$)[a]	2.09	2.09
Space Velocity (Nl/g-Fe$\cdot h$)[a]	3.01	3.01
GHSV (h^{-1})[c]	2215	2215
Weight Closure (%)	94.7	101.5
CO Conversion (%)	31.6	41.6
H_2+CO Conversion (%)	37.1	45.5
H_2/CO Usage	1.43	1.27
STY (*mols* H_2+CO/g-cat$\cdot h$)[a]	0.035	0.042
$P_{CO_2} \cdot P_{H_2} / P_{CO} \cdot P_{H_2O}$	0.50	0.50
Weight % of Outlet		
H_2	4.37	3.60
H_2O	8.02	12.5
CO	67.0	53.4
CO_2	10.9	17.4
Hydrocarbons	8.20	12.1
Oxygenates	0.53	0.96
Wax[d]	1.01	0.03
Yield (g/Nm^3 H_2+CO Converted)		
CH_4	16.7	16.8
C_2–C_4 Hydrocarbons	65.9	62.3
C_5–C_{11} Hydrocarbons	48.0	47.0
C_{12}+ Hydrocarbons	22.2	49.4
Oxygenates	8.81	13.9
Wax[d]	16.8	0.44
Total	162	189

[a] Based on unreduced catalyst
[c] Based on catalyst volume
[b] Maximum axial temperature difference
[d] Unanalyzed products collected from hot trap

Table 8 (cont'd). Summary of results for fixed bed run FA-33-2287.

Period	1	2
Weight % of Hydrocarbons		
CH_4	10.9	9.56
Ethane	8.40	6.25
Ethylene	4.72	3.62
Propane	3.20	2.77
Propylene	12.4	10.5
n Butane	2.76	2.31
1+2 Butenes	10.5	9.01
C_4 Isomers	1.17	1.05
n–Pentane	3.27	2.72
1+2 Pentenes	7.95	6.52
C_5 Isomers	1.25	1.30
n-Hexane	2.06	1.78
1+2 Hexenes	4.88	3.65
C_6 Isomers	1.08	1.04
n–Heptane	1.02	0.90
1+2 Heptenes	2.42	1.95
C_7 Isomers	0.70	0.79
n–Octane	0.71	0.51
1+2 Octenes	1.20	0.94
C_8 Isomers	0.28	0.30
n–Nonane	0.51	0.31
1+2 Nonenes	0.89	0.39
C_9 Isomers	0.11	0.04
n–Decane	0.59	0.64
1+2 Decenes	0.93	0.76
C_{10} Isomers	0.21	0.10
n–Undecane	0.46	0.96
1+2 Undecenes	0.67	1.05
C_{11} Isomers	0.22	0.17
C_2+[e]	78.1	90.2
C_2–C_4	43.1	35.5
C_5–C_{11}	31.4	26.8
$C_{12}+$	14.5	28.2
Wax[d]	11.0	0.25

[d] Unanalyzed products collected in hot trap

[e] Does not include wax

Table 9. Summary of results for fixed bed run FA-13-2217.

Catalyst: 4.00[a]g, 100 Fe/0.94 Cu/0.05 K (30/60 mesh)
Catalyst volume: 3.40 cc

Diluent: 36.3 g, Glass Beads (30/60 mesh)
Diluent volume: 24.0 cc

Period	1	2
Date	8/10/87	8/11/87
Time on Stream (h)	36.5	61.0
Balance Duration (h)	6.0	6.0
Average Temperature (°C)	219	236
Maximum Δ Temperature (°C)[b]	1.7	2.1
Pressure (MPa)	1.48	1.48
H_2/CO Feed Ratio	1.03	1.03
Space Velocity (Nl/g-cat$\cdot h$)[a]	2.08	2.08
Space Velocity (Nl/g-Fe$\cdot h$)[a]	3.0	3.0
GHSV (h^{-1})[c]	2444	2444
Weight Closure (%)	97.6	99.3
CO Conversion (%)	41.7	43.5
H_2+CO Conversion (%)	45.2	47.5
H_2/CO Usage	1.20	1.22
STY ($mols$ H_2+CO/g-cat$\cdot h$)[a]	0.042	0.044
$P_{CO_2} \cdot P_{H_2} / P_{CO} \cdot P_{H_2O}$	0.82	0.58
Weight % of Outlet		
H_2	3.64	3.38
H_2O	8.52	11.6
CO	55.7	53.0
CO_2	18.7	18.4
Hydrocarbons	11.9	10.3
Oxygenates	0.59	0.82
Wax[d]	0.98	2.60
Yield (g/Nm^3 H_2+CO Converted)		
CH_4	13.9	13.9
C_2–C_4 Hydrocarbons	55.2	51.8
C_5–C_{11} Hydrocarbons	72.0	60.1
C_{12}+ Hydrocarbons	43.0	51.8
Oxygenates	8.39	11.3
Wax[d]	13.9	35.9
Total	193	189

[a] Based on unreduced catalyst
[c] Based on catalyst volume
[b] Maximum axial temperature difference
[d] Unanalyzed products collected from hot trap

Table 9 (cont'd). Summary of results for fixed bed run FA-13-2217.

Period	1	2
Weight % of Hydrocarbons		
CH_4	7.55	7.81
Ethane	5.46	5.02
Ethylene	3.55	3.22
Propane	2.17	2.15
Propylene	8.67	8.53
n-Butane	1.93	1.90
1+2 Butenes	7.40	7.53
C_4 Isomers	0.81	0.83
n-Pentane	2.27	2.31
1+2 Pentenes	5.89	5.94
C_5 Isomers	0.75	1.04
n–Hexane	1.82	1.49
1+2 Hexenes	2.95	3.05
C_6 Isomers	0.93	0.81
n–Heptane	1.13	0.91
1+2 Heptenes	2.37	2.16
C_7 Isomers	0.39	0.78
n-Octane	1.48	1.15
1+2 Octenes	3.16	2.25
C_8 Isomers	0.27	0.33
n–Nonane	1.73	1.43
1+2 Nonenes	3.54	2.64
C_9 Isomers	0.40	0.34
n–Decane	1.76	1.36
1+2 Decenes	3.15	2.28
C_{10} Isomers	0.57	0.37
n–Undecane	1.56	1.12
1+2 Undecenes	2.47	1.69
C_{11} Isomers	0.51	0.37
C_2+[e]	84.9	72.0
C_2–C_4	30.0	29.2
C_5–C_{11}	39.1	33.8
$C_{12}+$	23.4	29.2
Wax[d]	7.57	20.2

[d] Unanalyzed products collected in hot trap

[e] Does not include wax

Table 10. Summary of results for fixed bed run FA-15-2097.

Catalyst: 4.02[a]g, 100 Fe/0.96 Cu/0.18 K (30/60 mesh)
Catalyst volume: 3.00 cc

Diluent: 36.3 g, Glass Beads (30/60 mesh)
Diluent volume: 24.0 cc

Period	1	2	3	4	5	6
Date	7/28/87	7/29/87	7/30/87	7/31/87	8/1/87	8/3/87
Time on Stream (h)	24.0	63.5	87.5	111.0	134.0	183.5
Balance Duration (h)	6.0	6.0	6.0	6.0	6.0	6.0
Average Temperature ($^\circ$C)	220	236	235	237	251	235
Maximum Δ Temperature ($^\circ$C)[b]	2.1	2.7	1.2	2.4	2.0	2.5
Pressure (MPa)	1.48	1.48	1.48	1.48	1.48	2.80
H_2/CO Feed Ratio	1.00	1.00	1.00	1.03	1.03	1.03
Space Velocity (Nl/g-cat$\cdot h$)[a]	2.09	2.09	4.18	5.50	2.09	4.12
Space Velocity (Nl/g-Fe$\cdot h$)[a]	3.02	3.02	6.03	7.95	3.02	5.95
GHSV (h^{-1})[c]	2800	2800	5590	7360	2800	5516
Weight Closure (%)	91.9	96.5	92.4	94.0	95.9	97.4
CO Conversion (%)	43.0	82.3	54.4	29.0	91.6	20.4
H_2+CO Conversion (%)	39.4	72.9	49.6	26.9	78.9	23.6
H_2/CO Usage	0.84	0.77	0.83	0.89	0.75	1.35
STY ($mols$ H_2+CO/g-cat$\cdot h$)[a]	0.037	0.068	0.092	0.066	0.074	0.043
$P_{CO_2} \cdot P_{H_2} / P_{CO} \cdot P_{H_2O}$	1.1	6.7	4.2	2.0	19.6	1.4
Weight % of Outlet						
H_2	4.71	2.55	4.02	5.52	2.41	5.24
H_2O	7.00	6.43	3.86	3.33	5.36	2.60
CO	57.9	17.1	46.0	70.4	8.16	76.7
CO_2	16.9	50.7	32.9	14.8	62.4	9.36
Hydrocarbons	10.7	16.2	11.4	5.20	19.5	3.35
Oxygenates	0.50	0.72	0.30	0.23	0.28	0.14
Wax[d]	2.33	6.25	1.59	0.59	1.96	2.65
Yield (g/Nm^3 H_2+CO Converted)						
CH_4	14.7	19.6	24.0	10.6	19.7	7.50
C_2–C_4 Hydrocarbons	54.2	66.4	58.6	33.7	59.3	41.2
C_5–C_{11} Hydrocarbons	75.5	51.0	49.8	50.5	63.2	45.2
C_{12}+ Hydrocarbons	59.3	62.3	28.9	38.8	29.9	71.6
Oxygenates	7.86	6.41	3.74	5.23	2.22	3.90
Wax[d]	36.3	55.4	19.8	13.6	15.7	71.6
Total	211	206	165	139	174	166

[a] Based on unreduced catalyst
[c] Based on catalyst volume
[b] Maximum axial temperature difference
[d] Unanalyzed products collected from hot trap

Table 10 (cont'd). Summary of results for fixed bed run FA-15-2097.

Period	1	2	3	4	5	6
Weight % of Hydrocarbons						
CH_4	7.22	9.85	14.9	7.90	11.4	4.63
Ethane	3.72	5.97	6.39	0.68	6.31	4.65
Ethylene	4.32	4.32	4.30	1.07	2.88	5.10
Propane	1.83	2.46	2.60	2.22	2.67	1.39
Propylene	7.75	9.88	10.8	10.2	10.9	5.89
n-Butane	1.69	1.94	2.17	1.87	2.03	1.26
1+2 Butenes	6.59	7.85	9.12	8.39	8.68	4.88
C_4 Isomers	0.70	0.87	1.00	0.85	0.99	0.52
n-Pentane	1.99	2.16	2.66	2.34	2.45	1.63
1+2 Pentenes	5.61	5.57	8.22	10.4	6.56	4.57
C_5 Isomers	0.34	1.03	1.59	0.54	1.33	1.14
n-Hexane	3.40	1.24	1.86	0.01	1.68	2.70
1+2 Hexenes	4.80	4.08	4.33	4.37	4.48	4.84
C_6 Isomers	1.91	0.83	1.04	0.65	0.94	0.95
n-Heptane	2.29	0.88	0.93	0.03	1.41	2.49
1+2 Heptenes	2.77	1.97	2.27	3.45	2.76	3.91
C_7 Isomers	0.72	0.47	0.66	0.49	0.62	1.36
n-Octane	0.21	0.66	0.42	0.32	1.44	1.11
1+2 Octenes	2.20	1.33	1.85	2.80	3.13	2.22
C_8 Isomers	0.05	0.34	0.20	0.20	0.84	0.64
n-Nonane	0.71	0.57	0.48	0.95	1.16	[f]
1+2 Nonenes	2.01	1.13	0.91	2.19	2.12	[f]
C_9 Isomers	0.12	0.13	0.09	0.20	0.40	[f]
n-Decane	1.06	0.58	0.59	1.34	1.03	[f]
1+2 Decenes	2.68	1.05	1.01	2.75	1.63	[f]
C_{10} Isomers	0.26	0.14	0.14	0.35	0.38	[f]
n-Undecane	1.11	0.49	0.60	1.49	0.90	[f]
1+2 Undecenes	2.59	0.81	0.87	2.56	1.14	[f]
C_{11} Isomers	0.24	0.14	0.14	0.37	0.32	[f]
C_2+[e]	74.9	62.4	72.8	81.9	79.4	51.2
C_2–C_4	26.6	33.3	36.3	25.3	34.4	23.7
C_5–C_{11}	37.1	25.6	30.9	37.8	36.7	27.5
$C_{12}+$	29.1	31.3	17.9	29.1	17.4	44.1
Wax[d]	17.8	27.8	12.3	10.2	9.13	44.1

[d] Unanalyzed products collected in hot trap

[e] Does not include wax

[f] No liquid organic product collected in this balance

Table 11. Summary of results for fixed bed run FA-17-2367.

Catalyst: 4.00[a] g, 100 Fe/1.05 Cu/0.5 K (30/60 mesh)
Catalyst volume: 3.30 cc

Diluent: 37.6 g, Glass Beads (30/60 mesh)
Diluent volume: 25.0 cc

Period	1	2	3	4	5
Date	8/24/87	8/25/87	8/26/87	8/27/87	8/28/87
Time on Stream (h)	35.5	59.5	83.5	108.0	131.0
Balance Duration (h)	6.0	6.0	6.0	6.0	6.0
Average Temperature (°C)	221	236	236	235	250
Maximum Δ Temperature (°C)[b]	3.6	6.1	6.5	4.2	7.3
Pressure (MPa)	1.48	1.48	1.52	1.52	1.48
H_2/CO Feed Ratio	1.07	1.07	1.07	1.07	1.07
Space Velocity (Nl/g-cat$\cdot h$)[a]	2.10	2.10	4.20	1.36	2.10
Space Velocity (Nl/g-Fe$\cdot h$)[a]	3.03	3.05	6.08	1.98	3.05
GHSV (h^{-1})[c]	2550	2550	5091	1655	2550
Weight Closure (%)	99.6	97.8	97.0	105.5	100.4
CO Conversion (%)	46.2	68.2	38.4	75.5	79.8
H_2+CO Conversion (%)	40.4	56.1	33.0	60.2	64.6
H_2/CO Usage	0.81	0.70	0.78	0.65	0.68
STY ($mols$ H_2+CO/g-cat$\cdot h$)[a]	0.038	0.053	0.062	0.037	0.061
$P_{CO_2} \cdot P_{H_2} / P_{CO} \cdot P_{H_2O}$	1.6	4.9	3.0	9.1	7.1
Weight % of Outlet					
H_2	4.67	4.05	5.33	3.68	3.55
H_2O	8.72	6.81	3.86	4.94	7.80
CO	50.1	30.2	58.9	21.6	18.7
CO_2	26.4	43.8	22.2	46.2	51.3
Hydrocarbons	7.73	8.99	4.98	11.0	12.1
Oxygenates	0.64	0.77	0.26	0.35	0.67
Wax[d]	1.75	5.36	4.43	12.3	5.95
Yield (g/Nm^3 H_2+CO Converted)					
CH_4	10.6	11.2	9.87	10.5	12.3
C_2–C_4 Hydrocarbons	48.4	50.1	45.2	51.7	55.5
C_5–C_{11} Hydrocarbons	49.4	34.6	35.9	45.7	34.8
C_{12}+ Hydrocarbons	43.2	66.5	89.1	157	79.2
Oxygenates	10.2	8.74	5.04	4.02	6.81
Wax[d]	28.0	60.7	84.7	140	60.1
Total	162	171	185	269	189

[a] Based on unreduced catalyst

[c] Based on catalyst volume

[b] Maximum axial temperature difference

[d] Unanalyzed products collected from hot trap

Table 11 (cont'd). Summary of results for fixed bed run FA-17-2367.

Period	1	2	3	4	5
Weight % of Hydrocarbons					
CH_4	7.00	6.91	5.48	3.94	6.75
Ethane	4.55	4.33	4.20	2.42	3.87
Ethylene	6.58	5.72	5.34	3.42	5.14
Propane	1.75	1.58	1.23	1.19	1.70
Propylene	9.15	9.49	7.09	6.29	10.1
n–Butane	1.65	1.42	1.09	0.96	1.33
1+2 Butenes	7.42	7.48	5.51	4.65	7.47
C_4 Isomers	0.83	0.83	0.62	0.55	0.88
n–Pentane	1.99	1.84	1.39	1.21	1.74
1+2 Pentenes	6.14	6.06	4.55	3.81	5.80
C_5 Isomers	0.47	0.49	0.36	0.33	0.50
n–Hexane	1.29	0.61	0.80	0.66	0.67
1+2 Hexenes	4.15	2.54	3.83	2.43	2.08
C_6 Isomers	0.88	0.65	1.00	0.59	0.65
n–Heptane	0.68	0.26	0.55	0.40	0.39
1+2 Heptenes	2.64	1.12	2.35	1.24	0.99
C_7 Isomers	0.45	0.92	0.73	0.38	0.37
n–Octane	0.61	0.23	0.30	0.22	0.21
1+2 Octenes	2.43	1.27	1.38	1.16	1.15
C_8 Isomers	0.28	0.12	0.30	0.15	0.18
n–Nonane	0.74	0.38	0.11	0.30	0.30
1+2 Nonenes	2.60	1.28	0.43	1.40	1.11
C_9 Isomers	0.29	0.22	0.06	0.18	0.20
n–Decane	0.83	0.38	0.17	0.24	0.28
1+2 Decenes	2.46	1.26	0.60	1.16	1.01
C_{10} Isomers	0.42	0.29	0.10	0.18	0.19
n–Undecane	0.75	0.28	0.18	0.18	0.26
1+2 Undecenes	1.95	0.89	0.62	0.88	0.91
C_{11} Isomers	0.52	0.22	0.12	0.14	0.17
C_2+^e	74.5	55.8	47.5	43.4	60.2
C_2–C_4	31.9	30.9	25.1	19.5	30.5
C_5–C_{11}	32.6	21.3	20.0	17.2	19.2
$C_{12}+$	28.5	40.9	49.5	59.4	43.6
Wax^d	18.5	37.3	47.1	52.7	33.1

^{d} Unanalyzed products collected in hot trap

^{e} Does not include wax

Table 12. Summary of results for fixed bed run FB-25-2447.

Catalyst: 4.05[a]g, 100 Fe/2.93 Cu/0.18 K (30/60 mesh)
Catalyst volume: 3.60 cc

Diluent: 36.8 g, Glass Beads (30/60 mesh)
Diluent volume: 25.0 cc

Period	1	2	3	4	5
Date	9/4/87	9/5/87	9/6/87	9/7/87	9/8/87
Time on Stream (h)	33.0	58.0	83.0	107.0	131.5
Balance Duration (h)	6.0	6.0	6.0	6.0	6.0
Average Temperature (°C)	221	235	235	250	234
Maximum Δ Temperature (°C)[b]	5.0	5.0	7.0	14.0	3.0
Pressure (MPa)	1.48	1.48	1.48	1.51	2.86
H_2/CO Feed Ratio	1.07	1.07	1.07	1.07	1.07
Space Velocity (Nl/g-cat·h)[a]	2.04	2.04	4.09	2.04	4.09
Space Velocity (Nl/g-Fe·h)[a]	3.01	3.01	6.01	3.01	6.01
GHSV (h^{-1})[c]	2366	2366	4734	2366	4731
Weight Closure (%)	91.5	92.4	96.0	96.7	95.4
CO Conversion (%)	41.2	54.5	25.6	81.7	17.6
H_2+CO Conversion (%)	42.9	54.4	26.0	72.2	19.5
H_2/CO Usage	1.16	1.07	1.10	0.83	1.30
STY ($mols$ H_2+CO/g-cat·h)[a]	0.039	0.050	0.047	0.066	0.036
$P_{CO_2} \cdot P_{H_2} / P_{CO} \cdot P_{H_2O}$	1.11	1.72	1.15	9.08	1.03
Weight % of Outlet					
H_2	4.00	3.54	5.51	2.72	5.91
H_2O	6.05	7.71	3.94	5.17	2.58
CO	54.7	45.8	71.9	17.5	80.2
CO_2	16.1	30.1	10.4	53.1	6.34
Hydrocarbons	8.81	9.92	5.55	17.9	3.59
Oxygenates	0.47	0.73	0.30	0.50	0.18
Wax[d]	9.82	2.20	2.36	3.04	1.20
Yield (g/Nm^3 H_2+CO Converted)					
CH_4	12.1	10.4	11.4	18.8	6.17
C_2–C_4 Hydrocarbons	60.5	55.8	51.1	67.1	40.2
C_5–C_{11} Hydrocarbons	58.2	40.5	54.8	59.7	55.6
C_{12}+ Hydrocarbons	156	33.8	72.9	36.5	49.9
Oxygenates	7.08	8.10	7.12	4.33	5.71
Wax[d]	148	24.3	56.8	26.4	38.1
Total	288	142	197	186	158

[a] Based on unreduced catalyst
[c] Based on catalyst volume

[b] Maximum axial temperature difference
[d] Unanalyzed products collected from hot trap

Table 12 (cont'd). Summary of results for fixed bed run FB-25-2447.

Period	1	2	3	4	5
Weight % of Hydrocarbons					
CH_4	4.31	7.80	6.00	10.3	4.06
Ethane	3.13	4.31	4.48	6.58	6.51
Ethylene	2.63	4.56	3.59	2.50	5.45
Propane	1.40	2.48	1.90	3.19	1.59
Propylene	6.15	12.5	8.15	11.5	5.70
n Butane	1.22	2.19	1.62	2.51	1.55
1+2 Butenes	4.81	10.1	6.51	9.46	5.08
C_4 Isomers	0.51	1.06	0.62	1.06	0.58
n–Pentane	1.41	2.92	2.01	3.10	2.03
1+2 Pentenes	4.72	9.58	5.97	7.27	5.13
C_5 Isomers	0.57	0.99	0.53	1.45	0.56
n–Hexane	0.01	0.01	1.86	1.64	2.85
1+2 Hexenes	2.62	3.48	4.21	3.83	7.37
C_6 Isomers	0.55	0.87	1.05	0.72	1.65
n–Heptane	0.77	0.78	1.13	1.03	2.19
1+2 Heptenes	1.54	1.87	2.24	1.92	4.51
C_7 Isomers	0.37	0.54	0.75	0.40	1.18
n–Octane	0.72	0.54	0.70	1.08	1.08
1+2 Octenes	1.34	1.39	1.85	1.93	2.94
C_8 Isomers	0.24	0.19	0.17	0.35	0.41
n–Nonane	0.56	0.53	0.51	1.07	0.18
1+2 Nonenes	1.29	1.27	1.22	1.78	0.42
C_9 Isomers	0.17	0.14	0.17	0.34	0.05
n–Decane	0.55	0.69	0.66	0.95	0.54
1+2 Decenes	1.18	1.44	1.37	1.47	1.09
C_{10} Isomers	0.20	0.20	0.22	0.38	0.13
n–Undecane	0.42	0.70	0.69	0.76	0.76
1+2 Undecenes	0.82	1.24	1.24	1.04	1.34
C_{11} Isomers	0.15	0.23	0.26	0.30	0.22
C_2+[e]	43.0	72.5	64.1	75.2	70.9
C_2–C_4	19.9	37.3	26.9	36.8	26.4
C_5–C_{11}	20.2	29.6	28.8	32.8	36.6
$C_{12}+$	55.6	25.3	38.3	20.0	32.9
Wax[d]	52.7	18.2	29.9	14.5	25.1

[d] Unanalyzed products collected in hot trap

[e] Does not include wax

Table 13. Summary of results for fixed bed run FA-27-2557.

Catalyst: 4.01[a]g, 100 Fe/2.95 Cu/0.45 K (30/60 mesh)
Catalyst volume: 3.60 cc

Diluent: 37.5 g, Glass Beads (30/60 mesh)
Diluent volume: 25.0 cc

Period	1	2	3	4	5
Date	9/14/87	9/15/87	9/16/87	9/17/87	9/18/87
Time on Stream (h)	38.0	62.5	86.5	110.5	135.0
Balance Duration (h)	6.0	6.0	6.0	6.0	6.0
Average Temperature (°C)	219	235	235	249	234
Maximum Δ Temperature (°C)[b]	7.0	3.0	2.6	4.0	4.7
Pressure (MPa)	1.41	1.41	1.41	1.41	2.79
H_2/CO Feed Ratio	1.07	1.07	1.07	1.07	1.07
Space Velocity (Nl/g-cat·h)[a]	2.04	2.03	4.07	2.02	4.07
Space Velocity (Nl/g-Fe·h)[a]	3.00	3.00	6.00	2.98	6.00
GHSV (h^{-1})[c]	2267	2263	4533	2250	4533
Weight Closure (%)	94.2	92.9	98.6	98.5	98.7
CO Conversion (%)	44.3	74.3	41.8	84.4	30.2
H_2+CO Conversion (%)	42.7	62.9	35.7	70.4	28.6
H_2/CO Usage	1.00	0.76	0.77	0.73	0.96
STY ($mols$ H_2+CO/g-cat·h)[a]	0.039	0.057	0.065	0.064	0.052
$P_{CO_2} \cdot P_{H_2} / P_{CO} \cdot P_{H_2O}$	3.47	10.8	3.81	9.23	2.10
Weight % of Outlet					
H_2	4.47	3.68	5.09	14.5	5.29
H_2O	3.45	3.69	3.47	6.55	3.57
CO	54.8	25.7	54.8	14.7	65.6
CO_2	25.8	48.8	25.1	50.5	16.4
Hydrocarbons	6.43	9.90	6.50	14.5	4.63
Oxygenates	0.30	0.35	0.44	0.80	0.37
Wax[d]	4.71	7.84	4.55	9.79	4.13
Yield (g/Nm^3 H_2+CO Converted)					
CH_4	8.42	9.87	9.63	8.97	8.55
C_2–C_4 Hydrocarbons	35.8	42.9	41.3	39.2	40.2
C_5–C_{11} Hydrocarbons	40.6	38.1	49.0	57.1	43.9
C_{12}+ Hydrocarbons	74.7	79.3	98.1	115	104
Oxygenates	4.36	3.40	7.95	7.22	8.18
Wax[d]	67.5	75.2	81.6	88.9	92.4
Total	164	174	206	228	204

[a] Based on unreduced catalyst
[c] Based on catalyst volume
[b] Maximum axial temperature difference
[d] Unanalyzed products collected from hot trap

Table 13 (cont'd). Summary of results for fixed bed run FA-27-2557.

Period	1	2	3	4	5
Weight % of Hydrocarbons					
CH_4	5.28	5.80	4.86	4.07	4.36
Ethane	2.93	3.63	4.62	1.64	0.69
Ethylene	4.91	4.64	4.18	2.55	2.40
Propane	1.28	1.27	1.07	0.94	1.67
Propylene	6.49	7.85	6.43	6.32	7.53
n-Butane	1.16	1.10	0.94	0.83	1.47
1+2 Butenes	5.11	6.02	5.05	4.92	5.98
C_4 Isomers	0.59	0.68	0.57	0.55	0.73
n–Pentane	1.48	1.56	1.34	1.27	1.88
1+2 Pentenes	4.56	5.23	4.73	4.77	7.34
C_5 Isomers	0.33	0.37	0.38	0.44	1.00
n–Hexane	0.76	0.73	0.91	0.63	0.70
1+2 Hexenes	2.91	3.16	3.67	2.93	2.75
C_6 Isomers	0.58	0.67	0.77	0.49	0.67
n–Heptane	0.51	0.49	0.53	0.35	0.43
1+2 Heptenes	1.97	2.20	2.11	1.80	1.68
C_7 Isomers	0.35	0.46	0.53	0.37	0.55
n–Octane	0.29	0.36	0.21	0.37	0.27
1+2 Octenes	1.43	1.78	1.29	2.36	0.88
C_8 Isomers	0.25	0.25	0.09	0.21	0.15
n–Nonane	0.50	0.38	0.25	0.62	0.14
1+2 Nonenes	2.33	1.67	1.73	2.71	0.67
C_9 Isomers	0.21	0.15	0.13	0.17	0.07
n–Decane	0.78	0.31	0.48	0.63	0.32
1+2 Decenes	3.06	1.34	2.44	2.60	1.16
C_{10} Isomers	0.22	0.14	0.17	0.18	0.07
n–Undecane	0.53	0.23	0.52	0.59	0.36
1+2 Undecenes	2.22	0.88	2.28	2.21	1.20
C_{11} Isomers	0.18	0.08	0.18	0.18	0.06
C_2+^e	52.4	50.0	54.0	55.6	48.5
C_2–C_4	22.5	25.2	20.9	17.8	20.5
C_5–C_{11}	25.4	22.4	24.7	25.9	22.4
$C_{12}+$	46.8	46.6	49.6	52.3	52.8
Wax[d]	42.3	44.2	41.2	40.3	47.1

[d] Unanalyzed products collected in hot trap

[e] Does not include wax

Table 15. Copper and potassium compositions of synthesized precipitated iron catalysts*.

Copper		Potassium	
Nominal	Actual**	Nominal	Actual**
0.0	-	0.01	0.005 ± .001
	-	0.02	0.016 ± .001
	-	0.05	0.037 ± .004
	-	0.10	0.082 ± .005
	-	0.20	0.19 ± .01
	-	0.50	1.01 ± .02
	-	1.00	0.83 ± .06
	-	2.00	1.7 ± .3
0.1	0.12 ± .01	0.00	-
0.3	0.29 ± .01	0.00	-
	0.27 ± .01	0.05	0.040 ± .002
	0.28 ± .01	0.20	0.185 ± .002
	0.28 ± .01	0.50	0.48 ± .07
1.0	1.04 ± .06	0.00	-
	0.94 ± .04	0.05	0.049 ± .004
	0.96 ± .03	0.20	0.18 ± .01
	1.05 ± .03	0.50	0.83 ± .04
3.0	2.97 ± .06	0.00	-
	2.83 ± .11	0.05	0.045 ± .001
	2.93 ± .12	0.20	0.18 ± .01
	2.95 ± .04	0.50	0.45 ± .03
10.0	9.7 ± .3	0.00	-
20.0	18.7 ± .4	0.00	-

---

* In parts by weight, relative to 100 parts by weight of Fe.

** As measured by atomic absorption spectroscopy.

Table 16. Surface areas of synthesized precipitated iron catalysts.

Nominal Composition (parts by weight)			Surface Area (m^2/g)	
Fe	Cu	K	Unreduced	Reduced*
100	0.0	0.00	180	10
	0.0	0.01	195	-
		0.02	205	-
		0.05	-	-
		0.10	-	-
		0.20	-	-
		0.50	-	-
		1.00	210	-
		2.00	-	-
	0.1	0.00	280	5
	0.3	0.00	328	5
		0.05	-	-
		0.20	-	-
		0.50	285	-
	1.0	0.00	234	-
		0.05	-	8
		0.20	-	-
		0.50	231	9
	3.0	0.00	300	5
		0.05	-	-
		0.20	-	-
		0.50	-	-
	10.0	0.00	380	-
	20.0	0.00	374	8

* In flowing H_2 for 4 hrs at 300°C.

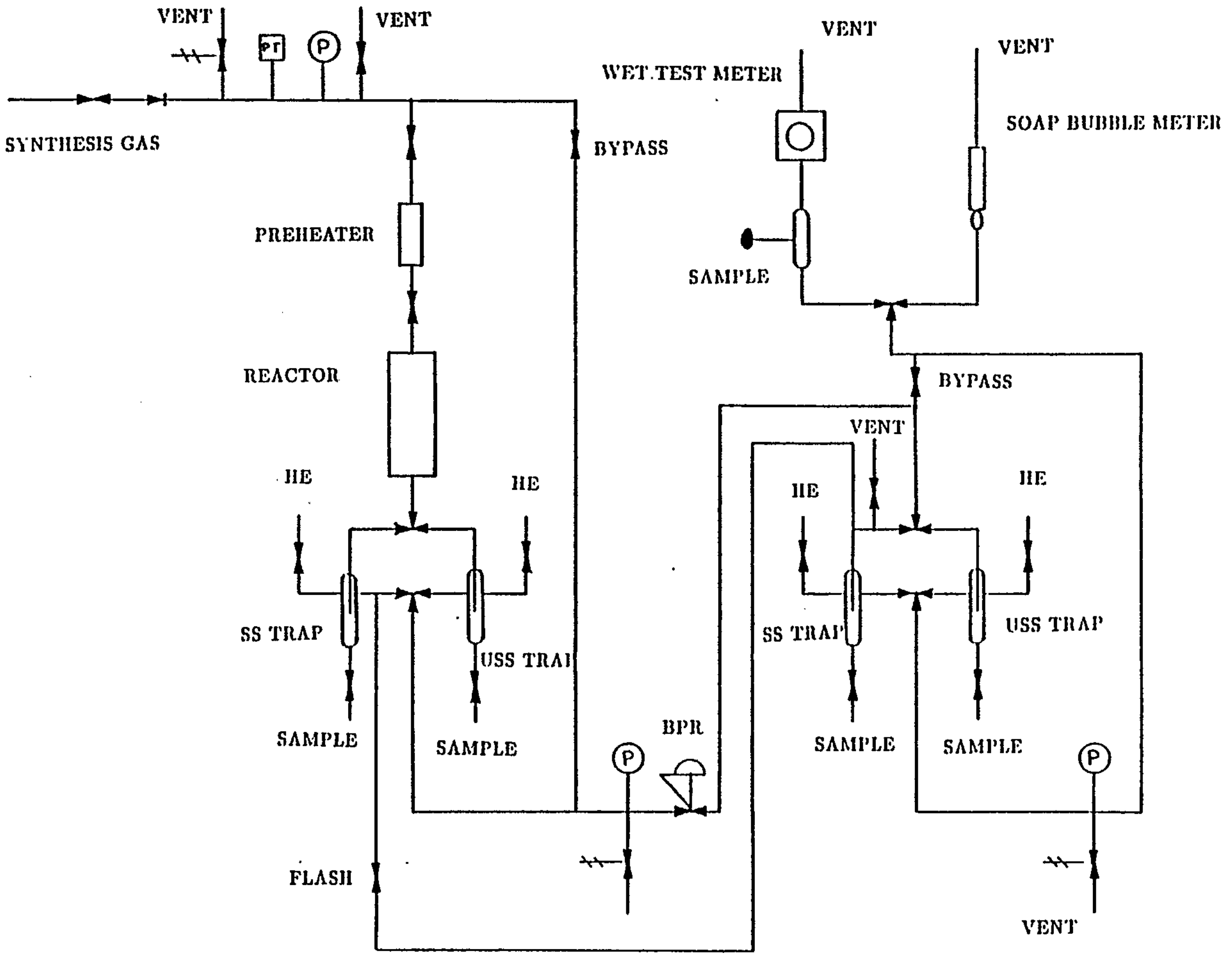

Figure 1. Process schematic of modified fixed bed reactors.

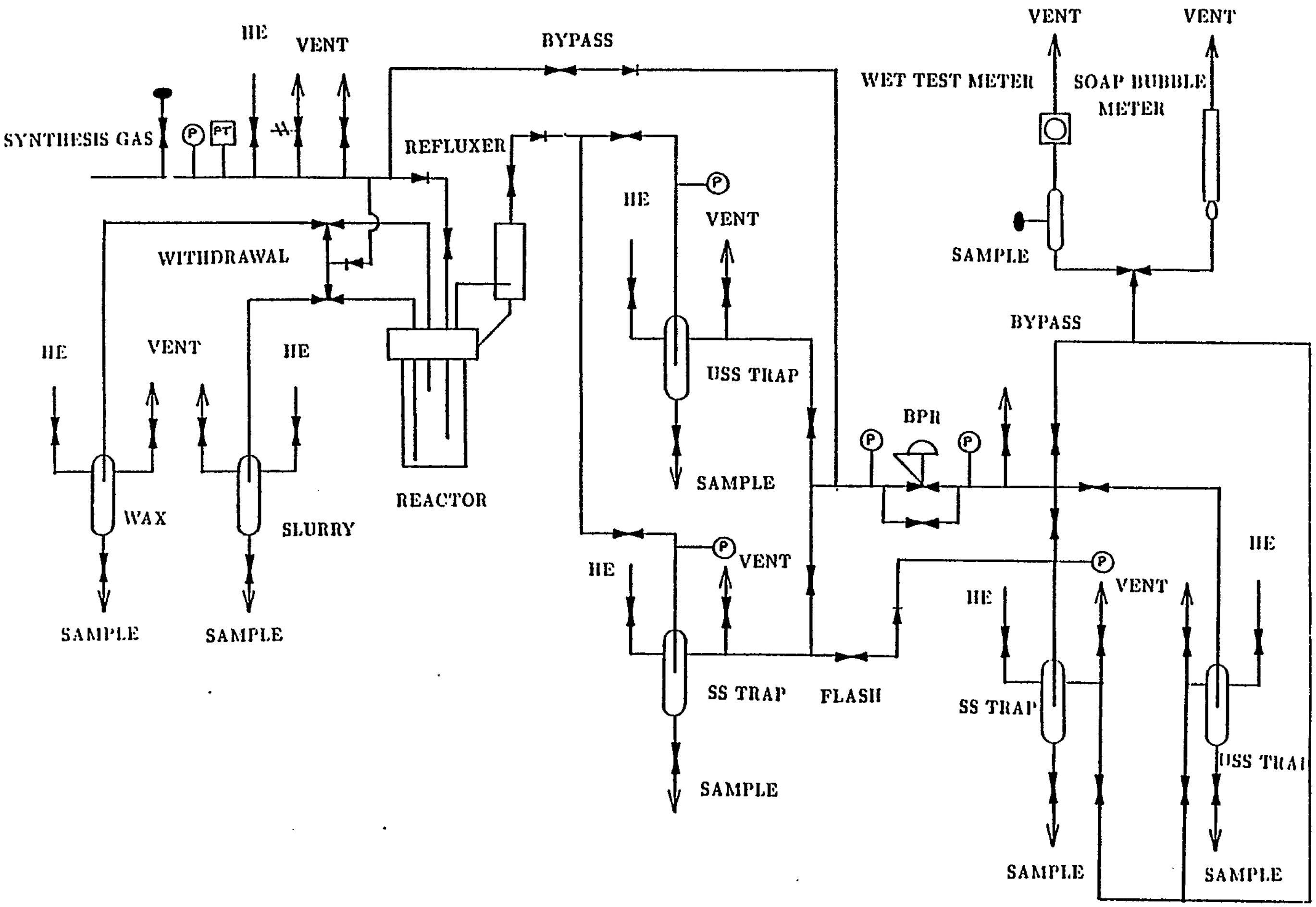

Figure 2. Process schematic of modified slurry reactor.

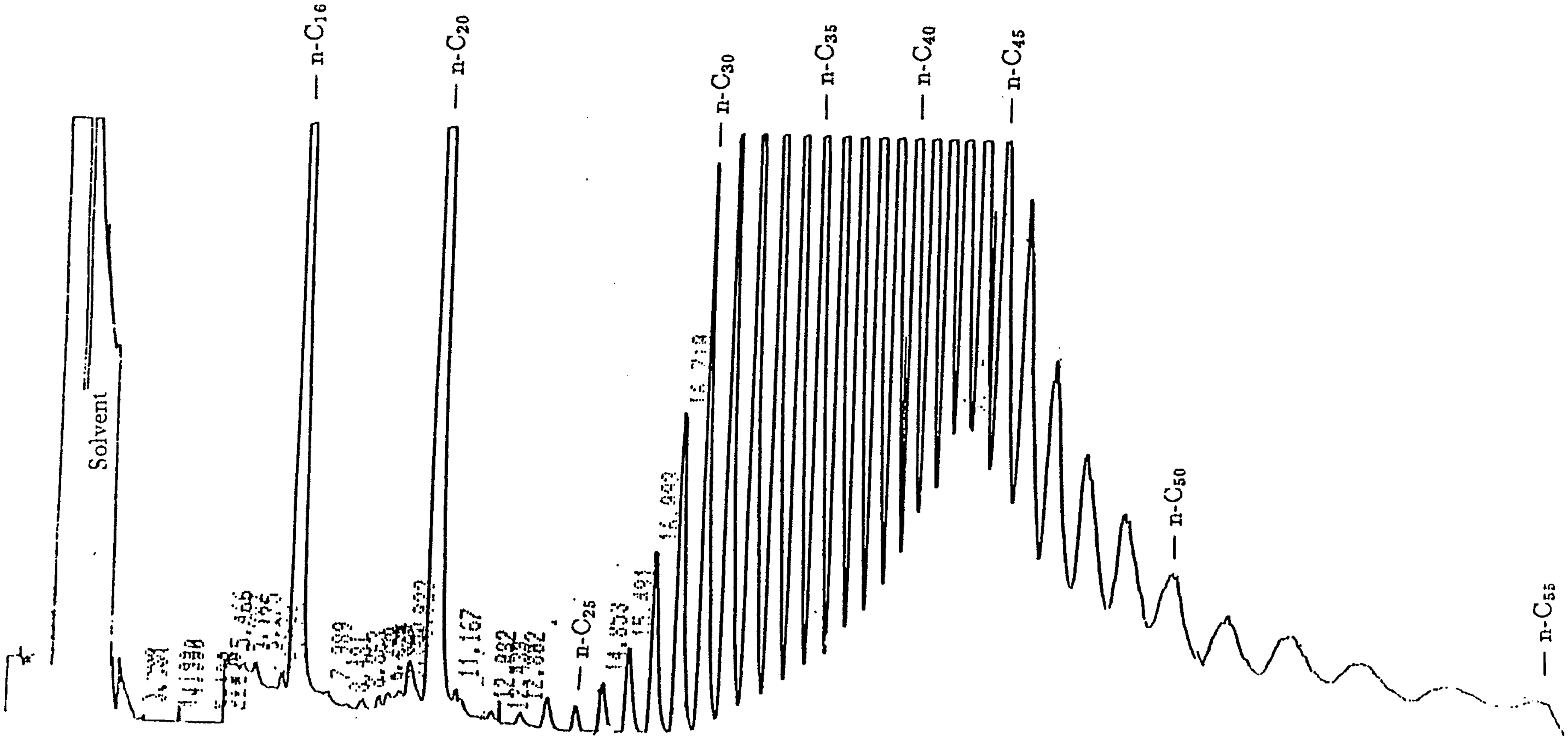

Figure 3. GC trace of FT-300 *n*-paraffin wax. Sigma 1 Chromatograph, RSL-150 fused silica column, FID.

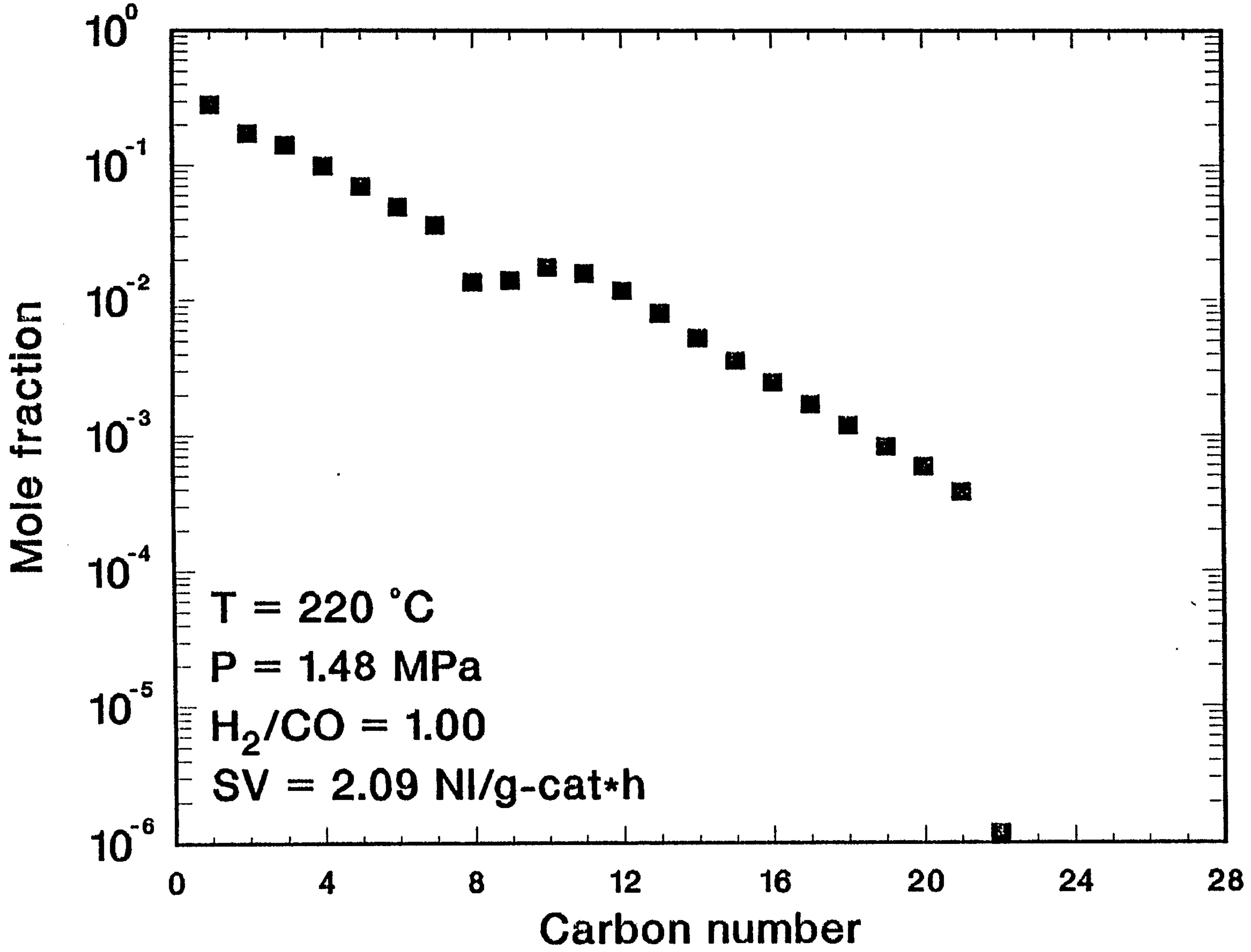

Figure 4. Anderson–Schulz–Flory plot for run FA–15–2097, balance 1.

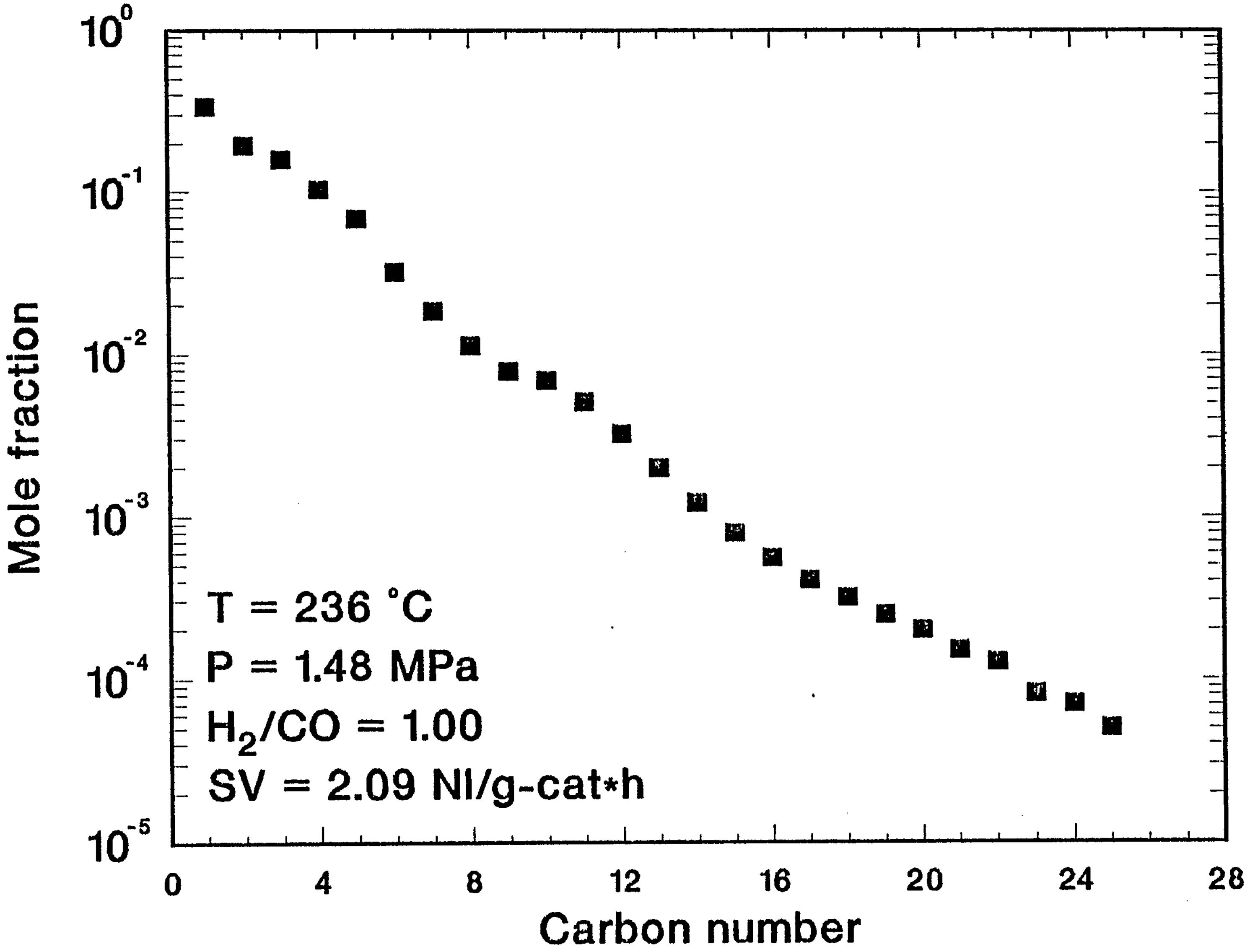

Figure 5. Anderson-Schulz-Flory plot for run FA-15-2097, balance 2.

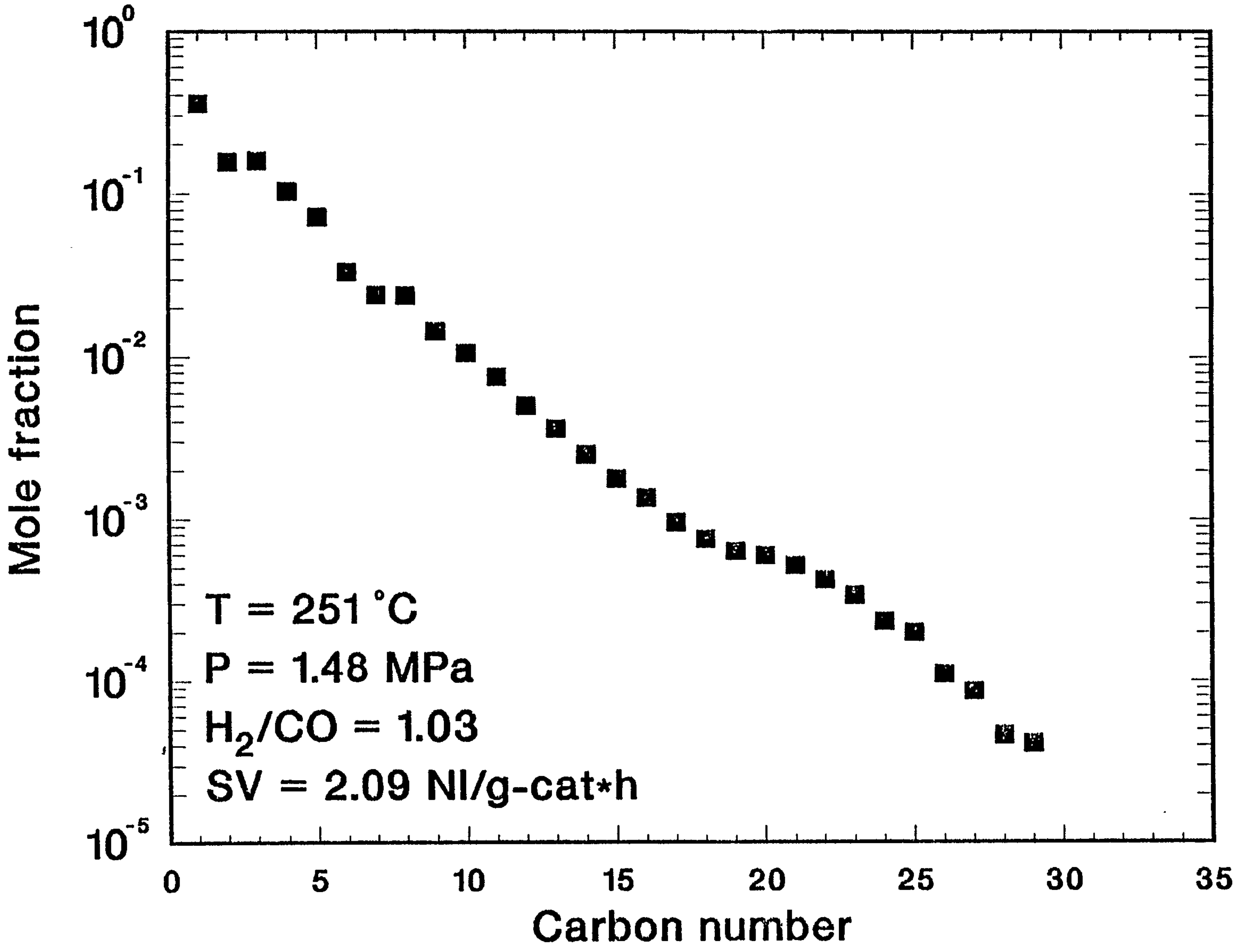

Figure 6. Anderson–Schulz–Flory plot for run FA-15-2097, balance 5.

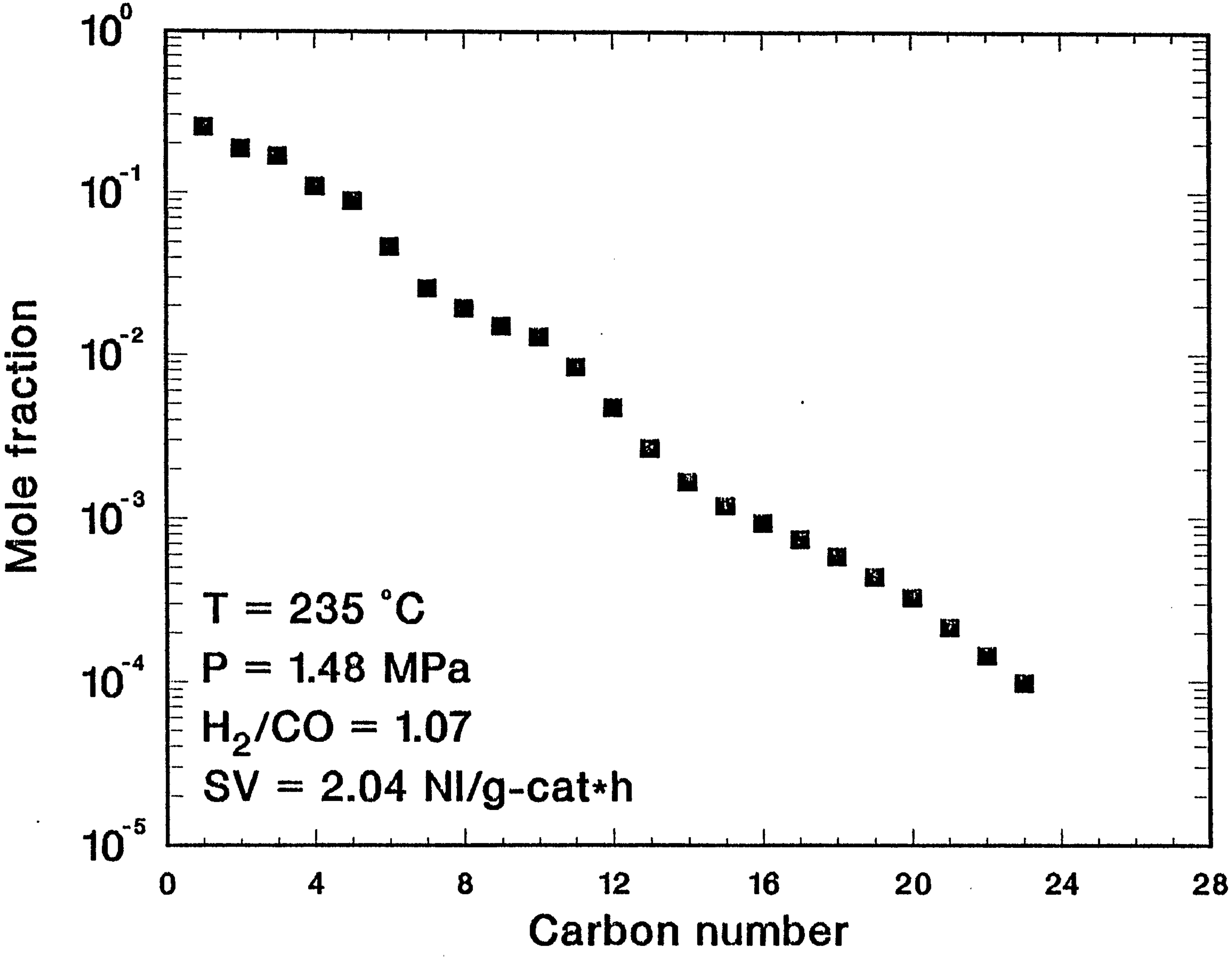

Figure 7. Anderson–Schulz–Flory plot for run FA-25-2447, balance 1.

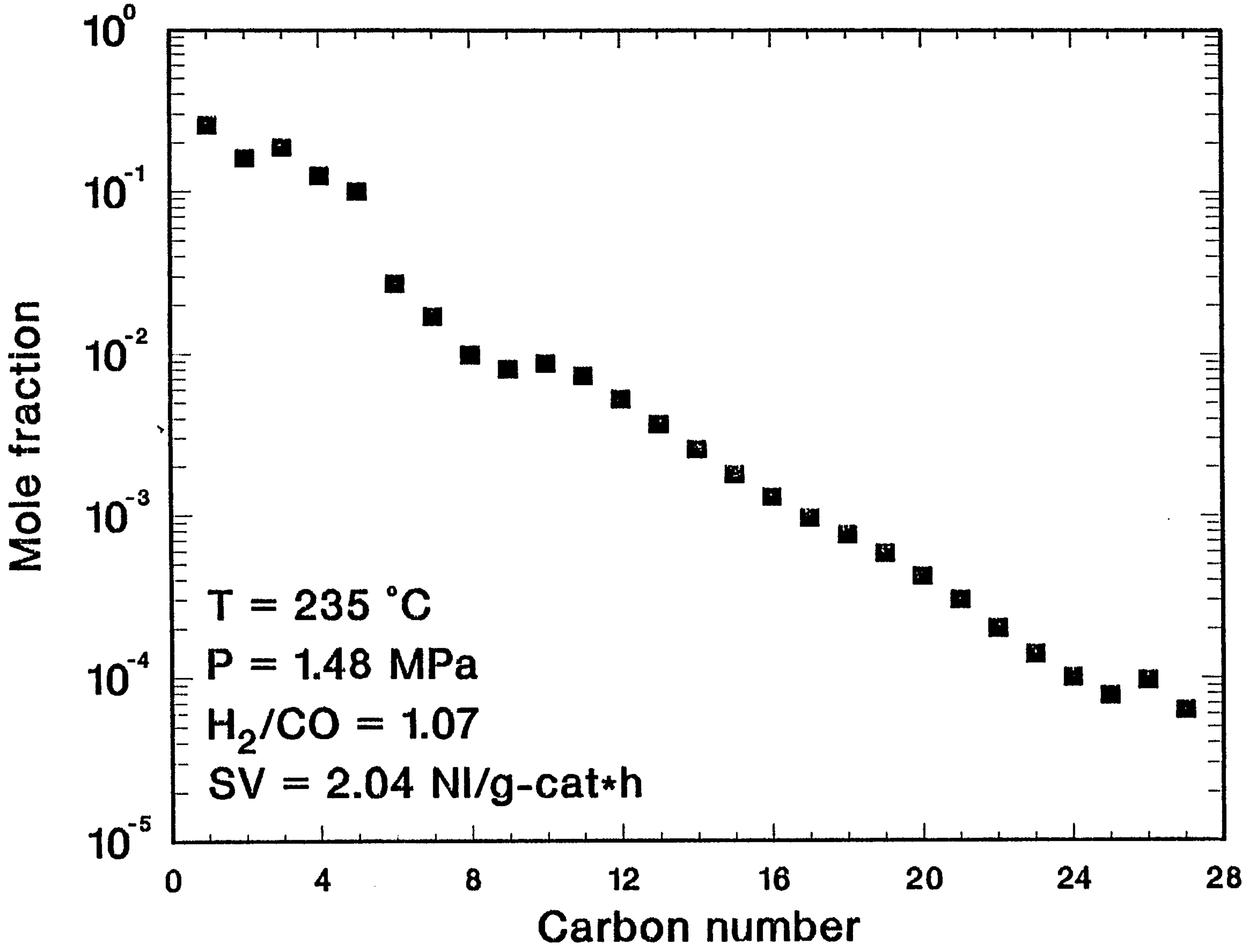

Figure 8. Anderson–Schulz–Flory plot for run FA-25-2447, balance 2.

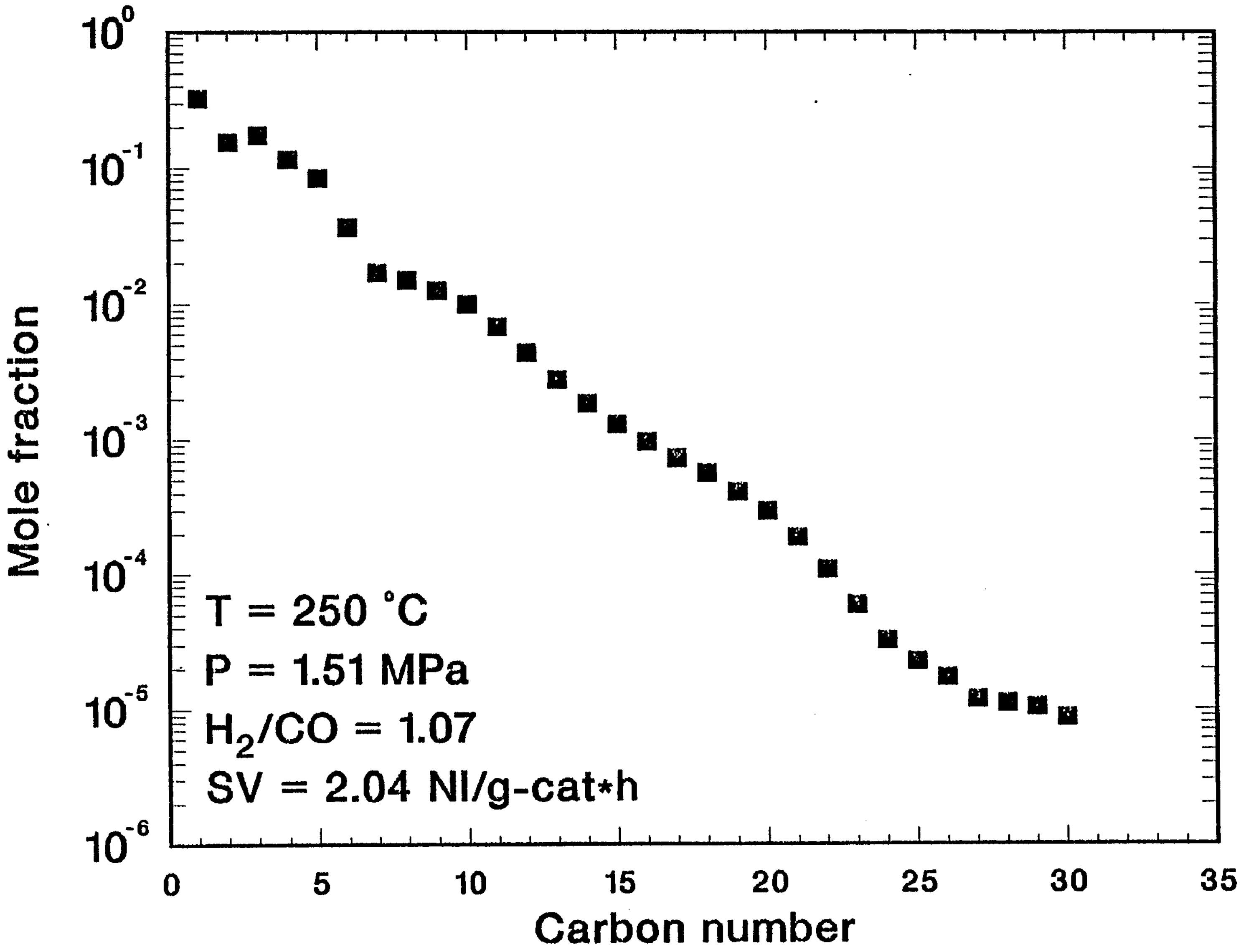

Figure 9. Anderson–Schulz–Flory plot for run FA–25–2447, balance 4.

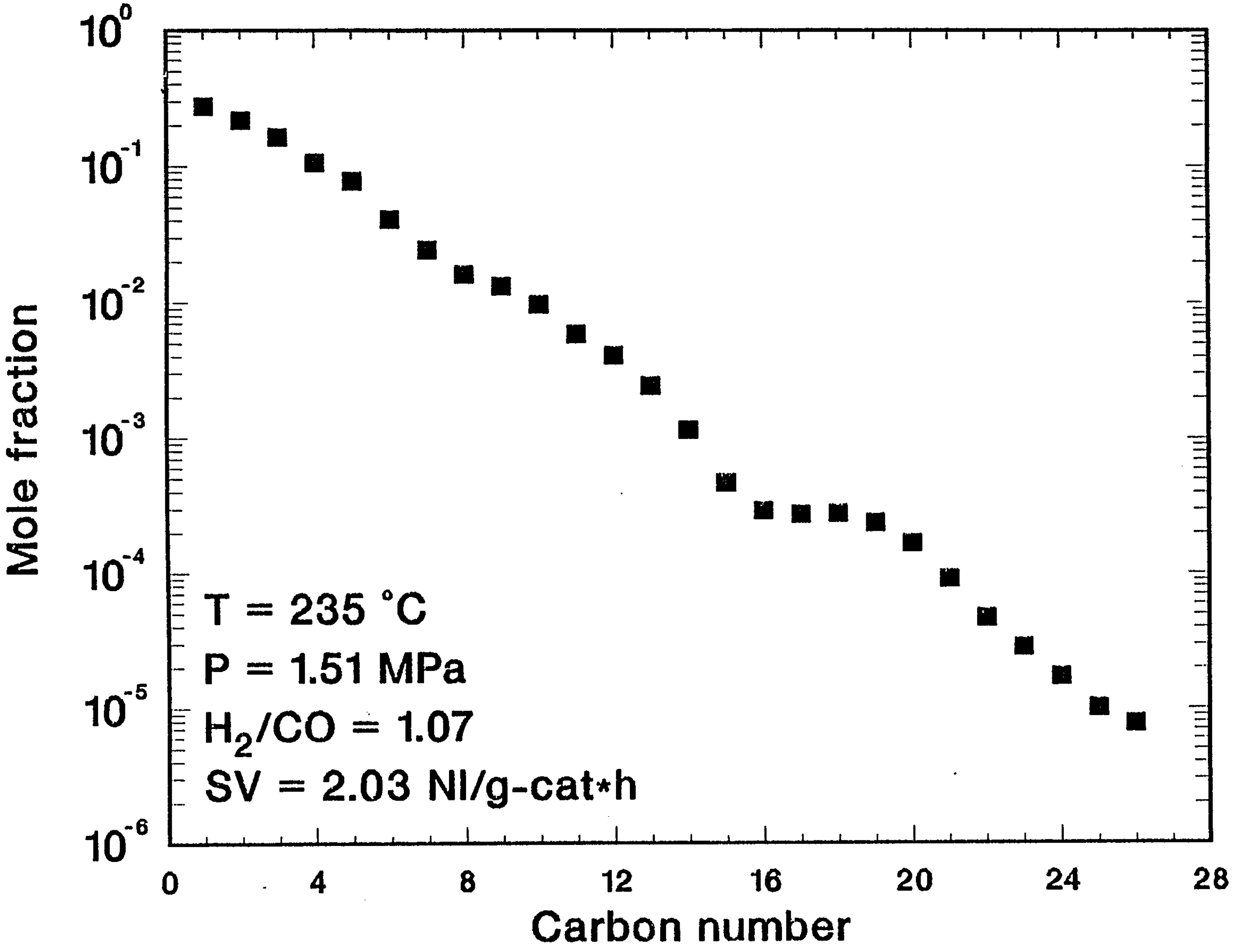

Figure 10. Anderson–Schulz–Flory plot for run FA–25–2557, balance 2.

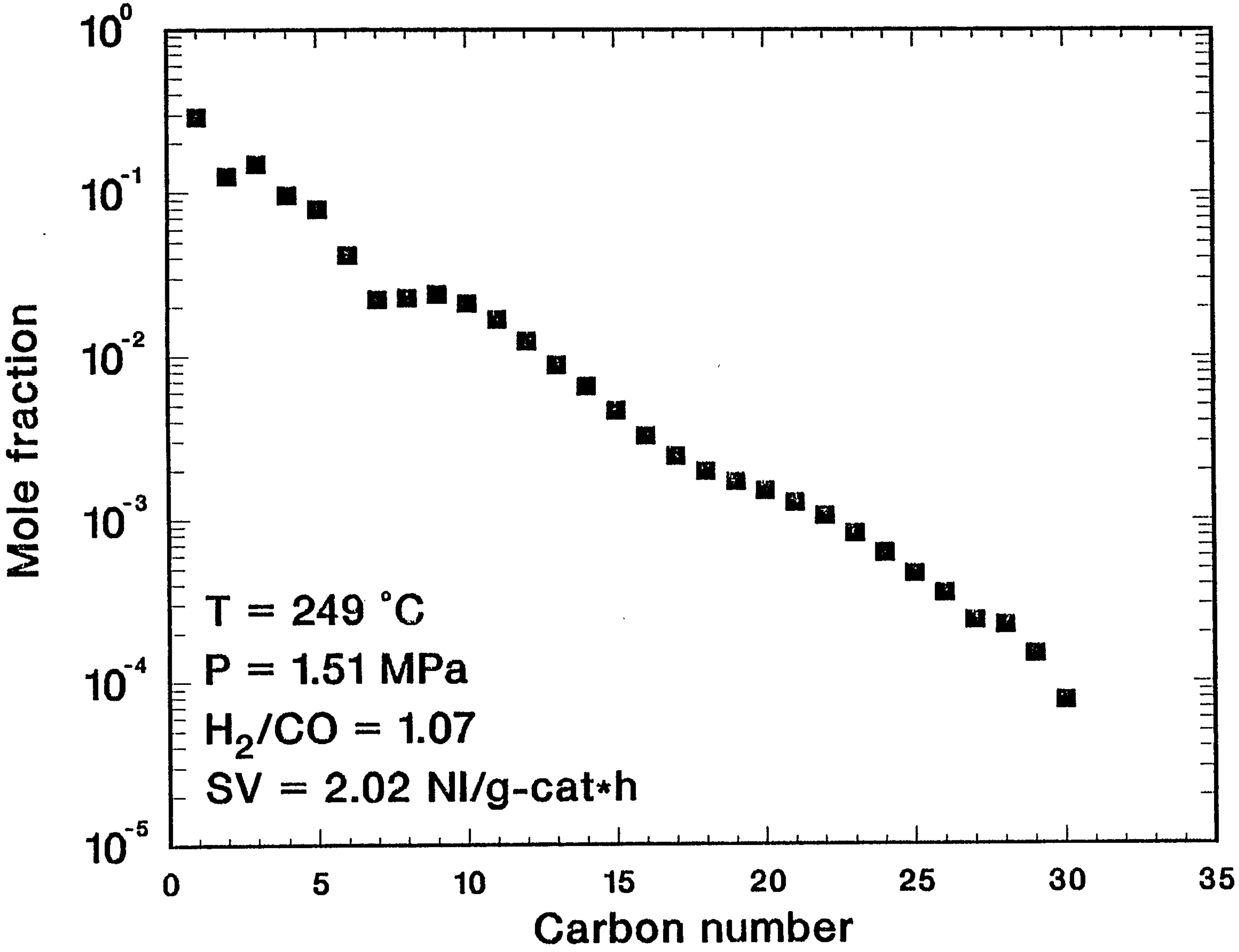

Figure 11. Anderson-Schulz-Flory plot for run FA-25-2557, balance 4.

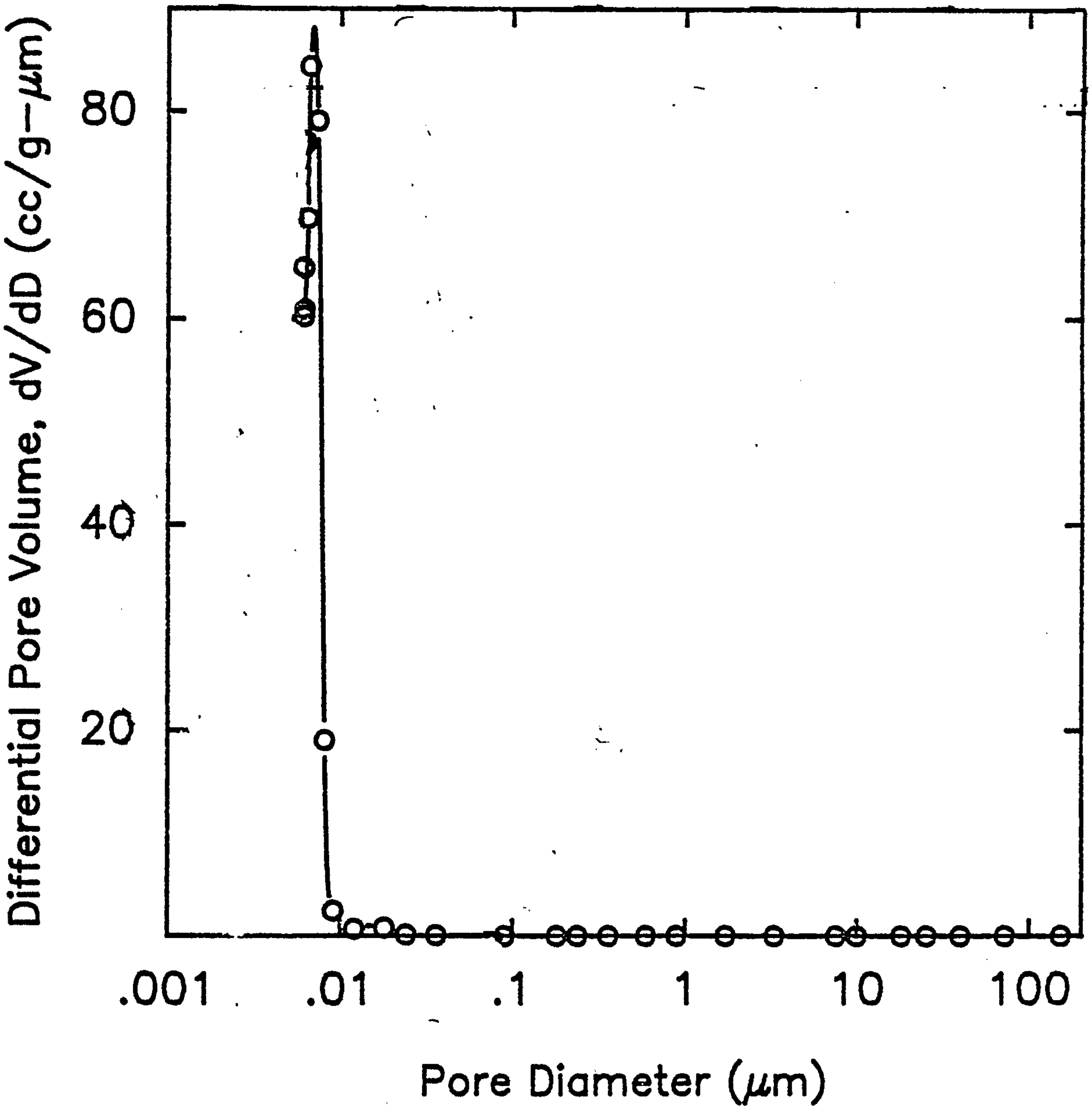

Figure 12. Differential pore volume distribution of 100 Fe/0.0 Cu/0.0 K catalyst following calcination in air for 4 *h* at 300 °C.

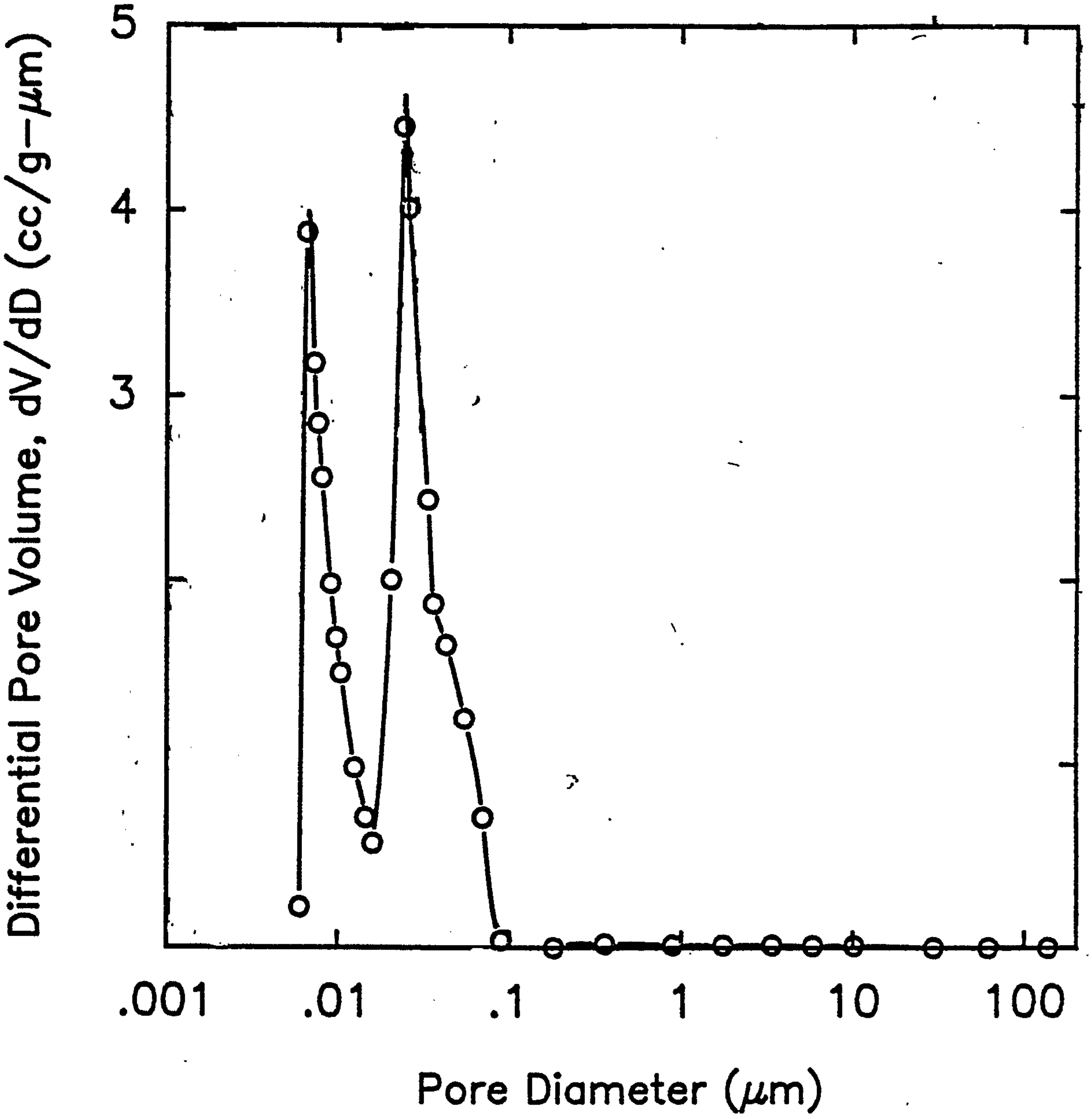

Figure 13. Differential pore volume distribution of 100 Fe/0.0 Cu/0.0 K catalyst following treatment in H_2 for 4 *h* at 300 °C.

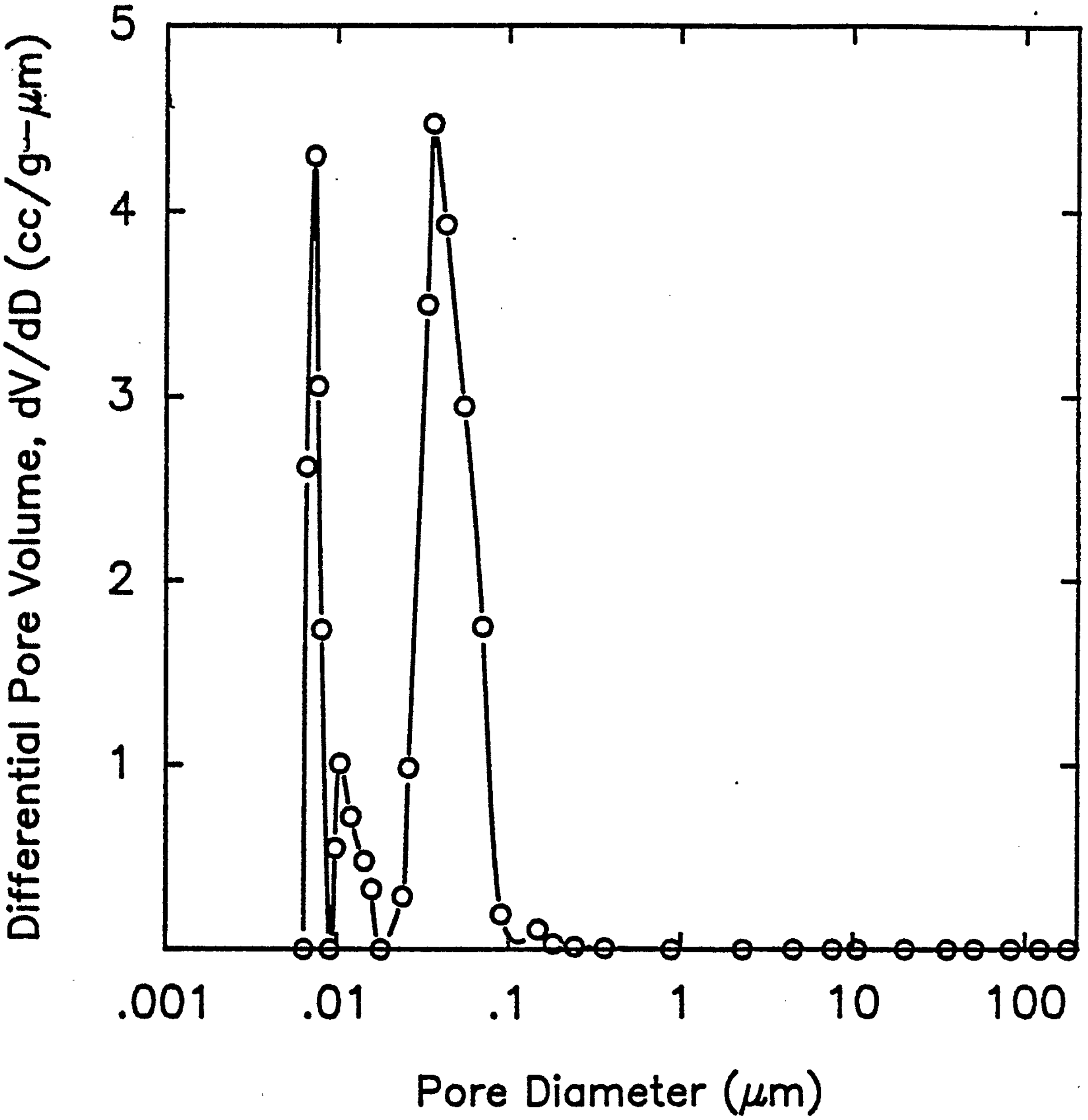

Figure 14. Differential pore volume distribution of 100 Fe/0.1 Cu/0.0 K catalyst following treatment in H_2 for 4 *h* at 300 °C.

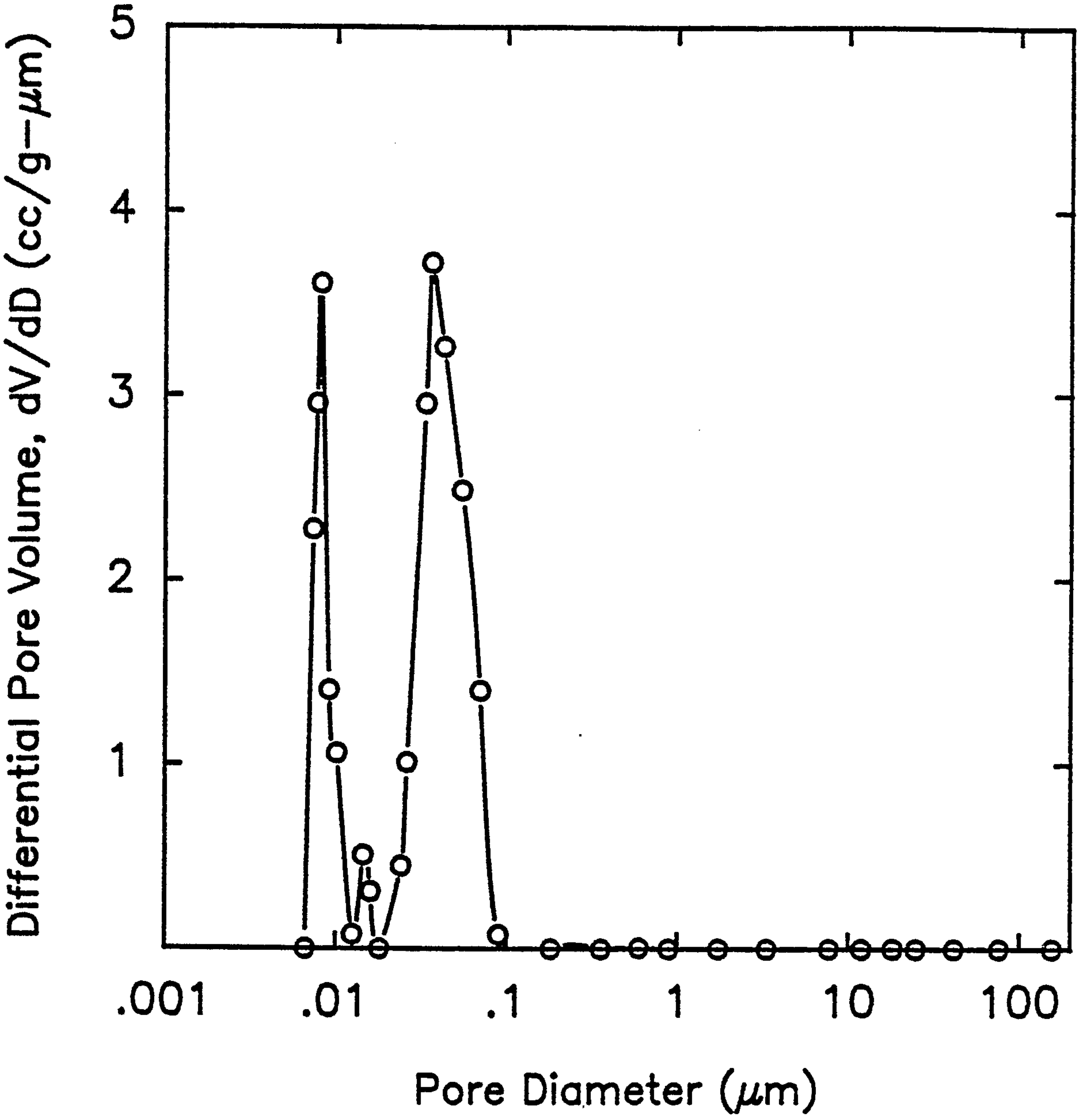

Figure 15. Differential pore volume distribution of 100 Fe/0.3 Cu/0.0 K catalyst following treatment in H_2 for 4 *h* at 300 °C.

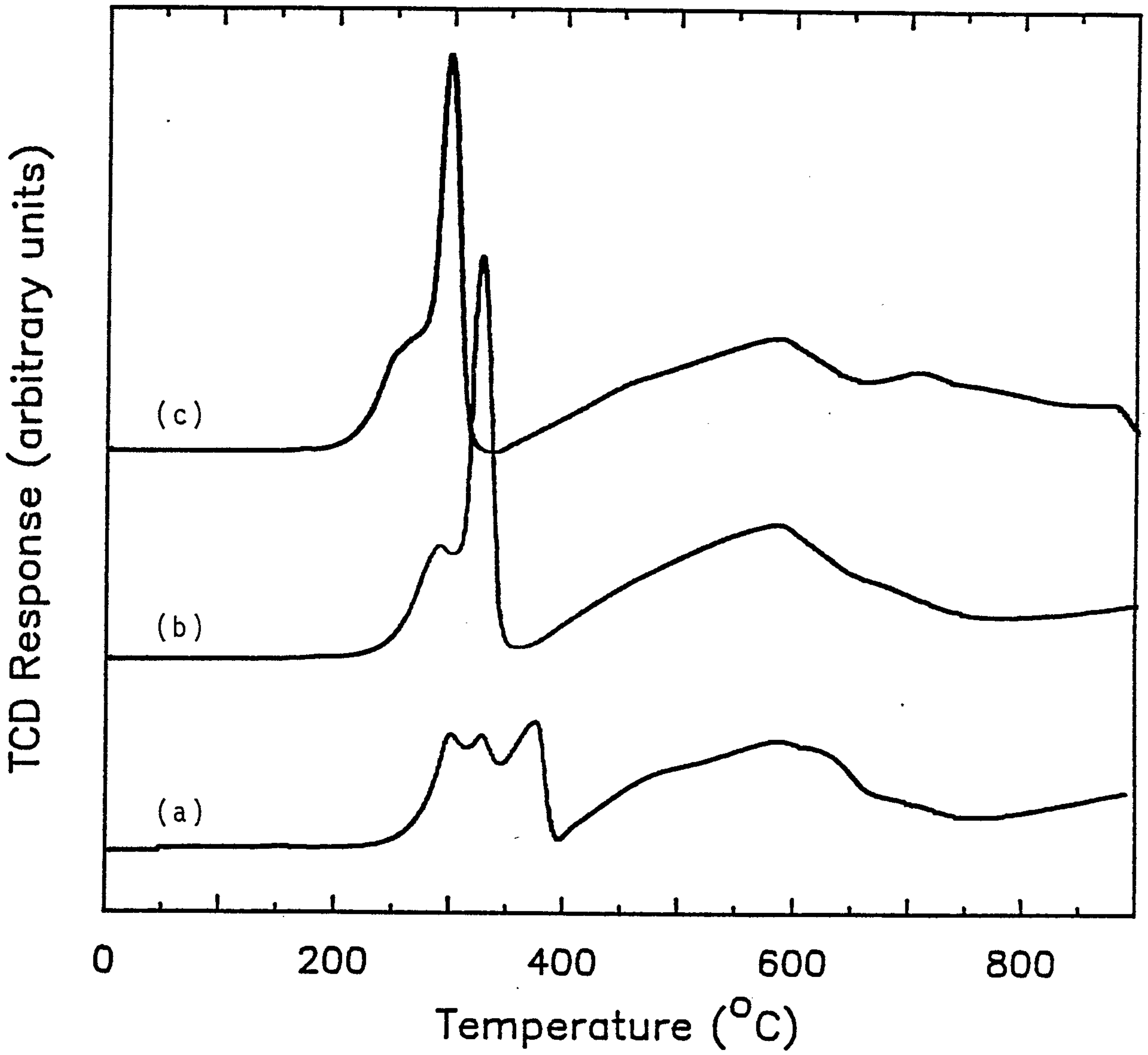

Figure 16. TPR profiles of: (a) 100 Fe/0.3 Cu/0.05 K; (b) 100 Fe/1.0 Cu/0.05 K; (c) 100 Fe/3.0 Cu/0.05 K.

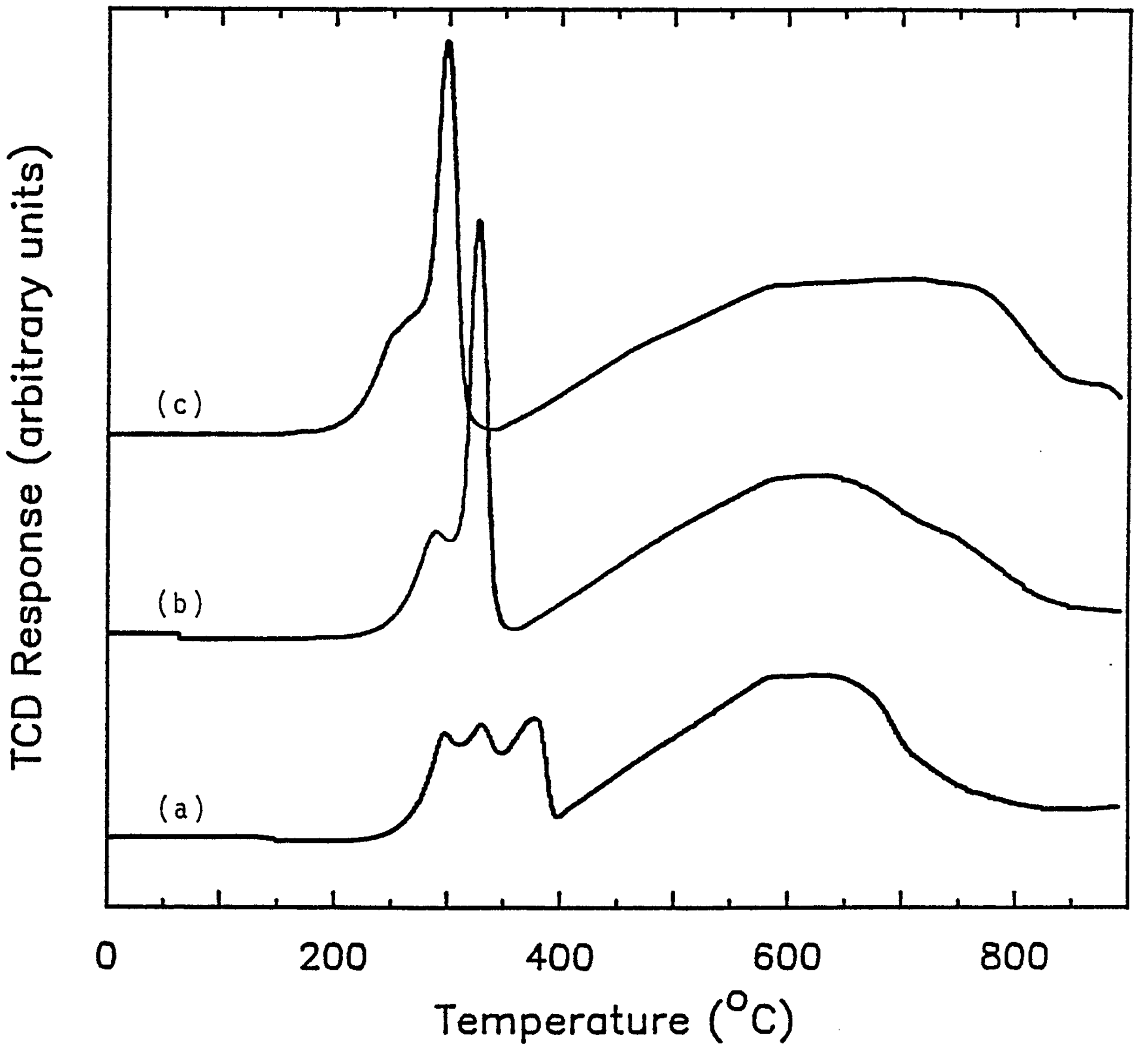

Figure 17. TPR profiles of: (a) 100 Fe/0.3 Cu/0.2 K; (b) 100 Fe/1.0 Cu/0.2 K; (c) 100 Fe/3.0 Cu/0.2 K.

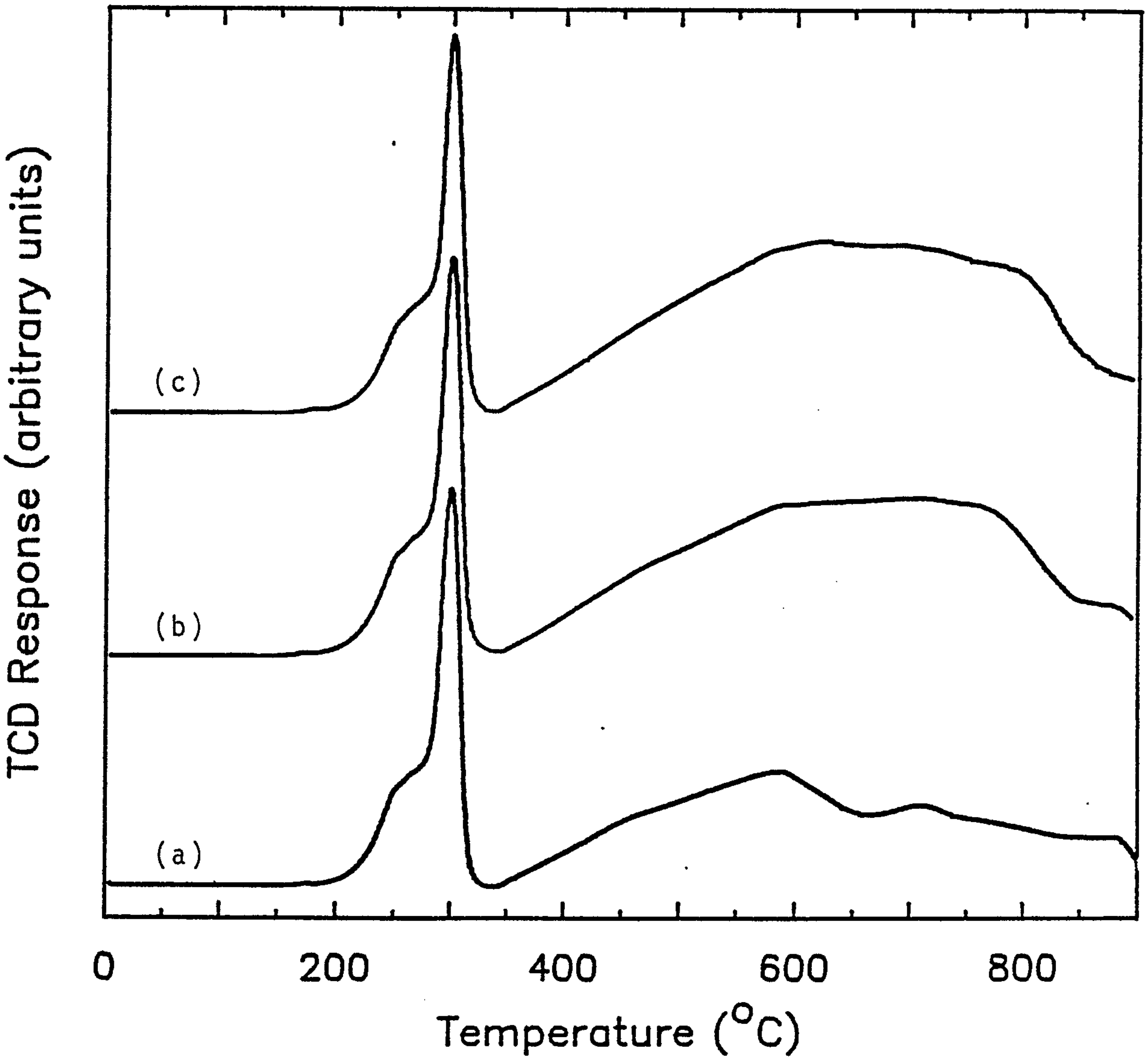

Figure 18. TPR profiles of: (a) 100 Fe/3.0 Cu/0.05 K; (b) 100 Fe/3.0 Cu/0.2 K; (c) 100 Fe/3.0 Cu/0.5 K.

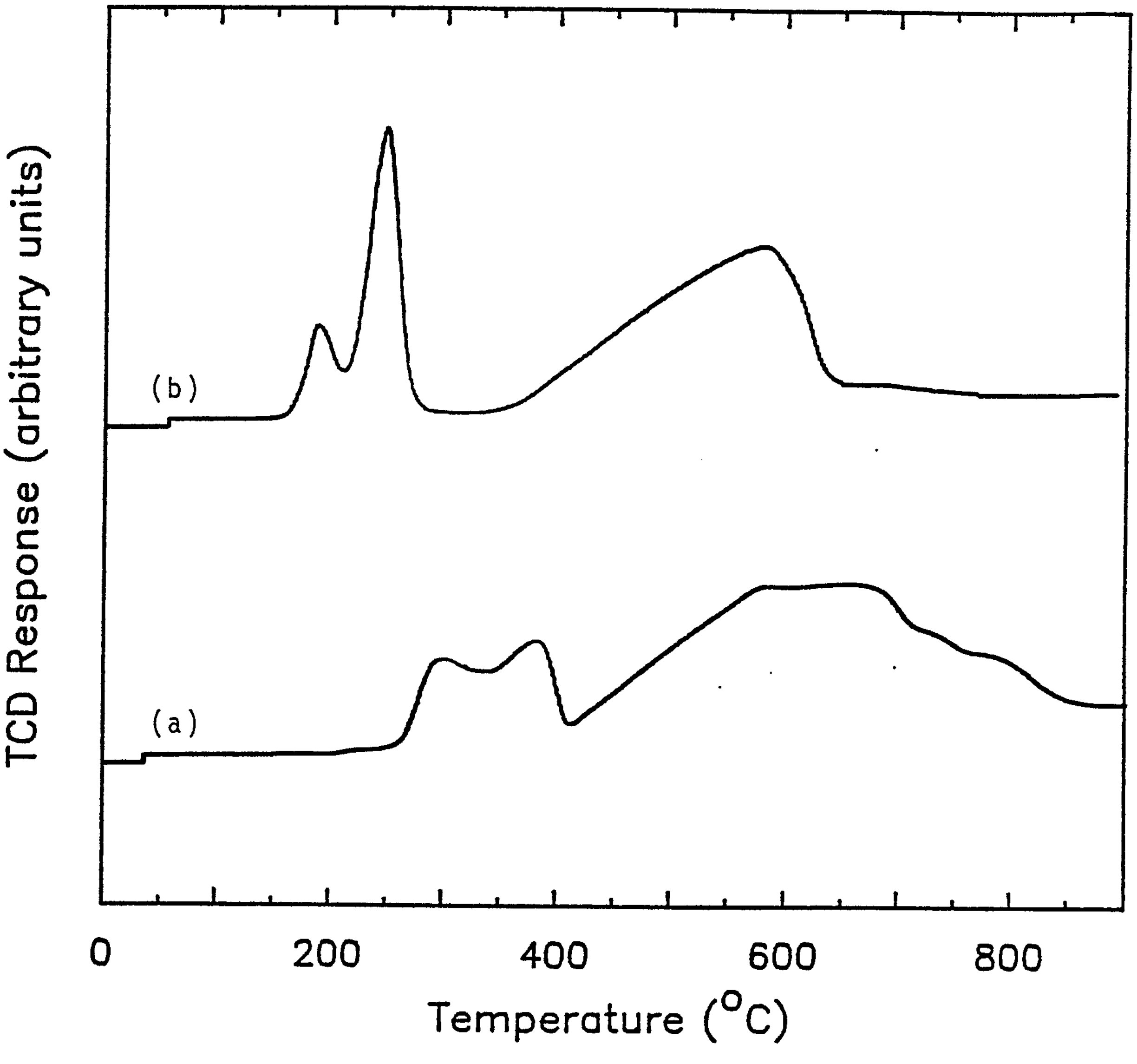

Figure 19. TPR profiles of: (a) 100 Fe/0.3 Cu/0.05 K; (b) 100 Fe/3.0 Cu/0.05 K.

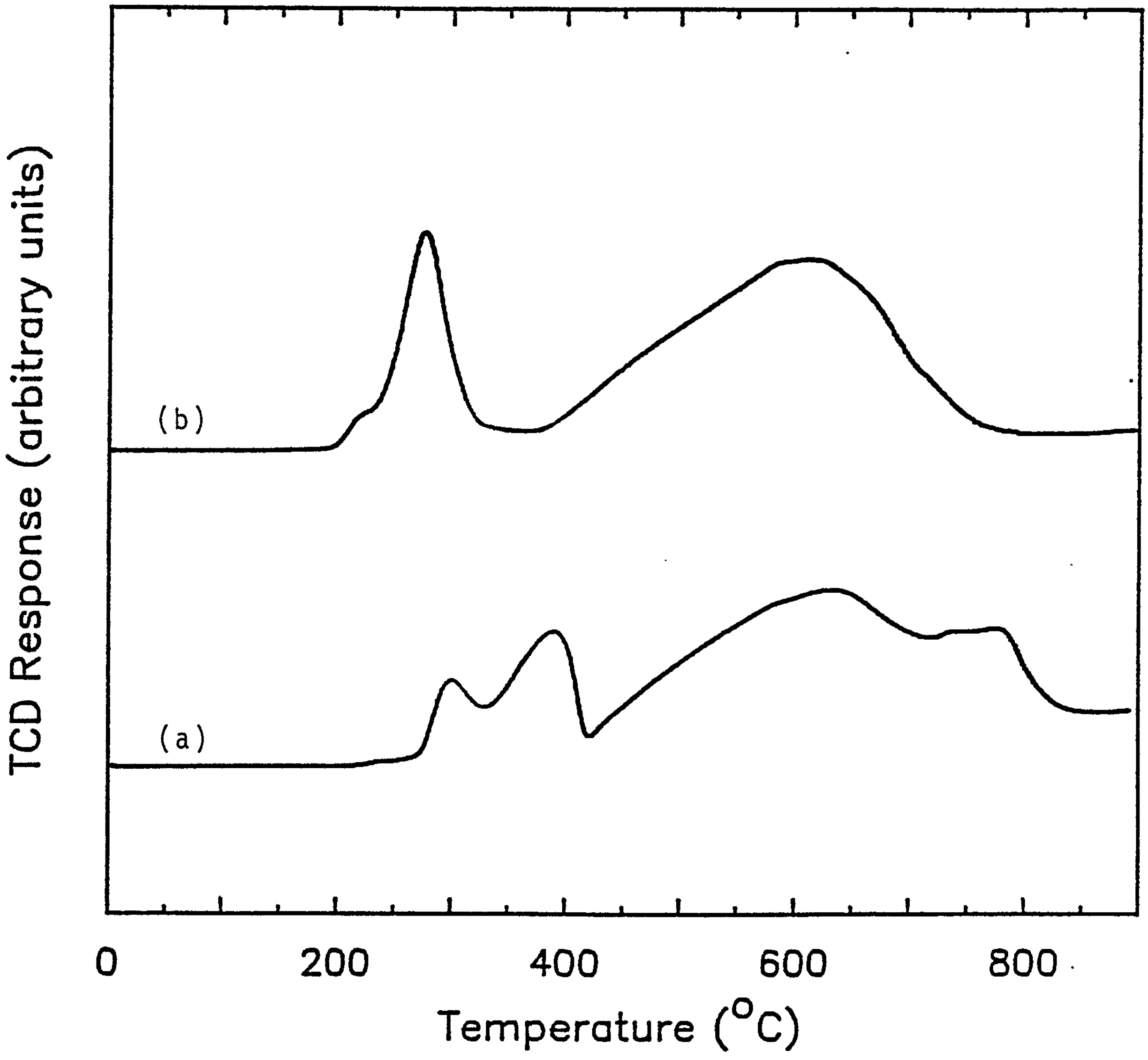

Figure 20. TPR profiles of: (a) 100 Fe/0.3 Cu/0.2 K; (b) 100 Fe/1.0 Cu/0.2 K.

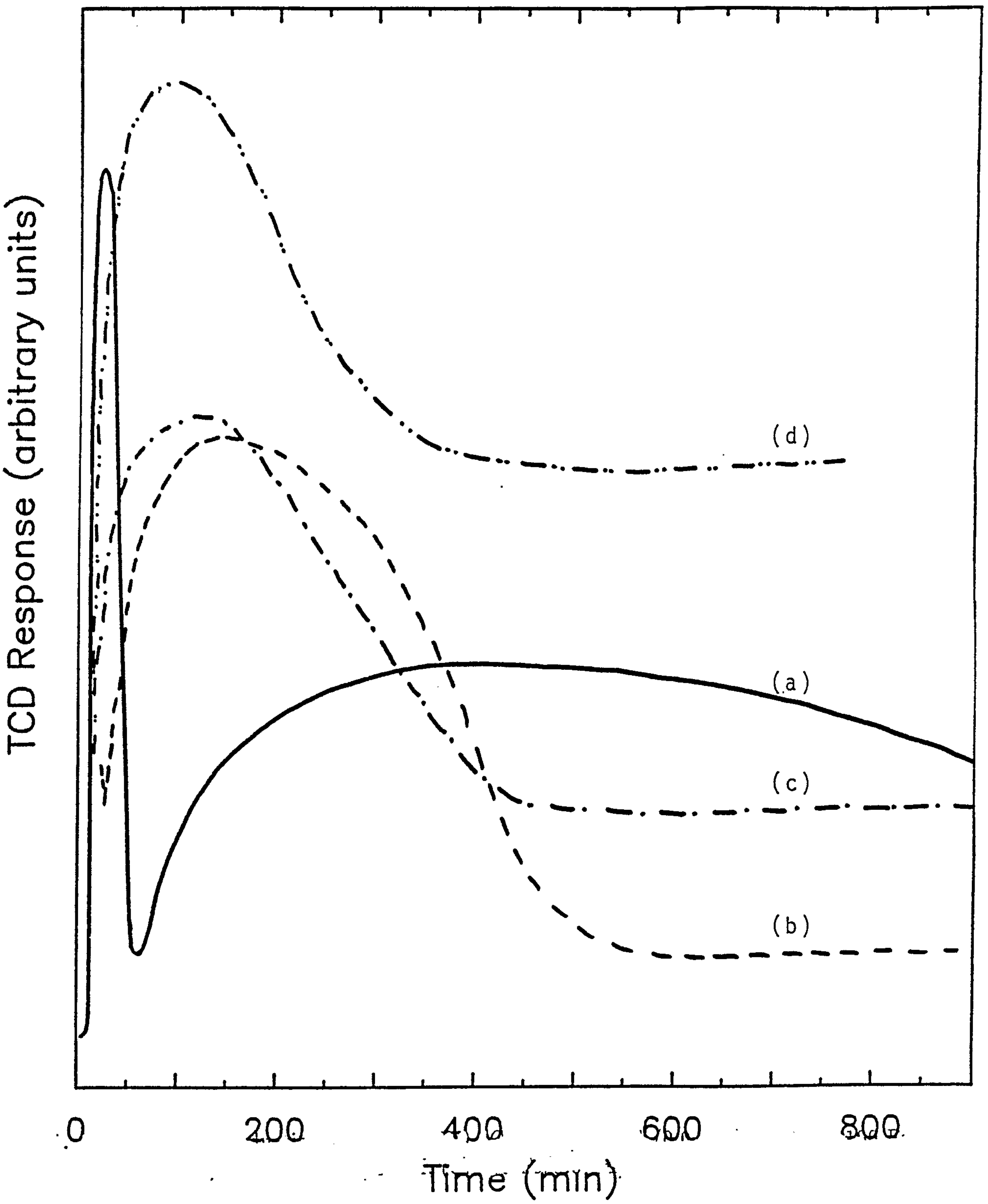

Figure 21. Isothermal H_2 reduction profiles at 300 °C of: (a) 100 Fe/0.0 Cu/0.0 K; (b) 100 Fe/0.3 Cu/0.0 K; (c) 100 Fe/1.0 Cu/0.0 K; (d) 100 Fe/3.0 Cu/0.0 K.

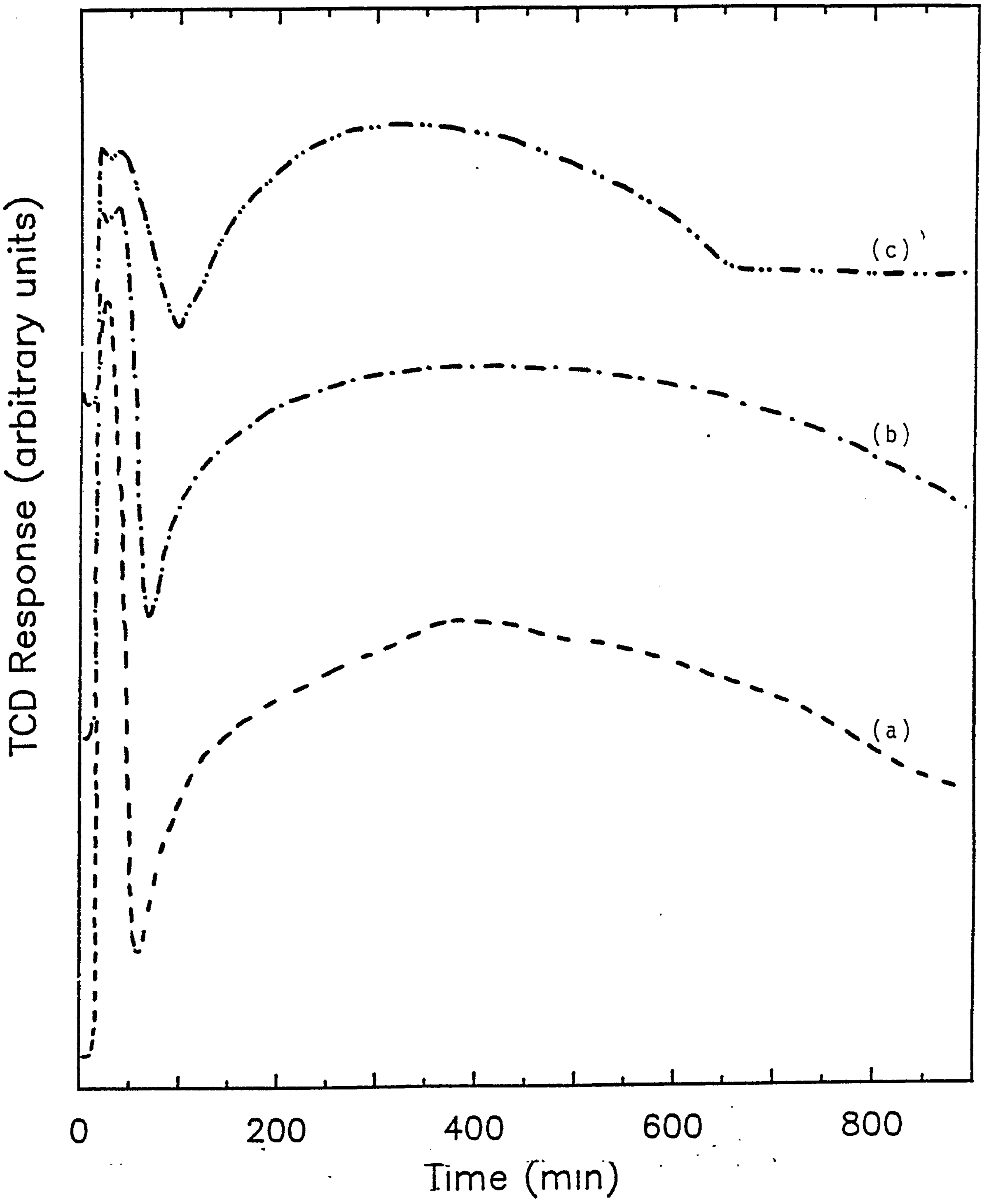

Figure 22. Isothermal H_2 reduction profiles at 300 °C of: (a) 100 Fe/0.0 Cu/0.2 K; (b) 100 Fe/0.0 Cu/1.0 K; (c) 100 Fe/0.0 Cu/2.0 K.

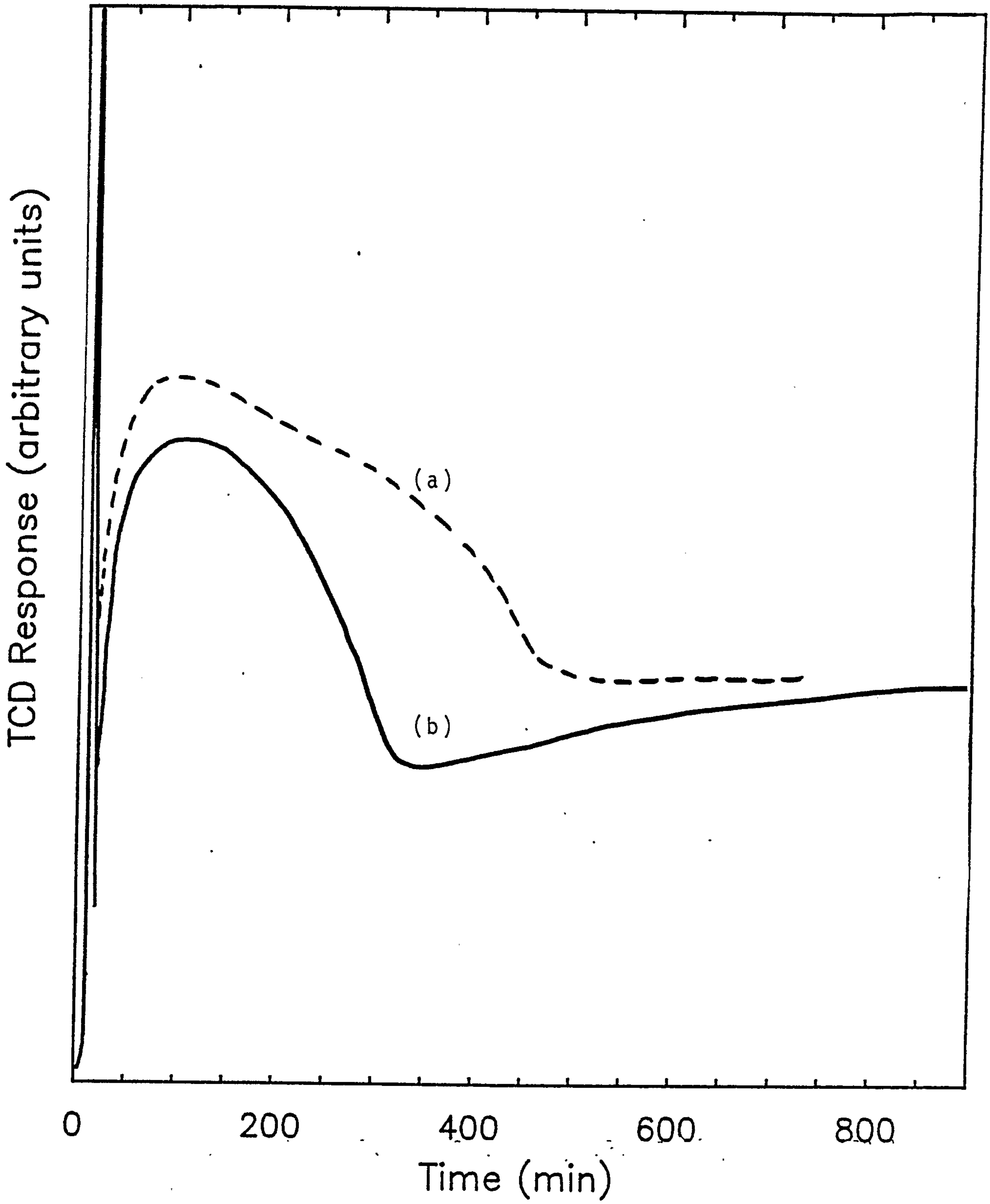

Figure 23. Isothermal H_2 reduction profiles at 300 °C of: (a) 100 Fe/1.0 Cu/0.2 K; (b) 100 Fe/3.0 Cu/0.2 K.

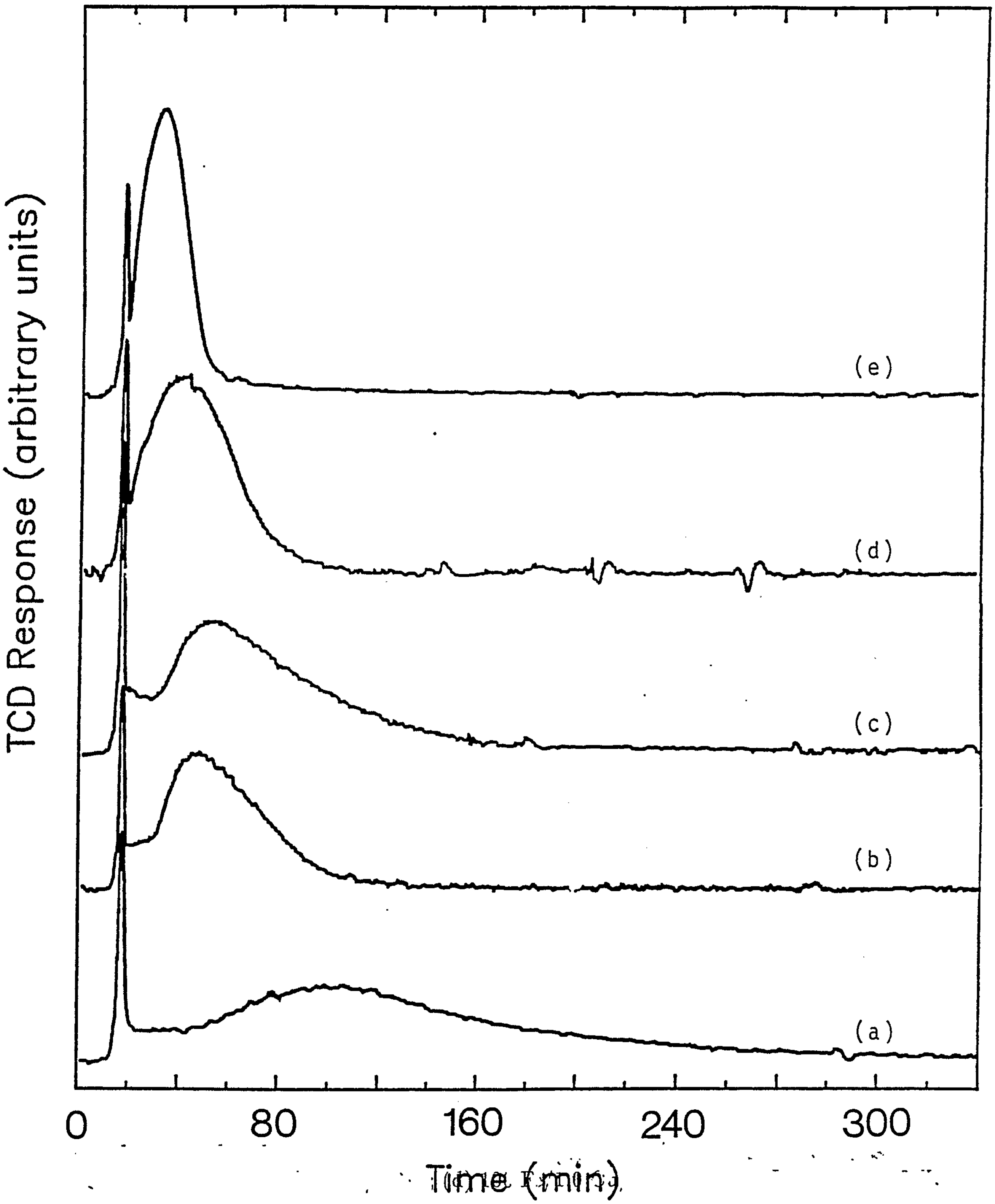

Figure 24. Isothermal CO reduction profiles at 300 °C of: (a) 100 Fe/0.0 Cu/0.0 K; (b) 100 Fe/0.0 Cu/0.2 K; (c) 100 Fe/0.0 Cu/1.0 K; (d) 100 Fe/1.0 Cu/0.0 K; (e) 100 Fe/1.0 Cu/0.2 K.

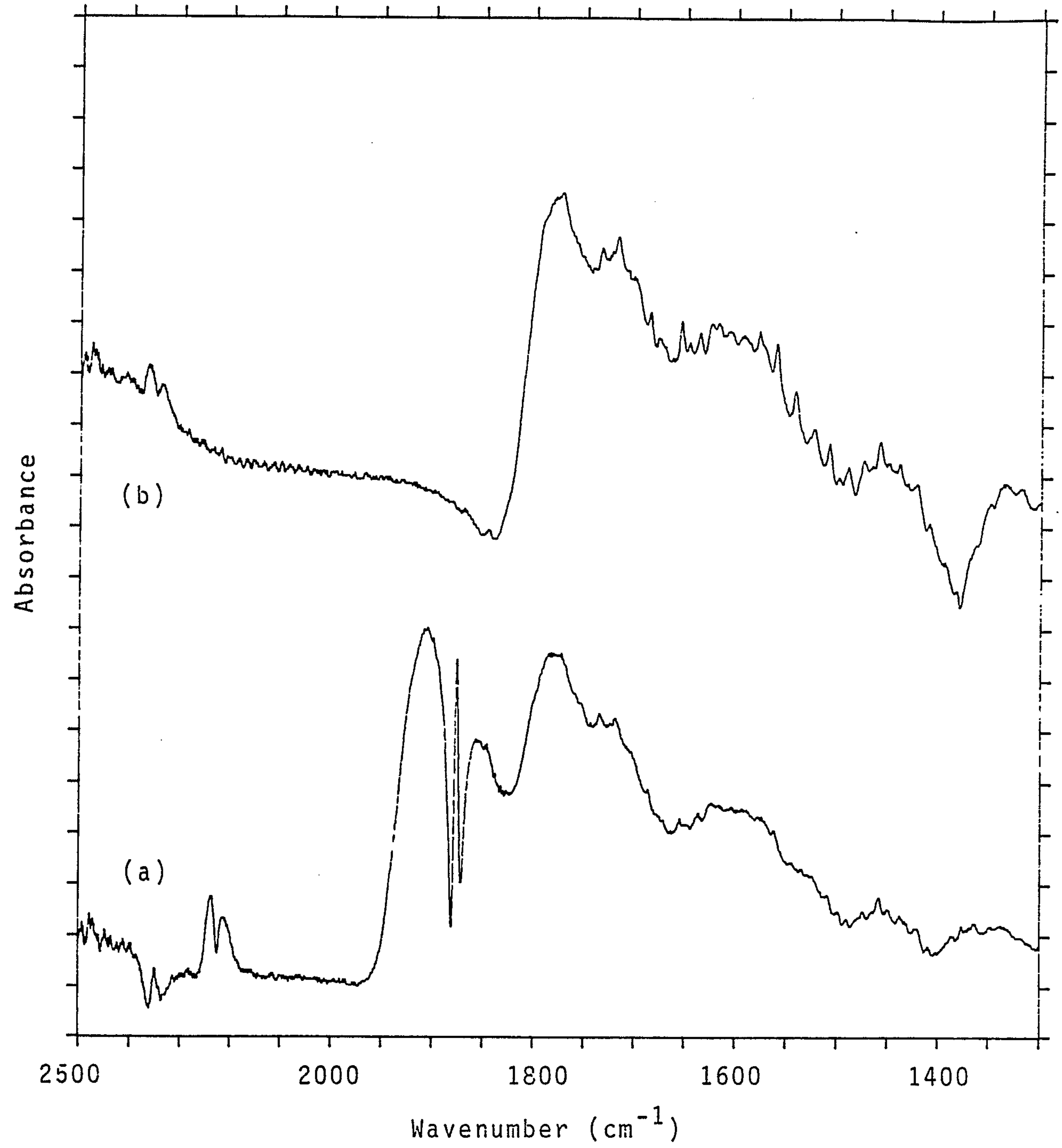

Figure 25. FT-IR spectra in N-O stretching region of 100 Fe/0.0 Cu/0.0 K deposited on BaF_2 crystal and calcined in O_2 for 1 *h* at 234 C: (a) following exposure to 11 torr of NO; (b) following removal of gaseous NO by cryogenic pumping.

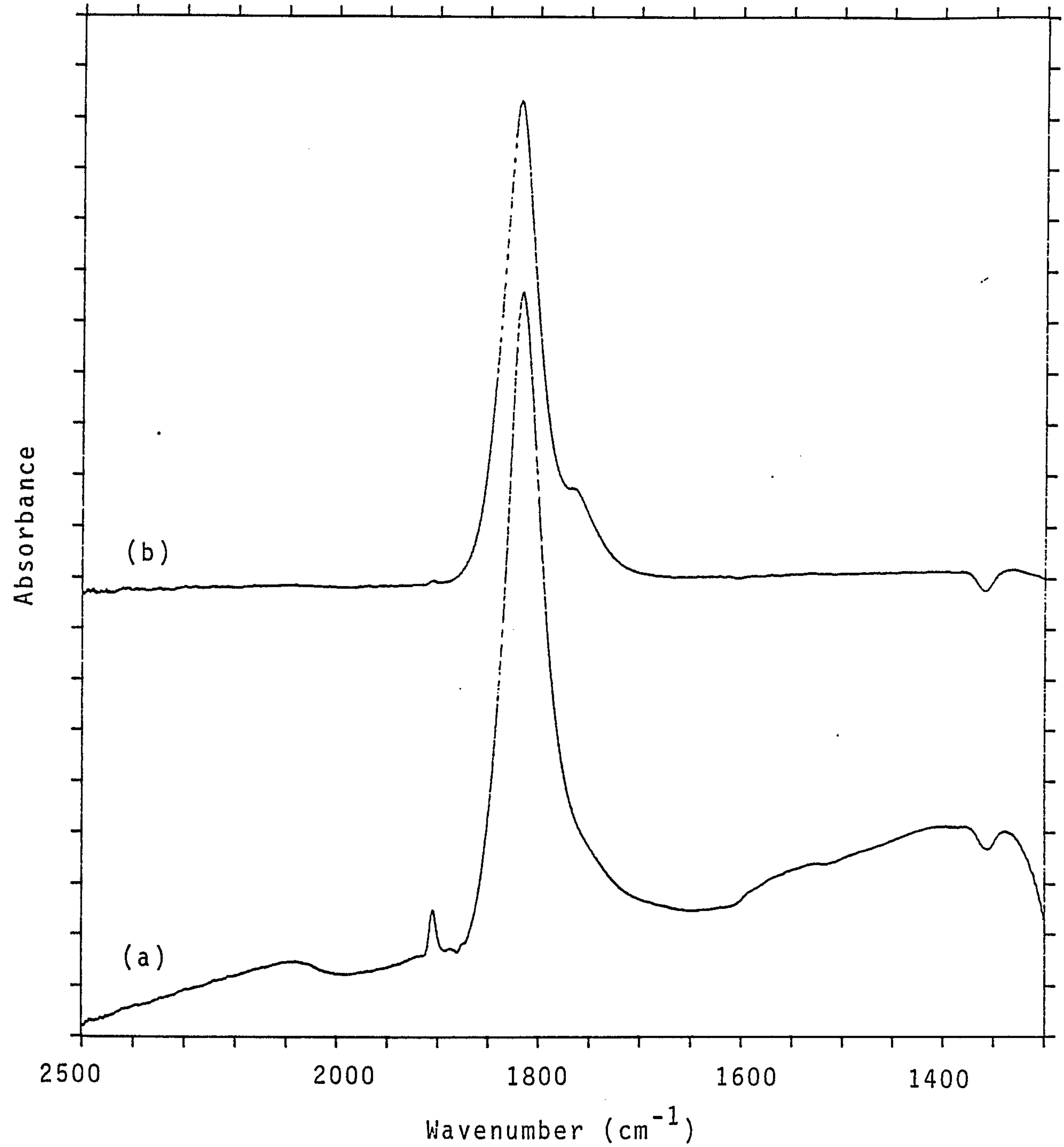

Figure 26. FT-IR spectra of 25 weight % Fe/SiO$_2$ calcined for 1 *h* in O$_2$ at 500 °C: (a) following exposure to 11 torr of NO; (b) following evacuation of gaseous NO.

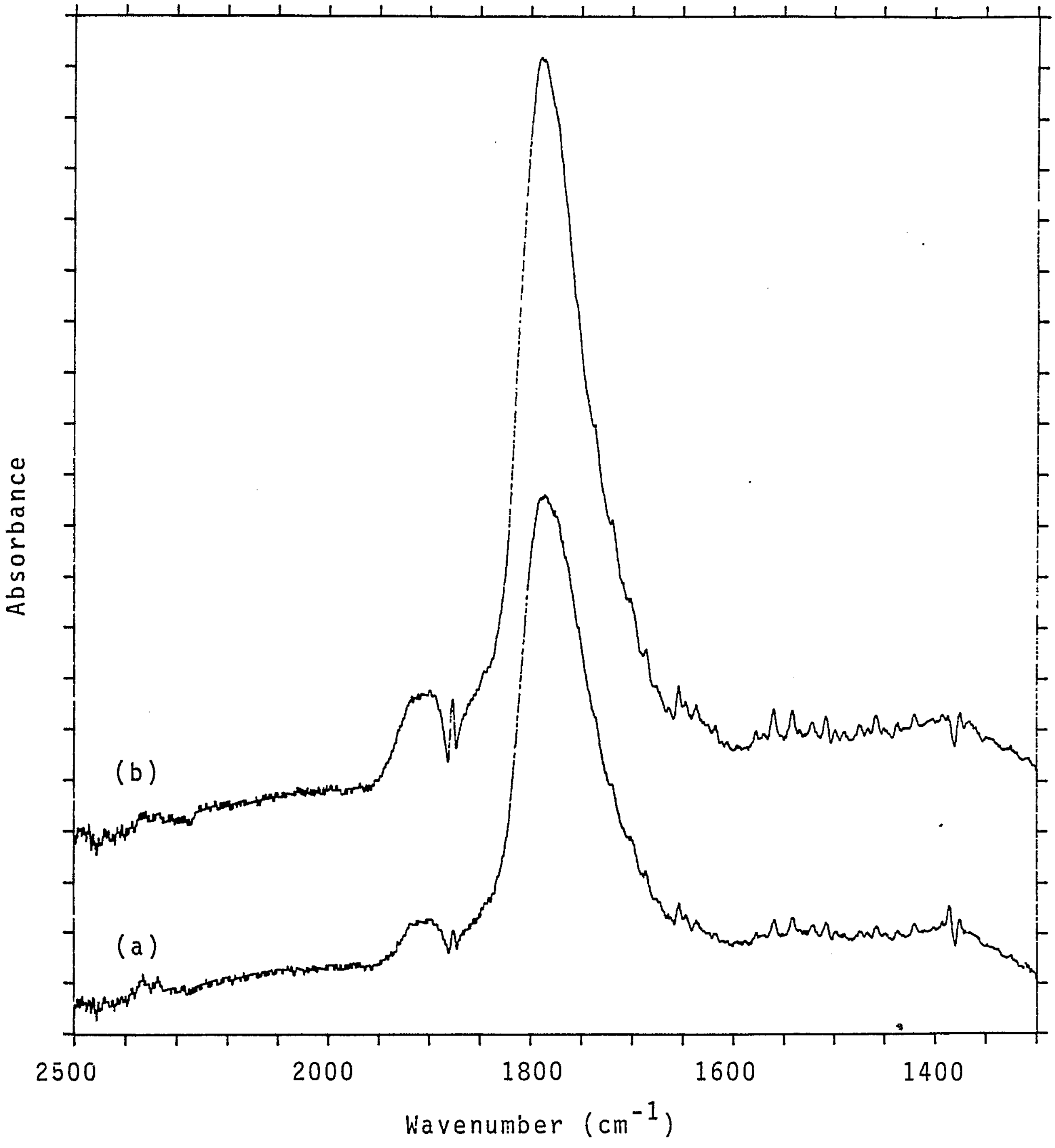

Figure 27. FT-IR spectra of 25 weight % Fe/SiO_2 containing 1 weight % K_2O, calcined for 1 *h* in O_2 at 500 °C: (a) following exposure to 11 torr of NO; (b) following exposure to 18 torr of NO.

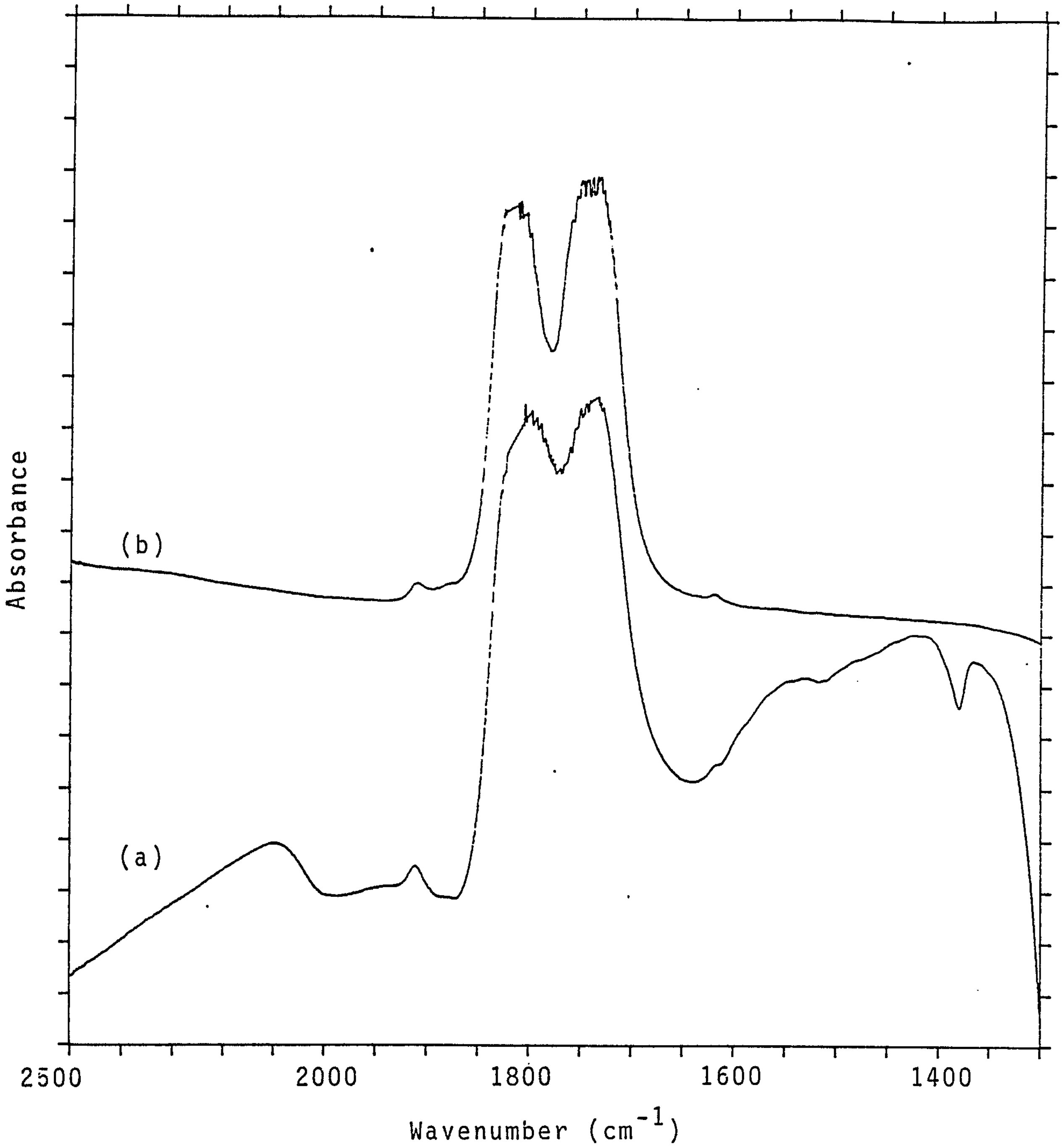

Figure 28. FT-IR spectra of 25 weight % Fe/SiO$_2$ calcined in O$_2$ and then reduced in H$_2$ for 1 *h* at 500 °C: (a) following exposure to 11 torr of NO; (b) following evacuation of gaseous NO.

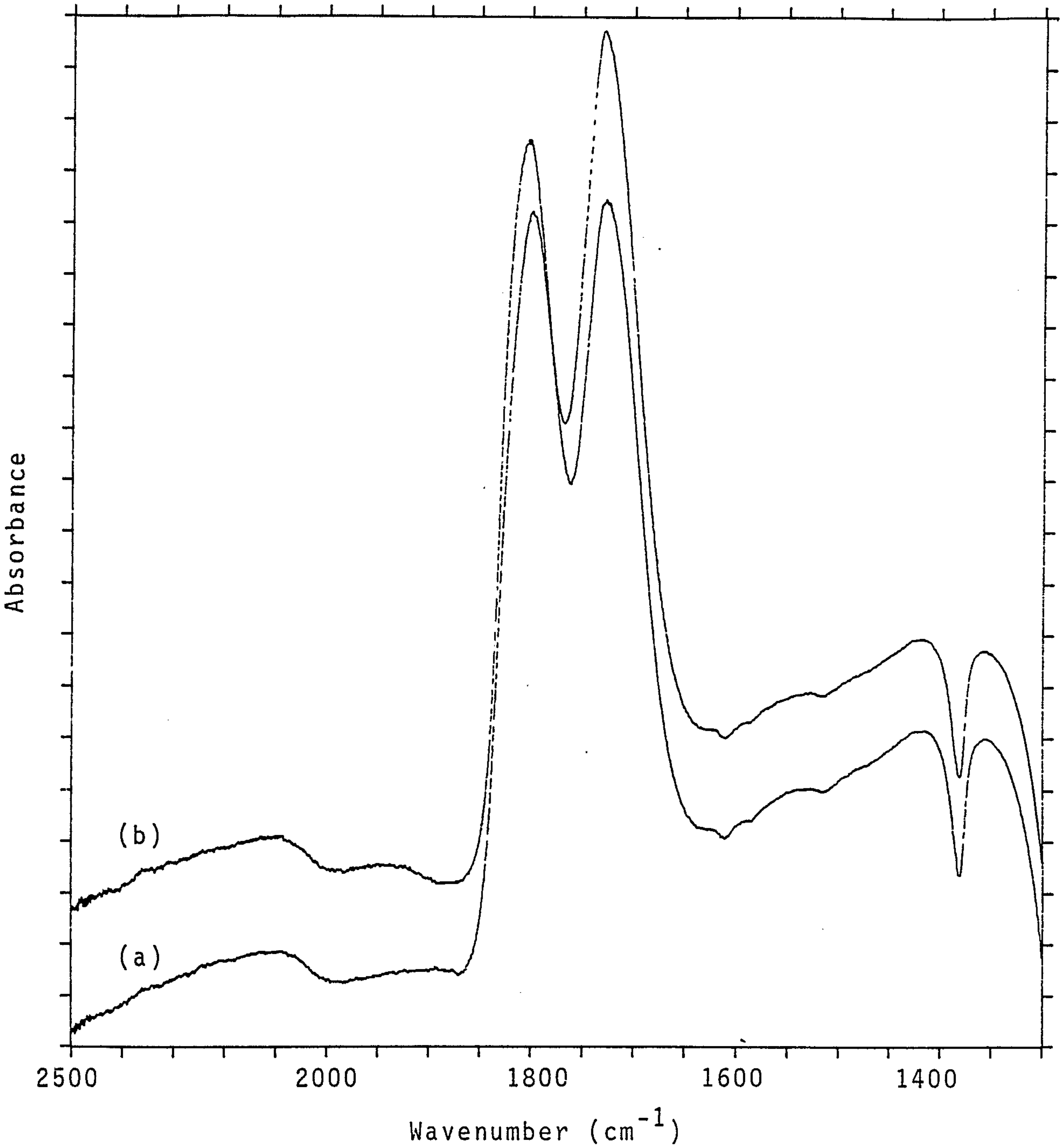

Figure 29. FT-IR spectra of 25 weight % Fe/SiO_2 containing 1 weight % K_2O, calcined in O_2 and then reduced in H_2 for 1 *h* at 500 °C: (a) following exposure to 11 torr of NO; (b) following evacuation of gaseous NO.

Appendix I

Calcination and Reduction Procedures for Precipitated Iron Catalysts

(a) Calcination Procedure.

After drying (Appendix II), precipitated iron catalysts were calcined with air at atmospheric pressure in either a fixed bed reactor (5 – 10 *g* samples) or in a large tubular reactor (50–80 *g*). The air flowrate during calcination was set at approximately 50 cm^3/g–cat$\cdot$*min* and the bed temperature was increased to 300 °C at a rate of 2°C/*min*. Once at 300 °C these conditions were maintained for 5 *h*. After that the heat supply was cut–off and the system was allowed to cool down to room temperature with air flowing through the catalyst bed. Calcined catalyst was later crushed, pelletized (if necessary) and sieved to obtain the desired mesh size range.

(b) Reduction Procedure.

Reduction was performed *in–situ* at atmospheric pressure at gas space velocities of 4–4.5 *Nl*/*g*–cat$\cdot$*h*. Initially the bed was heated to 150 °C at a rate of 2 °C/*min* in flowing helium, and was subsequently held at 150 ° for 2 *h*. Following this, CO was introduced and the bed temperature was raised to 280 ° at a rate of 1 °C/*min*. The bed temperature was maintained at 280 °C for 8 *h*, and then helium was again introduced to cool the bed to a temperature 50–60 °C below the desired initial reaction temperature. Following this the system was pressurized to the desired operating pressure and at this point the synthesis gas feed at the desired flowrate was introduced. The reactor temperature was gradually increased to the desired value. During this period the bed temperature was monitored frequently to prevent any temperature excursions above the desired reaction temperature. Once all process conditions, temperature, pressure, and space velocity, were achieved, the system was monitored closely during the first 3 *h* on stream to ensure their stability.

Appendix II

Summary of Catalyst Synthesis and Drying Procedure

(a) Iron/Copper Co – Precipitation Procedure.

Desired compositions of copper–promoted iron– based catalysts are prepared by a continuous co–precipitation technique. An aqueous solution containing $Fe(NO_3)_3$ ($\sim$ 0.6 *M*), together with a concentration of $Cu(NO_3)_2$ that corresponds to the desired Fe/Cu ratio in the final catalyst, and a second solution containing aqueous NH_3 ($\sim$ 2.7 *M*) are maintained in stirred vessels at 83 ± 3 °C. The two solutions are separately conveyed by fluid pumps to a stirred tubular reaction vessel that is thermostatted at 82 ± 1 °C. Precipitation (to form $FeOOH/Fe_2O_3$ and $Cu(OH)_2$ occurs continuously as the two solutions are pumped upward through the vessel, while an in–line pH electrode is used to monitor the pH of the reactor effluent. The flow rate of the NH_3 solution is normally fixed at $\sim$ 60 *ml/min*, while that of the Fe_3^+/Cu_2^+ solution is adjusted (typically to $\sim$ 90 *ml/min*) to give a precipitation pH of 6.0 ± 0.2. Collection of the slurried precipitate is made in ice–cooled vessels and is continued until one of the two solutions is consumed. The precipitate is then thoroughly washed by vacuum filtration to remove excess NH_3 and NO_3^- using $\sim$ 10 *l* of deionized, distilled water per 100 *g* (dry weight) of final catalyst. The washed precipitate is dried in a vacuum oven for 48 *h* at 50 °C, to remove most of the excess water, and then for an additional 12 to 24 *h* at 120 °C.

(b) Potassium Impregnation Procedure.

Addition of the desired levels of potassium promoter to precipitated Fe/Cu catalysts is performed by a pore–filling technique, using dried precipitate that has been crushed to pass a 40 mesh sieve. In this method, the required amount of $KHCO_3$ is dissolved in a volume of water that is $\sim$ 5 % larger than that needed to just fill all of the pores of the solid. The solution is then added to a weighed sample of catalyst, resulting in the so–called "incipient wetness" condition. This procedure ensures uniform and complete distribution of the potassium salt throughout the catalyst pore structure. For a typical batch of precipitated $FeOOH/Fe_2O_3$, for example, prepared by the method described in the preceding paragraph, $\sim$ 40 *ml* of water per 100 *g* (dry weight) of catalyst is required to achieve incipient wetness. Excess solvent is then removed by vacuum–aided evaporation, with continuous rotational agitation. The final product is dried further in a vacuum oven for 16 *h* at 120 °C.